Supplementary Information

Modular Synthesis of Benzothiophene-Fused Pentalene Reveals Substituent-Dependent Antiaromaticity

Ryosuke Isogai,[a] Kosuke Yasui,[b] and Aiko Fukazawa[*b]

[a] Department of Energy and Hydrocarbon Chemistry, Graduate School of Engineering, Kyoto University
[b] Institute for Integrated Cell-Material Science (WPI-iCeMS), Institute for Advanced Study, Kyoto University

Table of Contents

1. Experimental Details for the Synthesis

General. Melting points (mp) were determined with a Yanaco MP-S3 instrument. ^{1}H and $^{13}C\{^{1}H\}$ NMR spectra were recorded with a Bruker AVANCE III 500 MHz spectrometer (500 MHz for ^{1}H and 126 MHz for ^{13}C) in chloroform-*d* ($CDCl_3$) or dichloromethane-d_2 (CD_2Cl_2). The chemical shifts in ^{1}H and $^{13}C\{^{1}H\}$ NMR spectra are reported in δ ppm using residual protons of the solvents, *i.e.*, $CHCl_3$ (7.26 ppm) and CH_2Cl_2 (5.32 ppm), and the solvent signal of $CDCl_3$ (77.16 ppm) and CD_2Cl_2 (53.84 ppm), respectively, as an internal standard. In the case of $CDCl_3$ containing tetramethylsilane, tetramethylsilane (δ = 0 ppm) was used as an internal standard. High-resolution mass spectra (HRMS) were measured with a Bruker timsTOF (IMS-QTOF) system with the ionization method of ESI or APCI. Thin-layer chromatography (TLC) was performed on glass plates coated with 0.25 mm thickness of silica gel $60F_{254}$ (Merck). Column chromatography was performed using normal-phase silica gel Wakosil® HC-N (FUJIFILM Wako Pure Chemical Corporation), or Biotage® Sfär HC D (Biotage). All reactions were carried out under an atmosphere of N_2 in heat-dried glassware unless otherwise noted. Commercially available solvents and reagents were used without further purification unless otherwise mentioned. Anhydrous toluene, tetrahydrofuran (THF), and CH_2Cl_2 were purchased from FUJIFILM Wako Pure Chemical Corporation and further purified by Glass Contour solvent purifier systems. 2-bromothiophene was purchased from Sigma-Aldrich. Acetic acid (AcOH), Mg turnings, bromobenzene, 4-methoxybromobenzene, *n*-BuLi solution in hexane, triethylamine (Et_3N), 1,8-diazabicyclo[5.4.0]-7-undecene (DBU), tetra(*n*-butyl)ammonium iodide (TBAI), sodium hydroxide (NaOH), pyridinium chlorochromate (PCC), and *p*-toluenesulfonic acid monohydrate ($TsOH\cdot H_2O$) were purchased from Nacalai Tesque. 1-Bromo-3,5-bis(trifluoromethyl)benzene, 2-bromobenzenethiol, titanium tetrachloride ($TiCl_4$) solution in CH_2Cl_2 and cerium trichloride ($CeCl_3$) were purchased from Tokyo Chemical Industry (TCI). Sodium thiosulfate ($Na_2S_2O_3$), anhydrous dimethylformamide (DMF), methanol (MeOH), tri(*i*-propyl)silylacetylene, tri(*t*-butyl)phosphonium tetrafluoroborate (t-$Bu_3P\cdot HBF_4$), and molecular sieves 4A (MS 4 Å) were purchased from FUJIFILM Wako Pure Chemical Corporation. Iodobenzene diacetate ($PhI(OAc)_2$) was purchased from BIOSYNTH. Bicyclo[3.3.0]octane-2,6-dione (**7**) was prepared according to the literature method.[S1]

3,6-Bis[(2-bromophenyl)thio]-1,3a,4,6a-tetrahydropentalene (9). To a solution of **7** (6.91g, 50.0 mmol) in anhydrous THF (100 mL) was added a solution of $TiCl_4$ in CH_2Cl_2 (1.0 M, 105 mL, 0.105 mol) over 1 h at room temperature. After stirring for 20 min at the same temperature, a solution of 2-bromobenzenethiol (12.3 mL, 19.9 g, 0.110 mol) and Et_3N (29.2 mL, 21.2 g, 0.210 mol) in anhydrous THF (80 mL) was added slowly into the reaction vessel over 4 h. The resulting mixture was stirred for an additional 2.5 h, then quenched by saturated K_2CO_3 aqueous solution (100 mL). The aqueous layer was extracted with CH_2Cl_2 (3 × 200 mL). The combined organic layer was dried over Na_2SO_4, filtered, and concentrated under reduced pressure. The residue was adsorbed onto silica gel and purified by column chromatography to afford the desired compound (hexane to hexane/ CH_2Cl_2 10/1 as eluent) to afford 8.98 g of **9** as white solids (18.7 mmol, 37% yield). R_f =

0.19 (hexane/CH_2Cl_2 9/1). Mp: 95.2–95.8 °C. ^{1}H NMR (500 MHz, CD_2Cl_2): δ 2.54–2.64 (m, 4H), 3.52–3.57 (m, 2H), 7.09 (td, J = 7.6, 1.5 Hz, 2H), 7.26 (td, J = 7.9, 1.5 Hz, 2H), 7.31 (dd, J = 7.8, 1.5 Hz, 2H), 7.57 (dd, J = 7.9, 1.5 Hz, 2H). ^{13}C{^{1}H} NMR (125 MHz, $CDCl_3$): δ 36.9, 50.3, 124.8, 127.8, 127.9 131.4, 133.4, 134.7, 136.3, 136.4. HRMS (APCI): *m/z* Calcd. for $C_{20}H_{17}Br_2S_2$: 478.9133 ([*M*+H]$^+$). Found. 478.9130.

5b,6,11b,12-Tetrahydropentaleno[1,2-*b*:4,5-*b′*]dibenzothiophene (8). $Pd(OAc)_2$ (427 mg, 1.90 mmol) and P(*t*-Bu)$_3$·HBF_4 (1.07 g, 3.70 mmol) were added to a vial, and the atmosphere was replaced with nitrogen. Subsequently, anhydrous DMF (20 mL) and DBU (11.6 mL, 11.4 g, 74.8 mmol) were added to the vial, and the mixture was stirred for 20 minutes. Compound **9** (8.98 g, 18.7 mmol) was placed in a two-necked flask, and the atmosphere was replaced with nitrogen. DMF (20 mL) was then added to the flask. The contents of the vial were transferred into the two-necked flask, and the reaction mixture was heated to 140 °C. After 8 hours, the reaction mixture was cooled to room temperature, and all the volatiles were removed under reduced pressure to give the crude liquid. Purification by column chromatography with pre-adsorbed crude material (hexane/CH_2Cl_2 4/1 to hexane/CH_2Cl_2 1/1 as eluent) gave 5.05 g of **8** as white solids (15.9 mmol, 85% yield). R_f = 0.70 (hexane/CH_2Cl_2 1/1). Mp: 225.8–226.4 °C. ^{1}H NMR (500 MHz, CD_2Cl_2): δ 2.68 (dt, J = 15.3, 1.8 Hz, 2H), 3.37 (ddd, J = 15.3, 6.6, 3.7 Hz, 2H), 4.69 (ddd, J = 8.3, 3.7, 1.8 Hz, 2H), 7.23 (td, J = 7.2, 1.2 Hz, 2H), 7.22 (td, J = 7.2, 1.2 Hz, 2H), 7.55 (dt, J = 7.9, 0.9 Hz, 2H),7.55 (dd, J = 7.9, 0.9 Hz, 2H). ^{13}C{^{1}H} NMR (125 MHz, $CDCl_3$): δ 34.1, 51.9, 122.0, 123.8, 123.9, 124.6, 135.5, 138.0, 145.2, 146.6. HRMS (APCI): *m/z* Calcd. for $C_{20}H_{15}S_2$: 319.0610 ([*M*+H]$^+$). Found. 319.0610.

5b,6,11b,12-Tetrahydropentaleno[1,2-*b*:4,5-*b′*]dibenzothiophene-6,12-diyl diacetate (10). Compound **8** (3.41 g, 10.7 mmol) was placed in a two-necked flask, and the atmosphere was replaced with nitrogen. Anhydrous CH_2Cl_2 (80 mL) and AcOH (80 mL) were added, followed by $PhI(OAc)_2$ (10.3 g, 32.1 mmol) and TBAI (3.18 g, 8.60 mmol). The reaction mixture was heated to 40 °C and stirred. After 4 hours, the reaction was cooled to room temperature and quenched with 50 mL of saturated aqueous $Na_2S_2O_3$ solution. The aqueous layer was extracted with CH_2Cl_2 (3 × 50 mL), and the combined organic layers were collected. The solvent was removed under reduced pressure, and the crude product containing **10** was used for the next reaction without further purification.

5b,6,11b,12-Tetrahydropentaleno[1,2-*b*:4,5-*b′*]dibenzothiophene-6,12-diol (11). The crude product containing **10** obtained in the above experiment was placed to a 500 mL round-bottom flask and dissolved in 100 mL of MeOH under air. The flask was cooled to 0 °C, and an excess amount of NaOH (1.7 g, 43 mmol) was added. The mixture was gradually allowed to warm to room temperature and stirred for 1 hour. Then, the solvent was removed under reduced pressure. Water (100 mL) was added, and the aqueous layer was extracted with EtOAc (3 × 100 mL). The combined organic layers were collected, and the solvent was removed under reduced pressure. The crude product was purified by column chromatography (Biotage,

hexane/EtOAc 3/1 to EtOAc as eluent) to afford 2.22 g of **11** as white solids (6.33 mmol, 59% yield over 2 steps). R_f = 0.08 (hexane/ EtOAc 3/1). Mp: 212.6–212.9 °C. ^{1}H NMR (500 MHz, $CDCl_3$ containing TMS): δ 2.07 (d, J = 7.9Hz, 2H), 4.64 (t, J = 1.2 Hz, 2H), 5.43 (dt, J = 7.6, 1.5 Hz, 2H), 7.29 (td, J = 7.2, 1.2 Hz, 2H), 7.35 (td, J = 7.2, 1.2 Hz, 2H), 7.72 (dt, J = 7.9, 0.9 Hz, 2H), 7.55 (dt, J = 7.9, 0.9 Hz, 2H). ^{13}C{^{1}H} NMR (125 MHz, $CDCl_3$ containing TMS): δ 61.9, 76.2, 121.8, 123.7, 124.4, 134.9, 133.6, 139.4, 145.2, 147.9. HRMS (ESI): *m/z* Calcd. for $C_{20}H_{13}O_2S_2$: 349.0362 ([M–H]$^-$). Found. 349.0364.

5b,11b-Dihydropentaleno[1,2-*b*:4,5-*b*′]dibenzothiophene-6,12-dione (6). Compound **11** (2.21 g, 6.30 mmol) and Celite® (5.0 g) were placed in a 100 mL round-bottom flask, and anhydrous CH_2Cl_2 (60 mL) was added. PCC (3.00 g, 13.9 mmol) was added to the mixture, and the reaction mixture was stirred for 2 h. The resulting mixture was filtered through a plug of Celite® and washed with CH_2Cl_2 (100 mL). The filtrate was concentrated under reduced pressure, and the resulting residue was subjected to column chromatography (Biotage, hexane/EtOAc 1/1 to EtOAc as eluent**)** to afford 1.60 g of **6** as yellow solids (4.61 mmol, 73% yield). R_f = 0.64 (hexane/EtOAc 1/1). Mp: > 300 °C. ^{1}H NMR (500 MHz, $CDCl_3$ containing TMS): δ 4.92 (s, 2H), 7.42 (td, J = 7.3, 1.2 Hz, 2H), 7.46 (td, J = 7.6, 0.9 Hz, 2H), 7.85 (dd, J = 7.7, 0.9 Hz, 2H), 8.19 (dd, J = 7.3, 0.9 Hz, 2H). ^{13}C{^{1}H} NMR (125 MHz, $CDCl_3$ containing TMS): δ 57.5, 123.3 (2C), 126.3 (2C), 131.0, 136.4, 144.3, 168.9, 190.1. HRMS (APCI): *m/z* Calcd. for $C_{20}H_{11}O_2S_2$: 347.0195 ([M+H]$^+$). Found. 347.0195.

A General Procedure for the Synthesis of Bis(benzyl alcohol) 12a–d. Synthesis of 6,12-Bis[3,5-bis(trifluoromethyl)phenyl]-5b,6,11b,12-tetrahydropentaleno[1,2-*b*:4,5-*b*′]dibenzothiophene-6,12-diol (12a). Mg turnings (72.9 mg, 3.00 mmol) were placed in a dry vial, and the atmosphere was replaced with nitrogen. Anhydrous THF (5.0 mL) was added, followed by the dropwise addition of 1-bromo-3,5-bis(trifluoromethyl)benzene (517 µL, 879 mg, 3.00 mmol). The reaction mixture was heated to reflux and stirred for 30 min. After cooling to room temperature, the Grignard reagent solution was set aside.

In a separate vial, $CeCl_3$ (789 mg, 3.20 mmol) was added and dried under vacuum at 140 °C for 3 h. After cooling to room temperature, the vial was filled with nitrogen, cooled to –78 °C, and anhydrous THF (5.0 mL) was added under stirring. After being stirred for 10 min at –78 °C, the mixture was allowed to warm to room temperature and stirred for an additional 3 h. The resulting suspension was then cooled again to –78 °C, and the freshly prepared Grignard reagent (described above) was added dropwise. The mixture was stirred at –78 °C for 1 h, followed by the addition of a solution of **6** (346 mg, 1.00 mmol) in anhydrous THF (12 mL). After 3 h of stirring at –78 °C, the reaction mixture was allowed to warm to room temperature and poured into H_2O (50 mL). The aqueous layer was extracted with CH_2Cl_2 (5 × 50 mL), and the combined organic layer was dried over anhydrous Na_2SO_4, filtered, and concentrated under reduced pressure. The resulting crude product was purified by flash column chromatography (Biotage, hexane to hexane/EtOAc 4/1 as eluent) to afford 610 mg of **12a** as white solids (0.790 mmol, 79% yield). R_f = 0.48 (hexane/EtOAc 4/1). Mp:

262.3–262.7 °C. ^{1}H NMR (500 MHz, CD_2Cl_2): δ 3.36 (s, 2H), 4.75 (s, 2H), 7.10 (dt, J = 7.9, 0.6 Hz, 2H), 7.24 (ddd, J = 7.6, 7.5, 0.9 Hz, 2H), 7.36 (ddd, J = 8.2, 7.0, 1.2 Hz, 2H), 7.92 (dt, J = 8.2, 0.9 Hz, 2H), 7.98 (s, 2H), 8.09 (s, 4H). ^{13}C{^{1}H} NMR (125 MHz, CD_2Cl_2): δ 67.3, 81.4, 121.8, 122.5, 123.9 (q, J = 277.5 Hz), 124.4, 125.5(2C), 126.6, 132.5, 132.6 (q, J = 33.7 Hz), 143.9, 144.7, 146.5, 147.3. HRMS (ESI): *m/z* Calcd. for $C_{36}H_{18}F_{12}NaO_2S_2$: 797.0449 ([$M$+Na]$^{+}$). Found. 797.0443.

6,12-Diphenyl-5b,6,11b,12-tetrahydropentaleno[1,2-*b*:4,5-*b′*]dibenzothiophene-6,12-diol (12b). This compound was prepared in a similar manner to that described for **12a**. The Grignard reagent was prepared from Mg turnings (21.8 mg, 0.900 mmol) in anhydrous THF (1.5 mL) by the slow addition of bromobenzene (94.2 μL, 141 mg, 0.900 mmol), followed by heating at reflux temperature for 1 h. After the addition of the Grignard reagent into $CeCl_3$ (237 mg, 0.960 mmol; pre-dried under vacuum at 140 °C for 3 h) suspension in anhydrous THF (1.5 mL) at –78 °C and stirred for additional 1 h, a solution of **6** (104 mg, 0.300 mmol) in anhydrous THF (3.8 mL) was added into the reaction vessel and stirred for 2 h at –78 °C. After the resulting mixture was allowed to warm to room temperature, the reaction was quenched with saturated Na_2CO_3 aqueous solution (20 mL), and subjected for a standard aqueous workup, followed by the purification in a similar manner as described for **12a** by column chromatography (Biotage, hexane to hexane/EtOAc 1/1 as eluent**)** to afford 89.7 mg of **12b** as white solids (0.180 mmol, 59% yield). R_f = 0.52 (hexane/ EtOAc 1/1)**.** Mp: 183.4–183.7 °C. ^{1}H NMR (500 MHz, $CDCl_3$): δ 3.10 (s, 2H), 4.70 (s, 2H), 5.91 (d, J = 1.5 Hz, 1H), 7.16–7.22 (m, 4H), 7.29 (ddd, J = 7.9, 7.2, 2.1 Hz 2H), 7.38 (tt, J = 7.2, 1.2 Hz 2H), 7.45 (tt, J = 7.9, 1.5 Hz, 2H) , 7.56–7.60 (m, 4H), 7.84 (dt, J = 8.2, 0.9 Hz, 2H). ^{13}C{^{1}H} NMR (125 MHz, $CDCl_3$): δ 67.2, 81.6, 122.3, 123.7, 124.5, 124.7, 125.6, 127.8, 128.9, 133.1, 143.0, 144.2, 145.7, 146.0. HRMS (ESI): *m/z* Calcd. for $C_{32}H_{22}NaO_2S_2$: 525.0953 ([M+Na]$^{+}$). Found. 525.0952.

6,12-Bis(4-methoxyphenyl)-5b,6,11b,12-tetrahydropentaleno[1,2-*b*:4,5-*b′*]dibenzo-thiophene-6,12-diol (12c). This compound was prepared in a similar manner to that described for **12a**. The Grignard reagent was prepared from Mg turnings (21.8 mg, 0.900 mmol) in anhydrous THF (1.0 mL) by the slow addition of 4-methoxy-1-bromobenzene (113 μL, 168 mg, 0.900 mmol), followed by heating at a reflux temperature for 30 min. After the addition of the Grignard reagent into $CeCl_3$ (236.6 mg, 0.90 mmol; pre-dried under vacuum at 140 °C for 3 h) suspension in anhydrous THF (1.0 mL) at –78 °C and stirred for additional 1 h, a solution of **6** (104 mg, 0.300 mmol) in anhydrous THF (3.8 mL) was added into the reaction vessel and stirred for 3 h at –78 °C. After the resulting mixture was allowed to warm to room temperature, the reaction was quenched with H_2O (20 mL), and subjected for a standard aqueous workup, followed by the purification in a similar manner as described for **12a** by column chromatography (Biotage, hexane to hexane/EtOAc 1/4 as eluent) to afford 126 mg of **12c** as white solids (0.223 mmol, 73% yield). R_f = 0.46 (hexane/EtOAc 4/1). Mp: 203.8–204.4 °C. ^{1}H NMR (500 MHz, $CDCl_3$): δ 3.20 (s, 2H), 3.85 (s, 6H), 4.66 (s, 2H), 6.97 (dt, J = 8.9, 2.1 Hz, 4H), 7.19 (d, J = 0.9 Hz 2H), 7.20 (t, J = 0.9 Hz 2H), 7.29 (ddd, J = 8.2, 4.6, 3.6 Hz, 2H), 7.48 (dt, J = 8.9,

2.1 Hz, 4H), 7.86 (dt, J = 8.2, 0.9 Hz, 2H). $^{13}C\{^{1}H\}$ NMR (125 MHz, CD_2Cl_2): δ 55.7, 67.4, 81.5, 114.3, 122.4, 123.9, 124.6, 124.8, 127.0, 133.5, 136.6, 143.4, 146.0, 146.2, 159.6. HRMS (ESI): *m/z* Calcd. For $C_{34}H_{26}NaO_4S_2$: 585.1165 ([M+Na]$^+$). Found. 585.1164.

6,12-Di(thiophen-2-yl)-5b,6,11b,12-tetrahydropentaleno[1,2-*b*:4,5-*b′*]dibenzothiophene-6,12-diol (12d). This compound was prepared in a similar manner to that described for **12a**. The Grignard reagent was prepared from Mg turnings (21.8 mg, 0.900 mmol) in anhydrous THF (1.0 mL) by the slow addition of 2-bromothiophene (87.3 μL, 147 mg, 0.900 mmol), followed by heating at a reflux temperature for 30 min. After the addition of the Grignard reagent into $CeCl_3$ (237 mg, 0.960 mmol; pre-dried under vacuum at 140 °C for 3 h) suspension in anhydrous THF (1.0 mL) at –78 °C and stirred for additional 1 h, a solution of **6** (104 mg, 0.300 mmol) in anhydrous THF (3.8 mL) was added into the reaction vessel and stirred for 3 h at –78 °C. After the resulting mixture was allowed to warm to room temperature, the reaction was quenched with H_2O (20 mL), and subjected for a standard aqueous workup, followed by the purification in a similar manner to that described for **12a** by flash column chromatography (Biotage, hexane to hexane/EtOAc 3/1 as eluent) to afford 103 mg of **12d** as white solids (0.200 mmol, 67% yield). R_f = 0.53 (hexane/EtOAc 1/2). Mp: 161.6–161.9 °C. ^1H NMR (500 MHz, CD_2Cl_2): δ 3.25 (s, 2H), 4.82 (s, 2H), 7.02 (dd, J = 3.5, 1.2 Hz, 2H), 7.06 (dd, J = 4.9, 3.7 Hz, 2H), 7.26 (td, J = 7.5, 0.9 Hz, 2H), 7.32 (td, J = 8.1, 1.2 Hz 2H), 7.39 (dd, J = 4.9, 1.2 Hz, 2H), 7.47 (dd, J = 7.9, 0.9 Hz, 2H), 7.87 (d, J = 8.2 Hz, 2H). $^{13}C\{^{1}H\}$ NMR (125 MHz, CD_2Cl_2): δ 67.4, 80.6, 122.4, 123.9, 124.2, 124.9, 125.0, 125.6, 127.6, 133.2, 143.1, 145.1, 146.2, 148.8. HRMS (ESI): *m/z* Calcd. for $C_{28}H_{18}NaO_2S_4$: 537.0082 ([M+Na]$^+$). Found. 537.0083.

6,12-Bis{[tri(*i*-propyl)silyl]ethynyl}-5b,6,11b,12-tetrahydropentaleno[1,2-*b*:4,5-*b′*]dibenzo-thiophene-6,12-diol (12e). A lithium acetylide was prepared in situ by dropwise addition of *n*-BuLi solution in hexane (1.6 M; 563 μL, 0.900 mmol) to a solution of tri(*i*-propyl)silylacetylene (202 μL, 164 mg, 0.900 mmol) in anhydrous THF (1.5 mL) at –78 °C, stirring for 30 min, followed by additional stirring at room temperature for 1 h. After the addition of the lithium acetylide solution thus prepared into $CeCl_3$ (237 mg, 0.960 mmol; pre-dried under vacuum at 140 °C for 3 h) suspension in anhydrous THF (1.5 mL) at –78 °C and stirred for additional 1 h, a solution of **6** (104 mg, 0.300 mmol) in anhydrous THF (3.8 mL) was added into the reaction vessel and stirred for 3 h at –78 °C. After the resulting mixture was allowed to warm to room temperature, the reaction was quenched with saturated Na_2CO_3 aqueous solution (50 mL), and subjected for a standard aqueous workup, followed by the purification by flash column chromatography (Biotage, hexane to hexane/CH_2Cl_2 7/3 as eluent) to afford 61.9 mg of **12e** as white solids (87.0 μmol, 29% yield). R_f = 0.44 (hexane/EtOAc 10/1). Mp: 202.3–202.9 °C. ^1H NMR (500 MHz, $CDCl_3$): δ 1.13–1.16 (m, 42H), 2.76 (s, 2H), 4.83 (s, 2H), 7.35 (ddd, J = 7.9, 7.3, 1.2 Hz, 2H), 7.40 (td, J = 7.2, 1.2 Hz, 2H), 7.85 (dt, J = 7.9, 0.9 Hz, 2H), 8.14 (dt, J = 7.9, 0.9 Hz, 2H). $^{13}C\{^{1}H\}$ NMR (125 MHz, $CDCl_3$): δ 11.4, 18.8, 65.9, 71.7, 87.8, 107.0, 122.2, 123.7, 124.8, 124.9, 133.1, 141.5, 144.7, 145.6. HRMS (ESI): *m/z* Calcd. for $C_{42}H_{54}NaO_2S_2Si_2$:

733.2996 ([*M*+Na]$^+$). Found. 733.2996.

Typical procedure for the acid-promoted dehydration of 12a–e. Dehydration of 12a. A vial was charged with **12a** (77.5 mg, 0.100 mmol), TsOH·H_2O (57.1 mg, 0.300 mmol), and MS 4 Å (pre-dried under vacuum prior to use; 500 mg). After sealing with a cap, anhydrous toluene (4.0 mL) was added, and the mixture was stirred at 110 °C for 1 h. The reaction mixture was then cooled to room temperature and filtered through a plug of Celite®. The filtrate was concentrated under reduced pressure. The resulting residue was suspended in methanol, and the precipitate was collected by filtration to afford 47.9 mg of **4a** as red solids (64.8 μmol, 65% yield). The filtrate was concentrated under reduced pressure, and the residue was subjected to column chromatography (hexane to hexane/CH_2Cl_2 1/1 as eluent) to afford 7.0 mg of **4a** (9.5 μmol, 9% yield) and 17.4 mg of **13a** (22.9 μmol, 23% yield) as yellow solids.

6,12-Bis[3,5-bis(trifluoromethyl)phenyl]pentaleno[1,2-*b*:4,5-*b′*]dibenzothiophene (4a). R_f = 0.85 (hexane/CH_2Cl_2 1/1). Mp: > 300 °C. ^{1}H NMR (500 MHz, $CDCl_3$): δ 7.01 (d, J = 7.9 Hz, 2H), 7.08 (t, J = 7.5 Hz, 2H), 7.14 (t, J = 7.3 Hz, 2H), 7.53 (d, J = 7.9 Hz, 2H), 7.99 (s, 2H), 8.03 (s, 4H). ^{13}C{^{1}H} NMR spectrum was not obtained due to its poor solubility. HRMS (APCI): *m/z* Calcd. for $C_{36}H_{15}F_{12}S_2$: 739.0418 ([*M*+H]$^+$). Found. 739.0418.

[3,5-Bis(trifluoromethyl)phenyl](2-{1-[3,5-bis(trifluoromethyl)phenyl]-3*H*-benzo[*b*]cyclopenta-[*d*]thiophen-2-yl}benzo[*b*]thiophen-3-yl)methanone (13a). R_f = 0.72 (hexane/CH_2Cl_2 1/1). Mp: 91.2–91.7 °C. ^{1}H NMR (500 MHz, CD_2Cl_2): δ 4.07 (s, 2H), 7.14 (dd, J = 7.9, 1.2 Hz, 2H), 7.20 (dt, J = 6.9, 1.2, Hz, 2H), 7.28 (dt, J = 8.3, 1.2 Hz, 2H), 7.35 (dt, J = 7.5, 0.9 Hz, 2H), 7.43 (dt, J = 7.6, 1.2 Hz, 2H), 7.47 (dt, J = 8.2, 0.6 Hz, 2H), 7.64 (s, 2H), 7.86 (dt, J = 7.9, 0.9 Hz, 2H), 7.89–7.92 (m, 2H), 7.97–7.99 (m, 1H), 8.05 (s, 2H). ^{13}C{^{1}H} NMR (125 MHz, CD_2Cl_2): δ 42.5, 122.5, 122.6, 123.8, 124.2, 124.6, 125.0, 126.0, 126.3, 127.1, 129.9, 130., 132.0, 132.6, 126.7, 136.7, 128.5, 138.9, 139.8, 141.4, 143.3, 145.3, 146.9, 188.9. HRMS (APCI): *m/z* Calcd. for $C_{36}H_{17}F_{12}OS_2$: 757.0524 ([*M*+H]$^+$). Found. 757.0518.

6,12-Diphenylpentaleno[1,2-*b*:4,5-*b′*]dibenzothiophene (4b). This compound was prepared in a similar manner to that described for **4a**. The mixture of **12b** (50.3 mg, 0.100 mmol), TsOH·H_2O (57.1 mg, 0.300 mmol), and MS 4 Å (pre-dried, 500 mg) in anhydrous toluene (4.0 mL) was heated at 110 °C for 1 h. Purification in a similar manner to that described for **4a** gave 28.1 mg of **4b** as red solids (60.2 μmol, 60% yield). Further purification of thus obtained filtrate by column chromatography (hexane to hexane/CH_2Cl_2 7/3 as eluent) afforded an additional 1.3 mg of **4b** (R_f = 0.85 (hexane/CH_2Cl_2 1/1), 2.8 μmol, 3% yield). The ^{1}H NMR spectrum of this product showed good agreement with the data reported in the literature.[S2]

6,12-Bis(4-methoxyphenyl)pentaleno[1,2-*b*:4,5-*b′*]dibenzothiophene (4c). This compound was prepared in a similar manner to that described for **4a**. The mixture of **12c** (56.3 mg, 0.100 mmol), $TsOH·H_2O$ (57.1 mg, 0.300 mmol), and MS 4 Å (pre-dried, 500 mg) in anhydrous toluene (4.0 mL) was heated at 110 °C for 1 h. Purification in a similar manner to that described for **4a** gave 31.9 mg of **4c** as red solids (0.061 mmol, 61% yield). R_f = 0.64 (hexane/CH_2Cl_2 1/1). Mp: > 300 °C. ^{1}H NMR (500 MHz, $CDCl_3$): δ 3.92 (s, 6H), 7.00 (t, J = 7.0, 2H), 7.04 (d, J = 8.9 Hz, 4H), 7.10 (t, J = 7.6 Hz, 2H), 7.31 (d, J = 8.2 Hz, 2H), 7.48 (d, J = 7.6 Hz, 2H), 7.60 (d, J = 8.5 Hz, 4H). ^{13}C{^{1}H} NMR spectrum was not obtained due to its poor solubility. HRMS (APCI): *m/z* Calcd. for $C_{34}H_{23}O_2S_2$: 527.1134 ([M+H]$^+$). Found. 527.1136.

6,12-Di(thiophen-2-yl)pentaleno[1,2-*b*:4,5-*b′*]dibenzothiophene (4d). This compound was prepared in a similar manner to that described for **4a**. The mixture of **12d** (51.5 mg, 0.100 mmol), $TsOH·H_2O$ (57.1 mg, 0.300 mmol), and MS 4 Å (pre-dried, 500 mg) in anhydrous toluene (4.0 mL) was heated at 110 °C for 1 h. Purification in a similar manner to that described for **4a** gave 15.0 mg of **4d** as red solids (31.3 μmol, 31% yield). R_f = 0.64 (hexane/CH_2Cl_2 1/1). Mp: > 300 °C. ^{1}H NMR (500 MHz, $CDCl_3$): δ 7.03 (t, J = 7.6 Hz, 2H), 7.15 (t, J = 7.6 Hz, 2H), 7.22 (dd, J = 4.9, 4.3 Hz, 2H), 7.50–7.52 (m, 4H), 7.53 (dt, J = 5.2 Hz, 2H), 7.57 (d, J = 8.2 Hz, 2H). ^{13}C{^{1}H} NMR spectrum was not obtained due to its poor solubility. HRMS (APCI): *m/z* Calcd. for $C_{28}H_{15}S_4$: 479.0051 ([M+H]$^+$). Found. 479.0050.

6,12-Bis{[tri(*i*-propyl)silyl]ethynyl}pentaleno[1,2-*b*:4,5-*b′*]dibenzothiophene (4e).
This compound was prepared in a similar manner to that described for **4a**. The mixture of **12e** (35.6 mg, 50.0 μmol), $TsOH·H_2O$ (28.5 mg, 0.150 mmol), and MS 4 Å (pre-dried; 250 mg) in anhydrous toluene (2.0 mL) was added, and the mixture was heated at 110 °C for 1 h. Purification in a similar manner to that described for **4a** gave 18.7 mg of **12e** as red solids (27.6 μmol, 55% yield). R_f = 0.72 (hexane/CH_2Cl_2 2/1). Mp: > 300 °C. ^{1}H NMR (500 MHz, ($CDCl_3$): δ 1.14–1.21 (m, 42H), 7.00 (ddd, J = 8.2, 7.0, 1.2 Hz, 2H), 7.11 (ddd, J = 7.9, 7.5, 1.2 Hz, 2H), 7.44 (dt, J = 8.2, 0.9 Hz, 2H), 7.59 (dt, J = 7.9, 0.9 Hz, 2H). ^{13}C{^{1}H} NMR (125 MHz, $CDCl_3$): 27.2, 40.2, 56.5, 74.4, 117.2, 127.9, 129.8, 130.0, 131.0, 131.4, 132.3, 134.3, 138.0, 146.8, 175.4. HRMS (APCI): *m/z* Calcd. for $C_{42}H_{51}S_2Si_2$: 675.2965 ([M+H]$^+$). Found. 675.2965.

2. Supplementary Data for the Synthetic Investigations

Base and ligand screening for cyclization.

A series of screening experiments was carried out to evaluate the effect of the ligand and base for the Pd-catalyzed intramolecular cyclization of **9**, and the results were summarized in Table S1. Among the ligands evaluated, P(*t*-Bu)$_3$·HBF$_4$ improved the yield, while DBU was identified as the most effective base among those tested.

Table S1. Optimization of Pd-catalyzed Intramolecular Cyclization

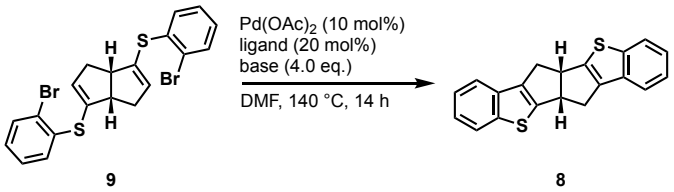

9 **8**

entry	ligand	base	NMR yield [a]
1 [b]	XPhos	Cs_2CO_3	0
2 [b]	MePhos	Cs_2CO_3	0
3 [b]	P(*o*-tol)$_3$	Cs_2CO_3	0
4	P(C_6F_5)$_3$	Cs_2CO_3	0
5	dppf [c]	Cs_2CO_3	0
6	PPh_3	Cs_2CO_3	7
7	PCy_3·HBF_4	Cs_2CO_3	14
8	P(*t*-Bu)$_3$·HBF_4	Cs_2CO_3	19
9	P(*t*-Bu)$_3$·HBF_4	K_2CO_3	trace
10	P(*t*-Bu)$_3$·HBF_4	Na_2CO_3	0
11	P(*t*-Bu)$_3$·HBF_4	NaOAc [d]	0
12	P(*t*-Bu)$_3$·HBF_4	NaOMe [d]	0
13	P(*t*-Bu)$_3$·HBF_4	DBU [d]	96

[a] 1,1,2,2-Tetrachloroethane was used as an internal standard for the estimation of NMR yields. [b] 38 h. [d] 10 mol% of the ligand was used. [d] 8.0 equivalent of the base was used.

Plausible reaction mechanism for the acid-promoted ring-opening reaction. Given the structure of the reactant **12a**, the product **13a**, and the reaction conditions, we hypothesized the following plausible mechanism. One of the hydroxy groups in **12a** is first likely protonated by TsOH, after which it may undergo dehydration to give **Int1**. This intermediate presumably undergoes C–C bond cleavage, accompanied by oxidation of the alcohol to a carbonyl group, thereby generating a stable cyclopentadienyl anion. Subsequent protonation of the cyclopentadienyl anion, followed by deprotonation on the carbonyl oxygen, could lead to the formation of **13a**. Under conditions where TsOH is present in excess, the C–C bond cleavage step may be inhibited, most likely because the hydroxy group in **Int1** is further protonated. This effect may account for the markedly suppressed formation of **13a** observed under strongly acidic conditions.

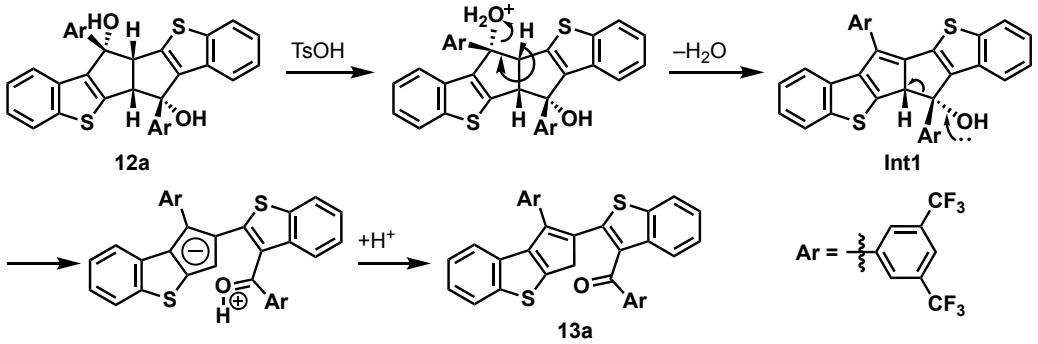

Scheme S1. Plausible reaction mechanism for the acid-promoted ring-opening reaction.

3. X-ray Crystallographic Data

X-ray Crystallographic Analysis of 4e. Red platelet single crystals were grown by slow diffusion of hexane into a solution of **4e** in $CHCl_3$ at an ambient temperature. Intensity data were collected at 100 K on synchrotron radiation (λ = 0.4108 Å) at the BL02B1 beamline in SPring-8 (JASRI). A total of 21271 reflections were measured with the maximum 2θ angle of 30.9°, of which 4476 were independent reflections (R_{int} = 0.0400). The structure was solved by direct methods (SHELXT-2018/2)[S3] and refined by the full-matrix least-squares on F^2 (SHELXL-2018/3).[S4] Two of the three *i*-Pr groups attached to the silicon atom exhibit minor disorder and, therefore, were solved using an appropriate disordered model. Thus, two *i*-Pr groups, (C13, C14, C15) and (C16, C17, C18), were modelled with two-site disorder (PART 1/PART 2), and their occupancies were refined to be 0.847/0.153 for (C13, C14, C15)/(C13A, C14A, C15A), and 0.849/0.151 for (C16, C17, C18)/ (C16A, C17A, C18A). For the minor disorder components, all non-hydrogen atoms were refined isotropically due to insufficient data to obtain reliable anisotropic displacement parameters. Geometric restraints (SIMU, DELU, and ISOR) were applied during the refinements to maintain reasonable geometry and displacement behavior. All non-hydrogen atoms except for the minor disorder components were refined anisotropically, and all hydrogen atoms were placed using AFIX instructions. The crystal data are as follows: Moiety formula = $C_{42}H_{50}S_2Si_2$, Formula weight (FW) = 675.12, crystal size = 0.10 × 0.10 × 0.01 mm^3, triclinic, *P*-1 (#2), a = 8.3908(2) Å, b = 8.8613(2) Å, c = 13.4687(3) Å, α = 97.962(2)°, β = 99.148(2)°, γ = 90.960(2)°, V = 978.40(4) $Å^3$, Z = 4, D_c = 1.146 g cm^{-3}, μ = 0.061 mm^{-1}, R_1 = 0.0394 ($I > 2\sigma(I)$), wR_2 = 0.1114 (all data), GOF = 1.083. Deposition Number 2504966 contains the supplementary crystallographic data for this compound. This data can be obtained free of charge by the joint Cambridge Crystallographic Data Centre and Fachinformationszentrum Karlsruhe Access Structures service.

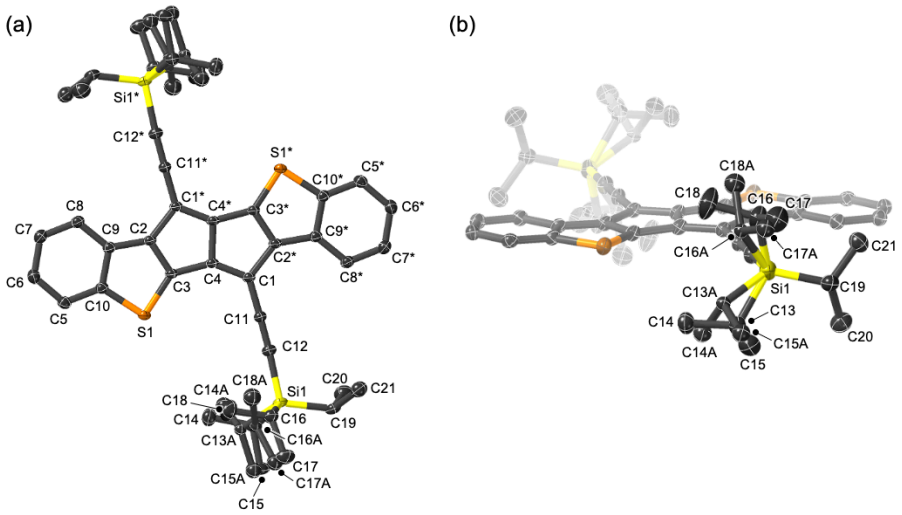

Fig. S1. X-ray crystal structure of **4e** (thermal ellipsoids drawn at 50% probability). Top view (a) and front view (b). Black: carbon, orange: sulfur, yellow: silicon. Hydrogen atoms are omitted for clarity.

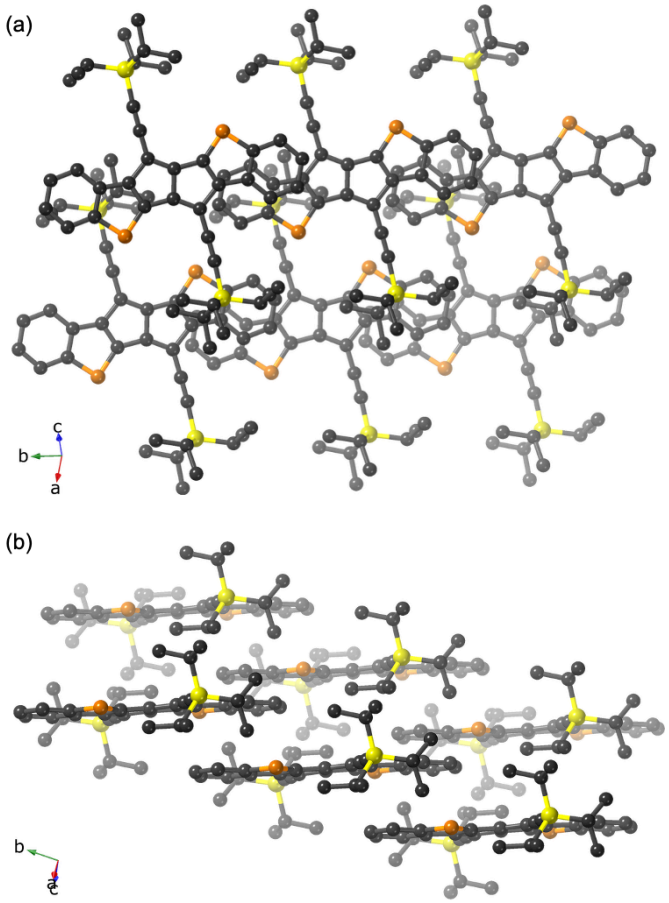

Fig. S2. Crystal packing structure of **4e**. Black: carbon, orange: sulfur, yellow: silicon. Hydrogen atoms are omitted for clarity.

4. Photophysical Properties

Method. UV/Vis/NIR absorption spectra were recorded on a Shimadzu UV-3600i Plus spectrometer using sample solutions prepared in spectrophotometric-grade THF purchased from Nacalai Tesque in a 1 cm-square quartz cuvette. The absorption spectra thus obtained are shown in Fig. 4a.

5. Electrochemical Properties

Methods. Cyclic voltammograms of compounds **4a**–**e** were recorded on an ALS/chi-610E electrochemical analyzer (BAS). The CV cell consisted of a glassy carbon electrode, a Pt wire counter electrode, and an $Ag/AgNO_3$ reference electrode. The measurements were carried out under an argon atmosphere using a 0.5 mM sample solution in THF or CH_2Cl_2 containing 0.10 M tetrabutylammonium hexafluorophosphate ([*n*-Bu_4N][PF_6]) as a supporting electrolyte. The redox potentials were calibrated with a ferrocene/ferrocenium ion couple as an internal standard. The obtained cyclic voltammograms are shown in Fig. 4b, and the data are summarized in Table S2.

The energy levels of the HOMO and the LUMO were estimated by the following equations:

$$\text{HOMO [eV]} = -(E_{\text{onset,ox}} + 4.8)$$
$$\text{LUMO [eV]} = -(E_{\text{onset,red}} + 4.8)$$

Table S2. Electrochemical Data for **4a**–**e**[a]

Cmpd.	$E_{\text{onset,ox}}$ / V[b]	$E_{\text{onset,red}}$ / V[c]	HOMO / eV[d]	LUMO / eV[d]	$\Delta E_{\text{H–L}}$ / eV[e]
4a	+0.41	–0.90	–5.21	–3.90	1.31
4b	+0.17	–1.20	–4.97	–3.60	1.37
4c	+0.08	–1.29	–4.88	–3.51	1.37
4d	+0.14	–1.11	–4.94	–3.69	1.25
4e	+0.26	–0.91	–5.06	–3.89	1.17

[a] Data from cyclic voltammograms (scan rate: 50 mV s^{-1}, supporting electrolyte: [*n*-Bu_4N][PF_6]). [b] In CH_2Cl_2. [c] In THF. [d] Estimated using the values of the onset potentials of the cyclic voltammograms based on the method reported in the literature.[S5] [e] HOMO–LUMO energy gap estimated using the difference between the onset potentials vs. Fc/Fc^+.

6. Theoretical Calculations

Computational Methods. All density functional theory (DFT) calculations in this article were performed with the Gaussian16 Revision B.01 suite of programs[S6] with default thresholds and algorithms. In order to benchmark density functionals, the geometry optimizations for the model compound **4e′**, where the tri(*i*-propyl)silyl groups of **4e** were replaced with trimethylsilyl groups, were carried out with various density functionals (B3LYP, M06, M06-2X, ωB97X-D, and M11) and the 6-31++G(d) basis set, and the resulting C–C bond lengths of the pentalene framework were compared with those determined by the single-crystal X-ray diffraction analysis of **4e** (Fig. S3). Since the C–C bond lengths optimized with the M06-2X density functional showed the best agreement with those of the crystal structure, the geometry optimizations of **2**, **4a**, **4b**, **4c**, **4d,** and **4f** were carried out at the M06-2X/6-31++G(d) level of theory. For all geometry optimizations, the stationary points were optimized without any symmetry assumptions and characterized by frequency analysis at the same level of theory (the number of imaginary frequencies, NIMAG, was 0). The Cartesian coordinates for the optimized geometries are given in Tables S5–15. Orbital energy diagrams and the pictorial representations of the selected Kohn-Sham molecular orbitals of **4a**, **4b**, **4c**, **4d**, and **4e′**are shown in Fig. S4. TD-DFT vertical excitation energy calculations for the optimized geometries of **4a**, **4b**, **4c**, **4d**, and **4e′** were performed using the TD-M06-2X/6-311++G(2d,p) level of theory, and the results are summarized in Table S3.

The nucleus-independent chemical shift (NICS)[S7] values for **2**, **4a**, **4b**, **4c**, **4d**, and **4e′** were calculated at the M06-2X/6-311+G(2d,p) level of theory using the optimized geometries. For NICS(1.7)$_{zz}$ computations, dummy atoms were placed 1.7 Å above the centroid of monocycilc rings.[S8] For 2D-NICS(1.7)$_{zz}$ maps,[S8] a 2D grid of dummy atoms was generated 1.7 Å above the *xy* Cartesian plane with an interval of 0.2 Å. Input file preparation and result analysis for NICS calculations were carried out using the py.Aroma 4 program.[S9] The *xy* planes were set to the mean planes defined by the pentalene frameworks. Anisotropy of the induced current density (ACID) for the optimized geometries of **4a**, **4b**, **4c**, **4d**, and **4e′** was calculated at the M06-2X/6-31G(d) level of theory using the ACID method[S10] implemented in Gaussian 16 Revision B.01 suite of programs (NMR=CSGT IOp(10/93=2)). The magnetic field in the ACID calculations was chosen to be parallel to the *z*-axis. Only the π-electron contribution was used. The graphics were generated using POV-Ray and are shown in Fig. 5b.

To estimate the electron occupancies for $2p_z$ orbitals of the carbon atoms in the pentalene framework, natural atomic orbital analyses were carried out for the optimized geometry of **4f** at the M06-2X/6-31++G(d) level of theory with the NBO 7.0 program via Gaussian 16 using the NAOMO keyword.[S11] The results were summarized in Table S4 and Fig. 5c.

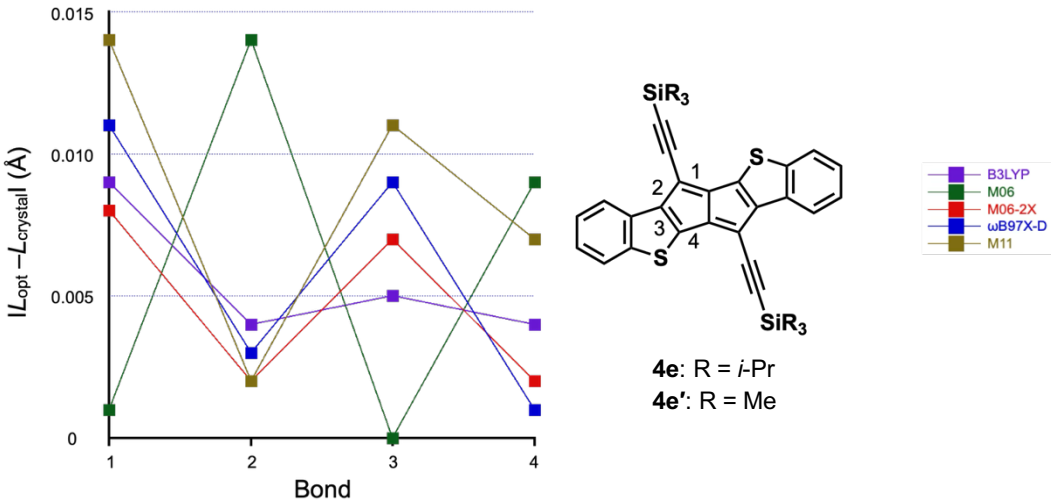

Fig. S3. Assessment of density functionals for the geometry optimization of benzothiophene-fused pentalenes **4**. Differences between the C–C bond lengths of the pentalene framework in the optimized geometries of **4e′** with various density functionals and those in the crystal structure of **4e**.

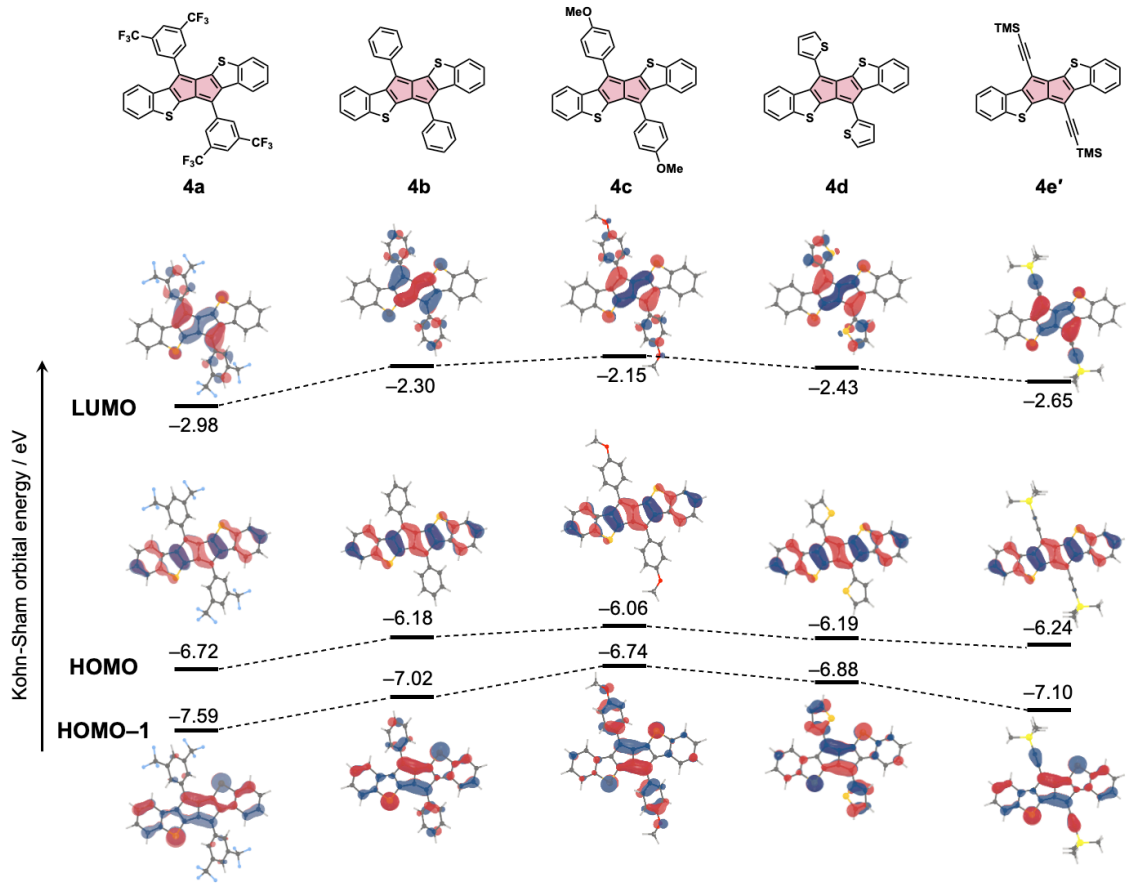

Fig. S4. Orbital energy diagrams and the pictorial representations of the selected Kohn-Sham molecular orbitals (isovalue = 0.03) for the optimized geometries of **4a**, **4b**, **4c**, **4d**, and **4e′** calculated at the M06-2X/6-311++G(2d,p) level of theory.

Table S3. Selected Excitation Energies, Main CI Coefficients, and Oscillator Strengths for a Series of Benzothiophene-fused Pentalenes[a]

Cmpd	Excitation	Transition energy / eV (Wavelength / nm)	Oscillator strength *f*	Transitions (c^2 values)[b]
4a	$S_0 \rightarrow S_1$	1.37 eV (908 nm)	0.0000	HOMO→LUMO (0.4864)
	$S_0 \rightarrow S_2$	2.73 eV (453 nm)	0.1948	HOMO–1→LUMO (0.4732)
				HOMO–4→LUMO (0.0119)
4b	$S_0 \rightarrow S_1$	1.47 eV (843 nm)	0.0000	HOMO→LUMO (0.4883)
	$S_0 \rightarrow S_2$	2.82 eV (439 nm)	0.2491	HOMO–1→LUMO (0.4759)
4c	$S_0 \rightarrow S_1$	1.50 eV (829 nm)	0.0000	HOMO→LUMO (0.4888)
	$S_0 \rightarrow S_2$	2.76 eV (450 nm)	0.3575	HOMO–1→LUMO (0.4761)
4d	$S_0 \rightarrow S_1$	1.41 eV (880 nm)	0.0000	HOMO→LUMO (0.4886)
	$S_0 \rightarrow S_2$	2.64 eV (469 nm)	0.2947	HOMO–1→LUMO (0.4778)
4e′	$S_0 \rightarrow S_1$	1.26 eV (985 nm)	0.0000	HOMO→LUMO (0.4922)
	$S_0 \rightarrow S_2$	2.65 eV (468 nm)	0.2472	HOMO–1→LUMO (0.4730)

[a] Calculated at the TD-M06-2X/6-311++G(2d,p) level of theory. [b] Configuration-interaction (CI) contributions were evaluated from the TD-DFT CI coefficients. For each excited state, the squared CI coefficients (c^2) of transitions with $|c| > 0.1$ are listed. Note that c^2 values are not normalized to 100% and therefore do not represent exact percentage contributions.

Table S4. Selected Natural Atomic Orbital Occupancies Pentalene Carbons of **4f**[a]

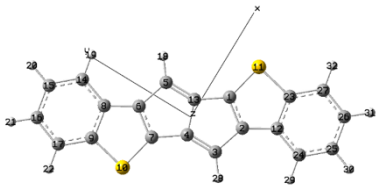

NAO	Atom, No	lang	Type(AO)	Occupancy	Energy
11	C1	p_z	Val(2p)	1.08229	–0.15439
30	C2	p_z	Val(2p)	1.07871	–0.12136
48	C3	p_z	Val(2p)	0.92026	–0.12593
67	C4	p_z	Val(2p)	1.06170	–0.12232
85	C5	p_z	Val(2p)	0.92026	–0.12593
104	C6	p_z	Val(2p)	1.07871	–0.12136
122	C7	p_z	Val(2p)	1.08229	–0.15439
241	C13	p_z	Val(2p)	1.06170	–0.12232

[a] Calculated at the M06-2X/6-31++G(d) level of theory.

7. Appendix

7.1 NMR Spectra of New Compounds

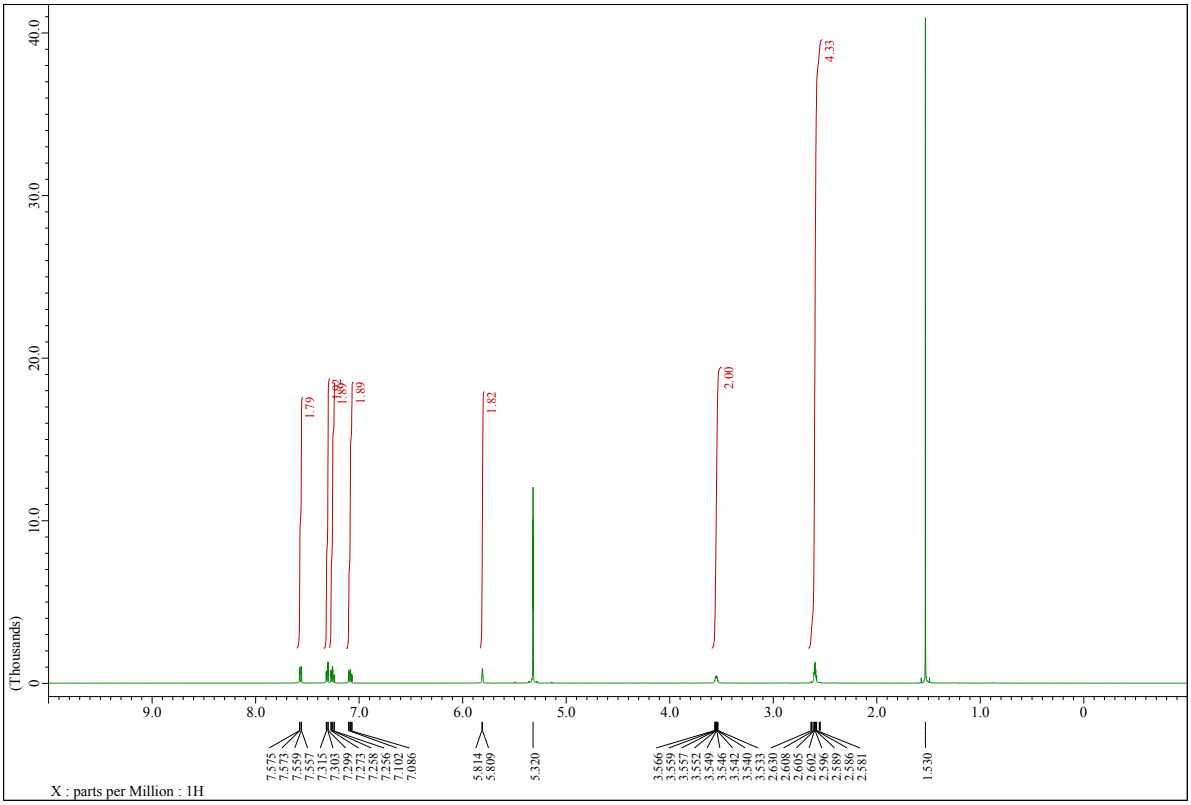

Fig. S5. ^{1}H NMR spectrum of **9** (500 MHz, CD_2Cl_2).

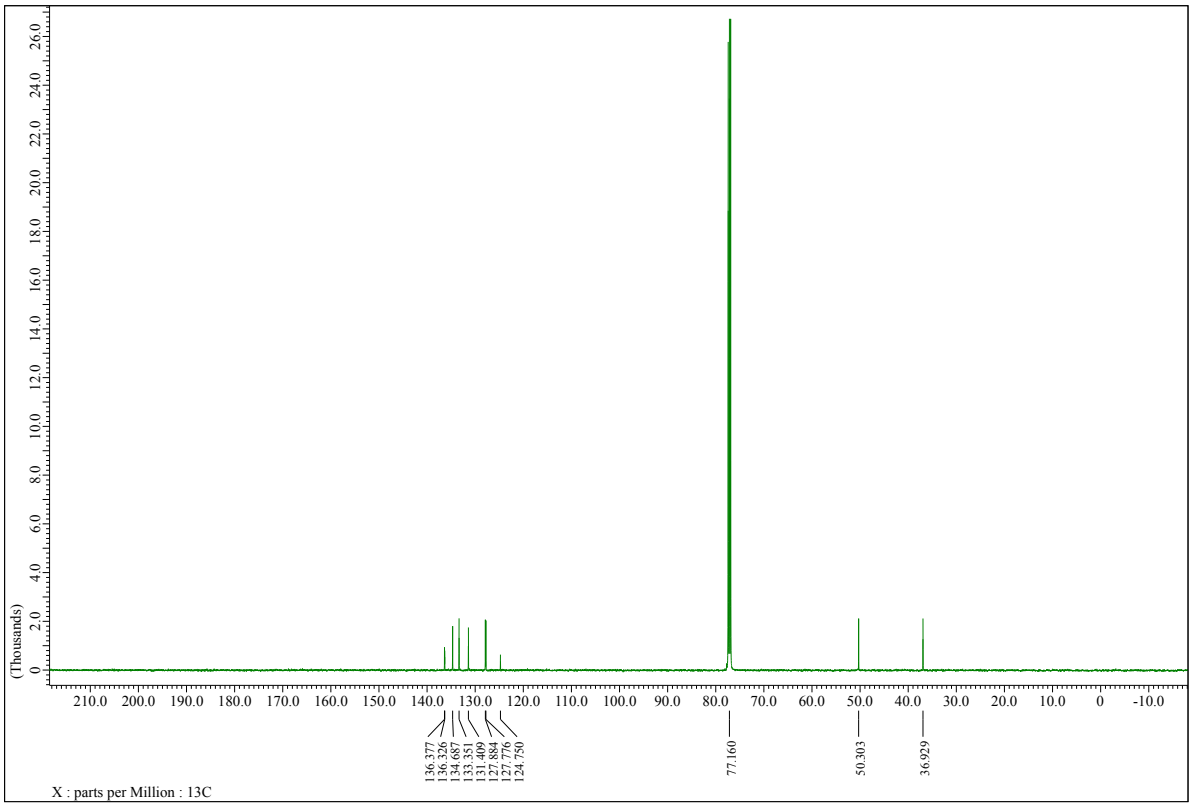

Fig. S6. $^{13}C\{^{1}H\}$ NMR spectrum of **9** (126 MHz, $CDCl_3$).

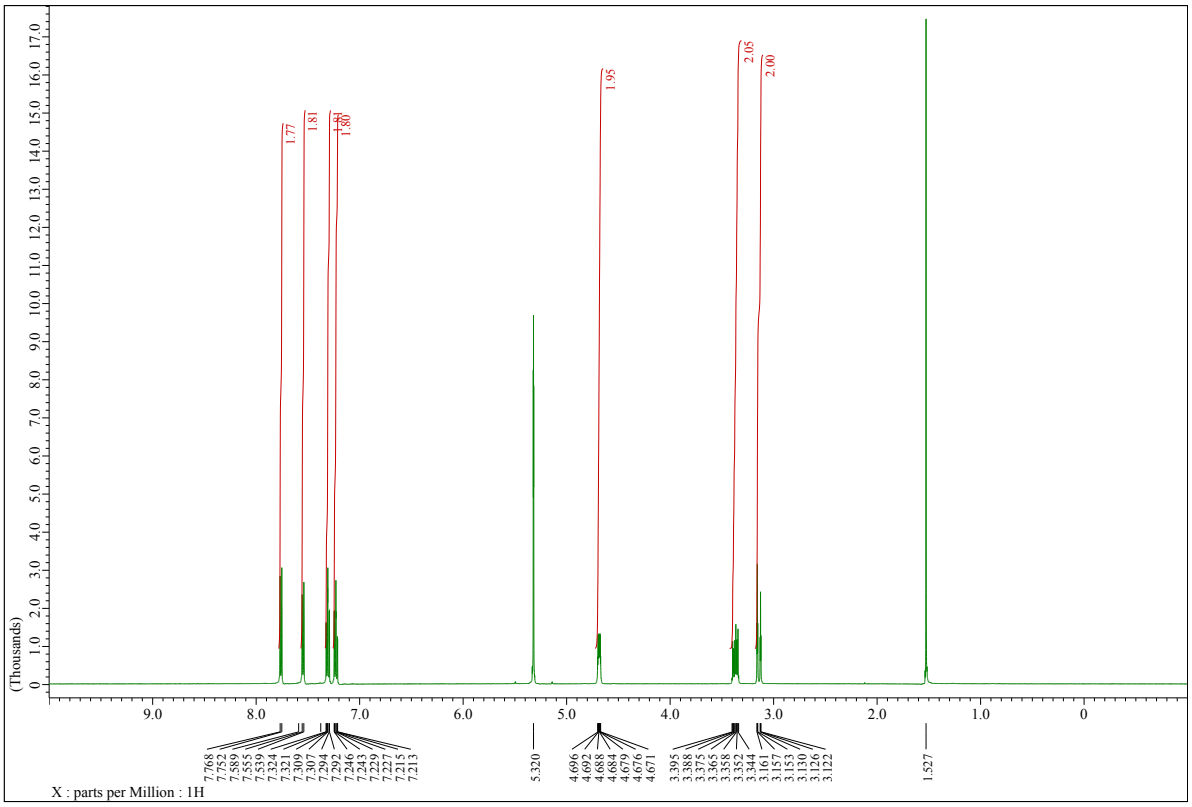

Fig. S7. ^{1}H NMR spectrum of **8** (500 MHz, CD_2Cl_2).

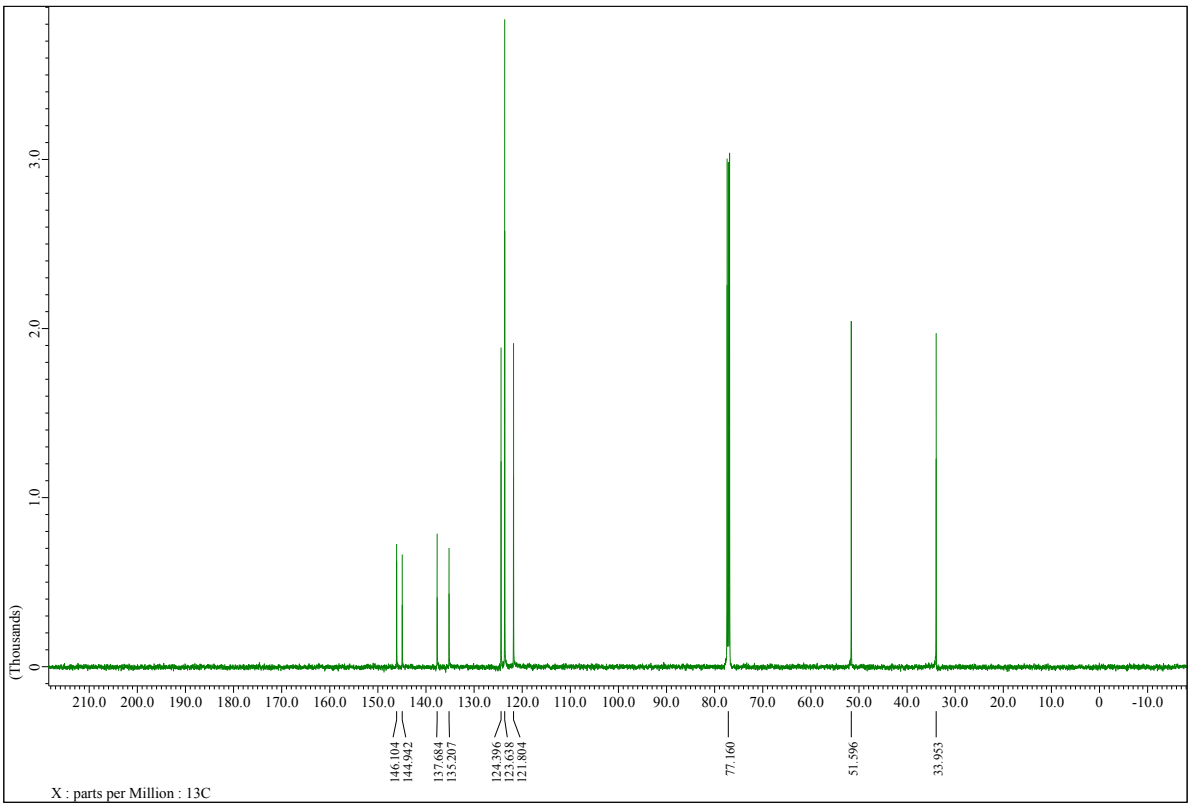

Fig. S8. ^{13}C{^{1}H} NMR spectrum of **8** (126 MHz, $CDCl_3$).

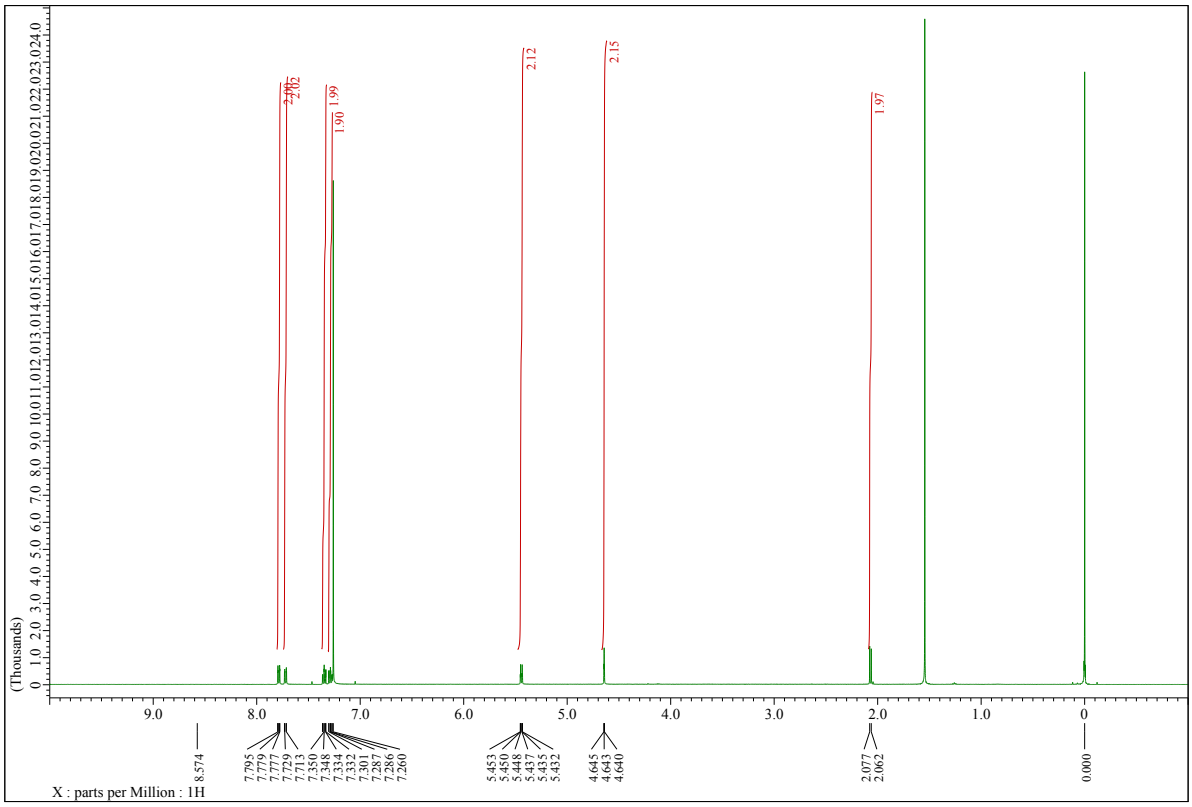

Fig. S9. ^{1}H NMR spectrum of **11** (500 MHz, $CDCl_3$ containing TMS).

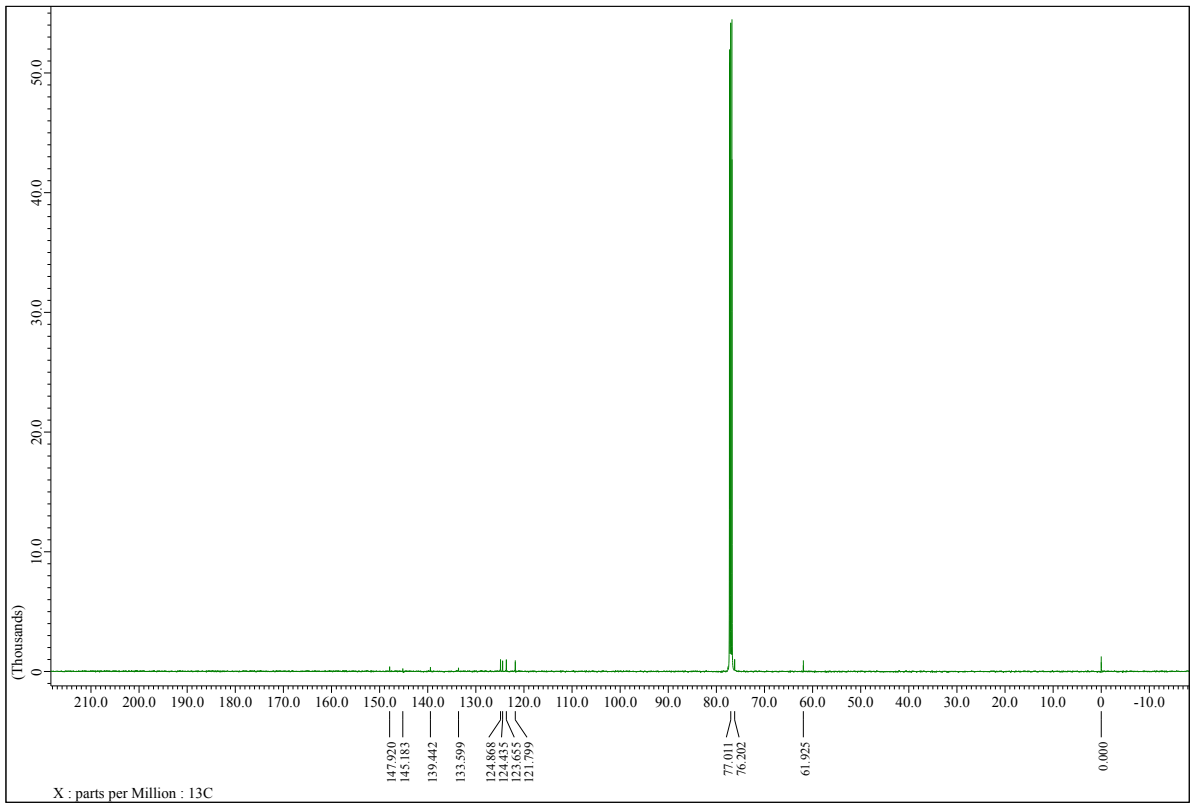

Fig. S10. $^{13}C\{^{1}H\}$ NMR spectrum of **11** (126 MHz, $CDCl_3$ containing TMS).

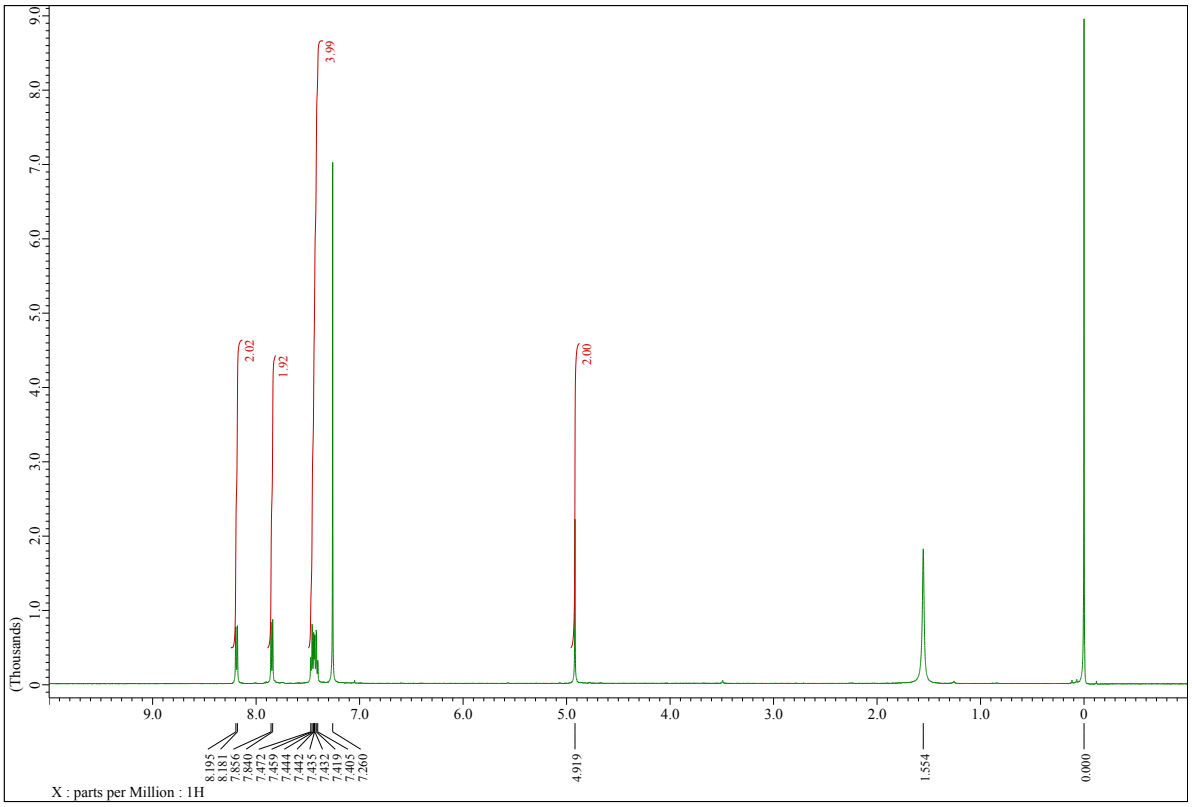

Fig. S11. ^{1}H NMR spectrum of **6** (500 MHz, $CDCl_3$ containing TMS).

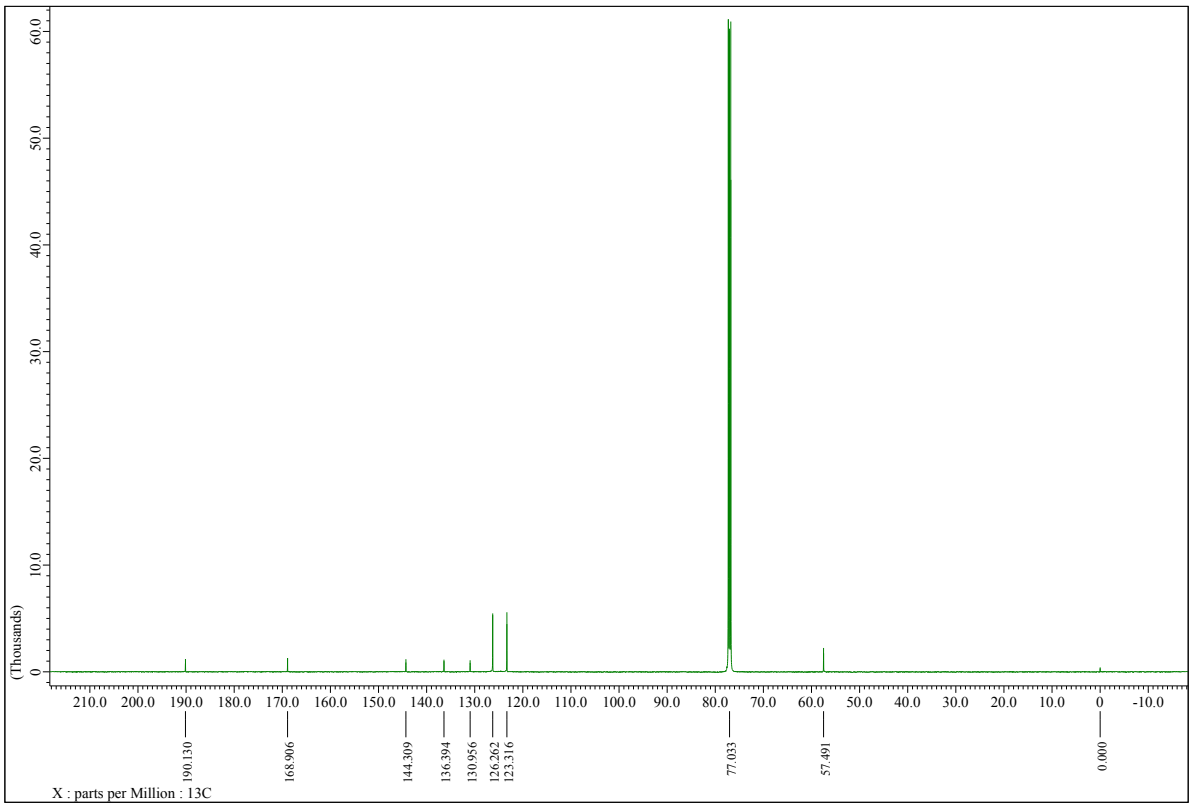

Fig. S12. $^{13}C\{^{1}H\}$ NMR spectrum of **6** (126 MHz, $CDCl_3$ containing TMS).

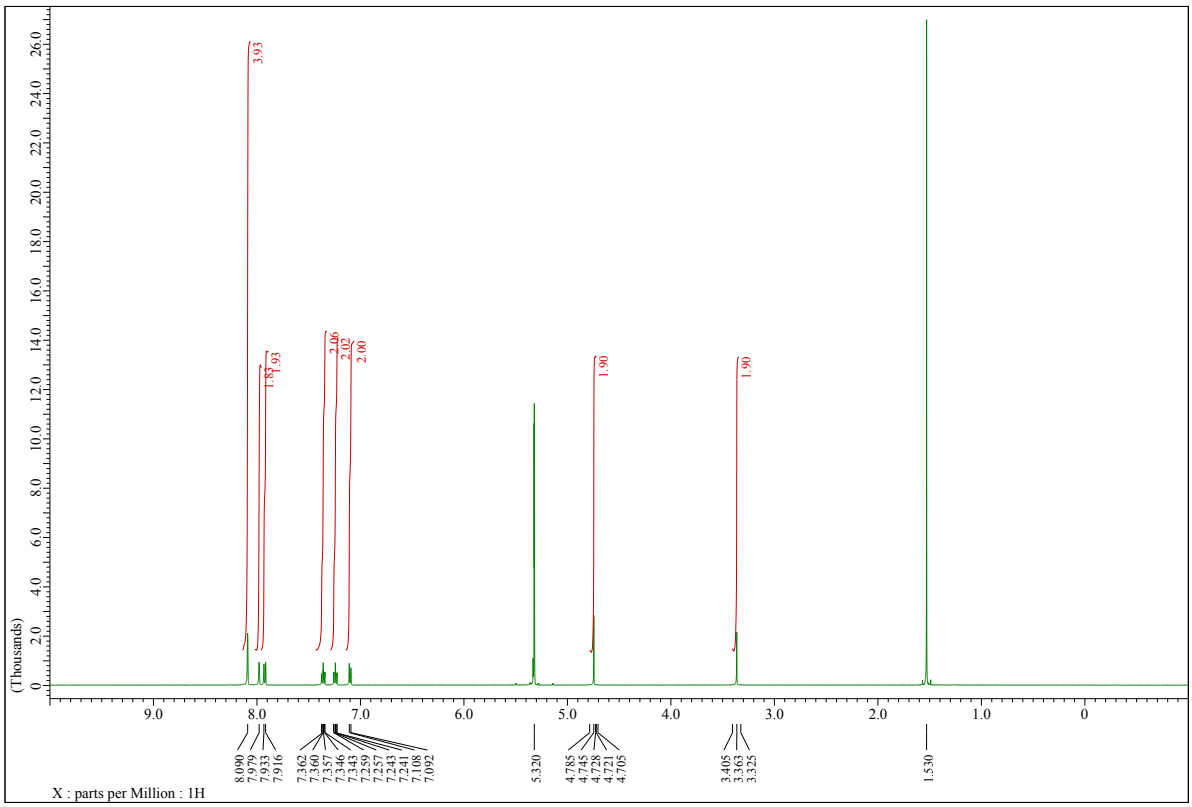

Fig. S13. ^{1}H NMR spectrum of **12a** (500 MHz, CD_2Cl_2).

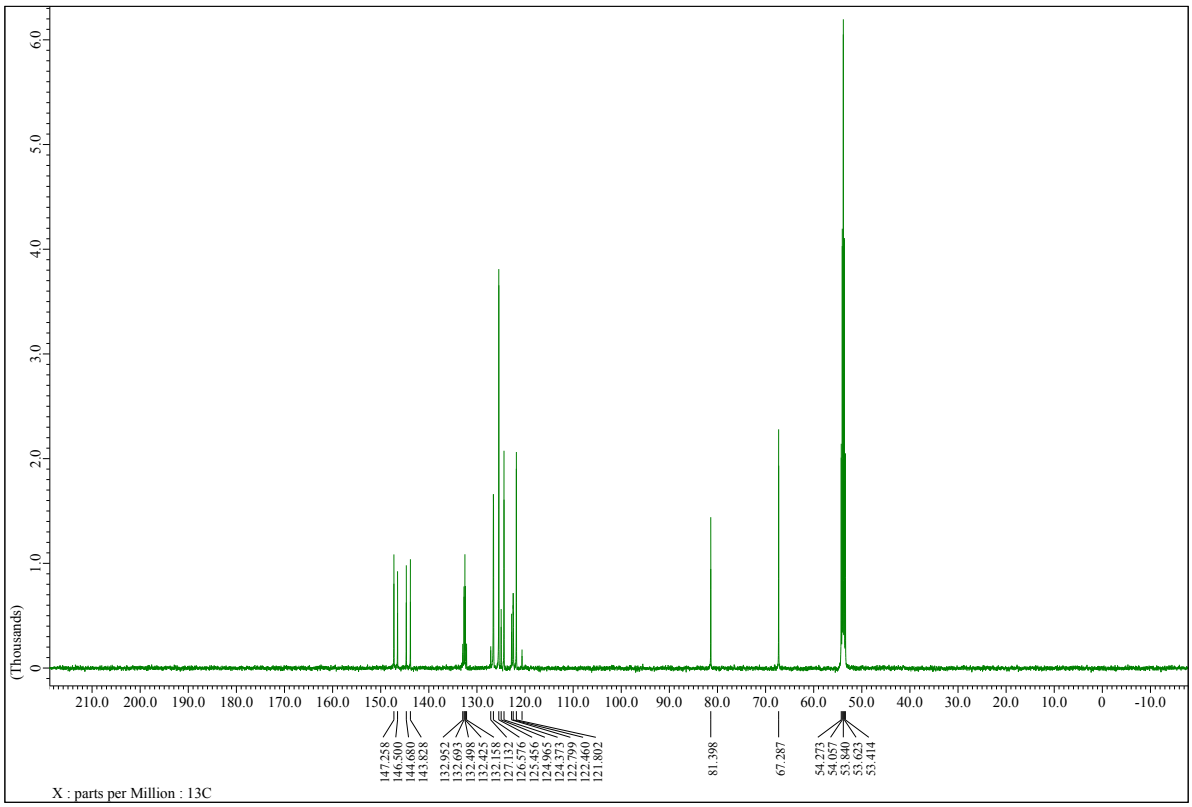

Fig. S14. $^{13}C\{^{1}H\}$ NMR spectrum of **12a** (126 MHz, CD_2Cl_2).

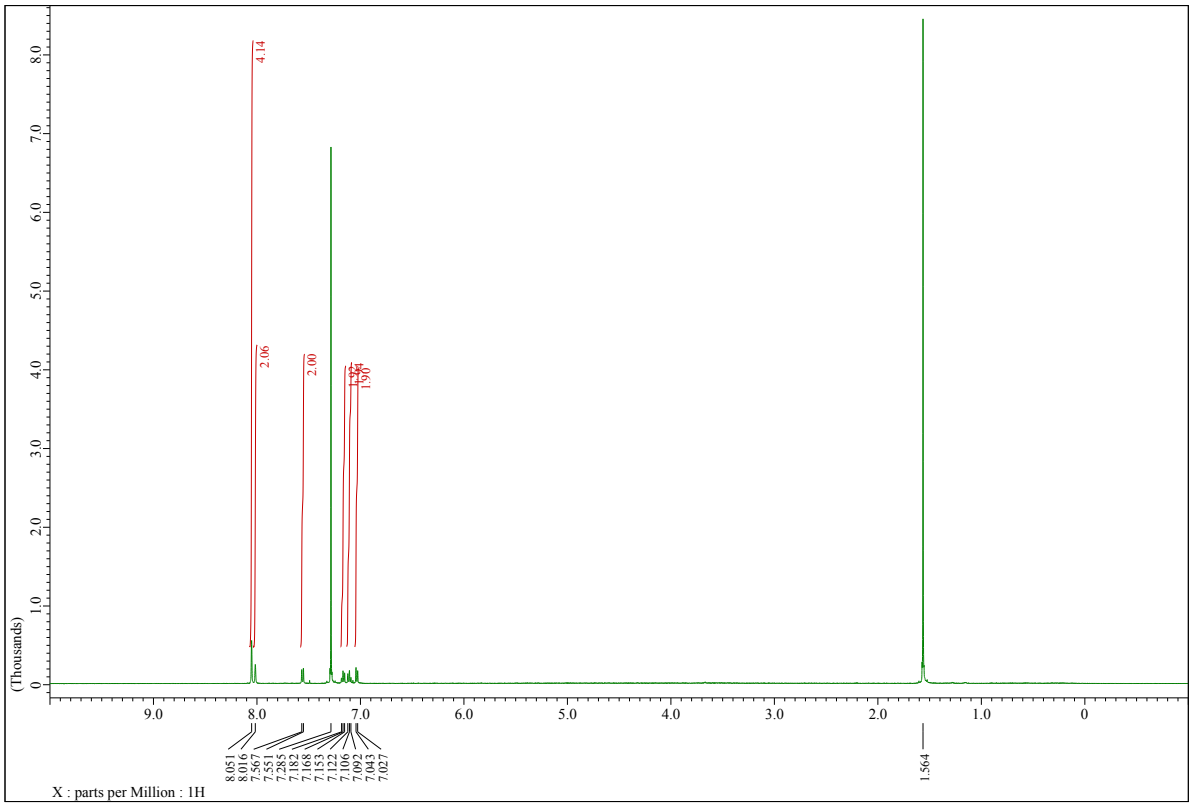

Fig. S15. ^{1}H NMR spectrum of **4a** (500 MHz, $CDCl_3$).

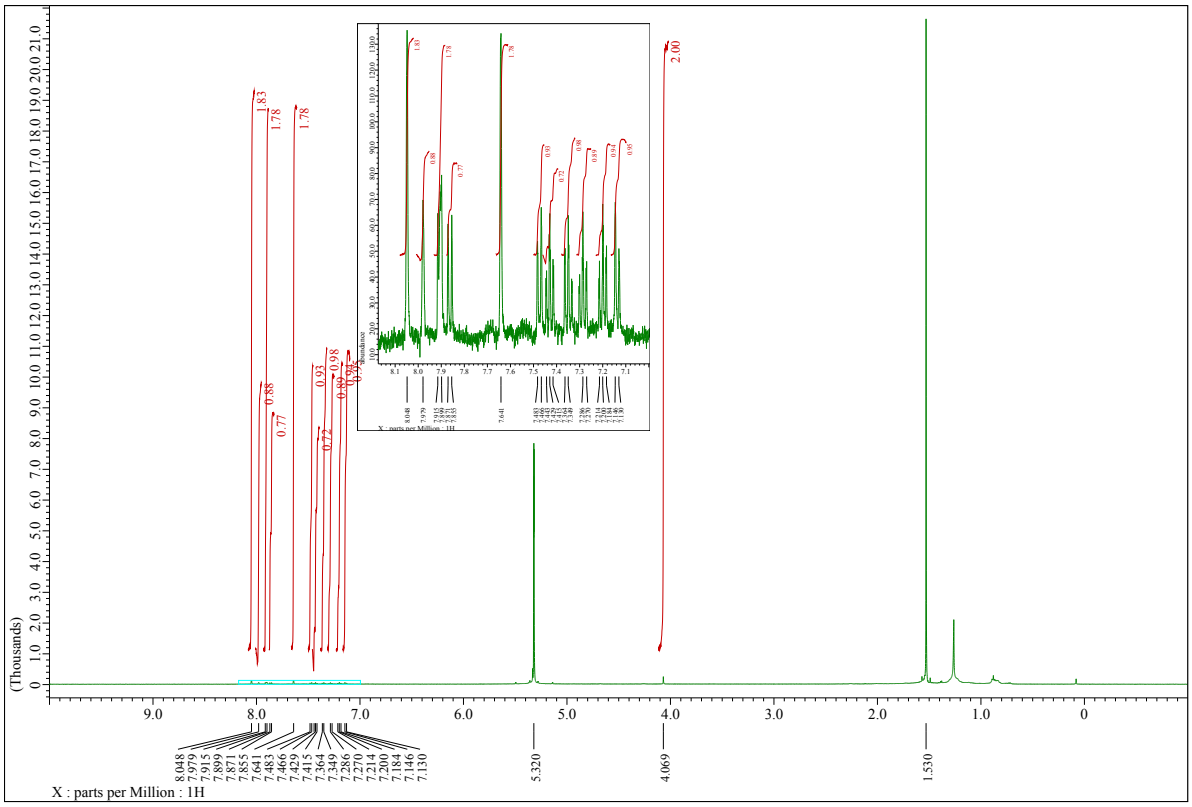

Fig. S16. ^{1}H NMR spectrum of **13a** (500 MHz, CD_2Cl_2).

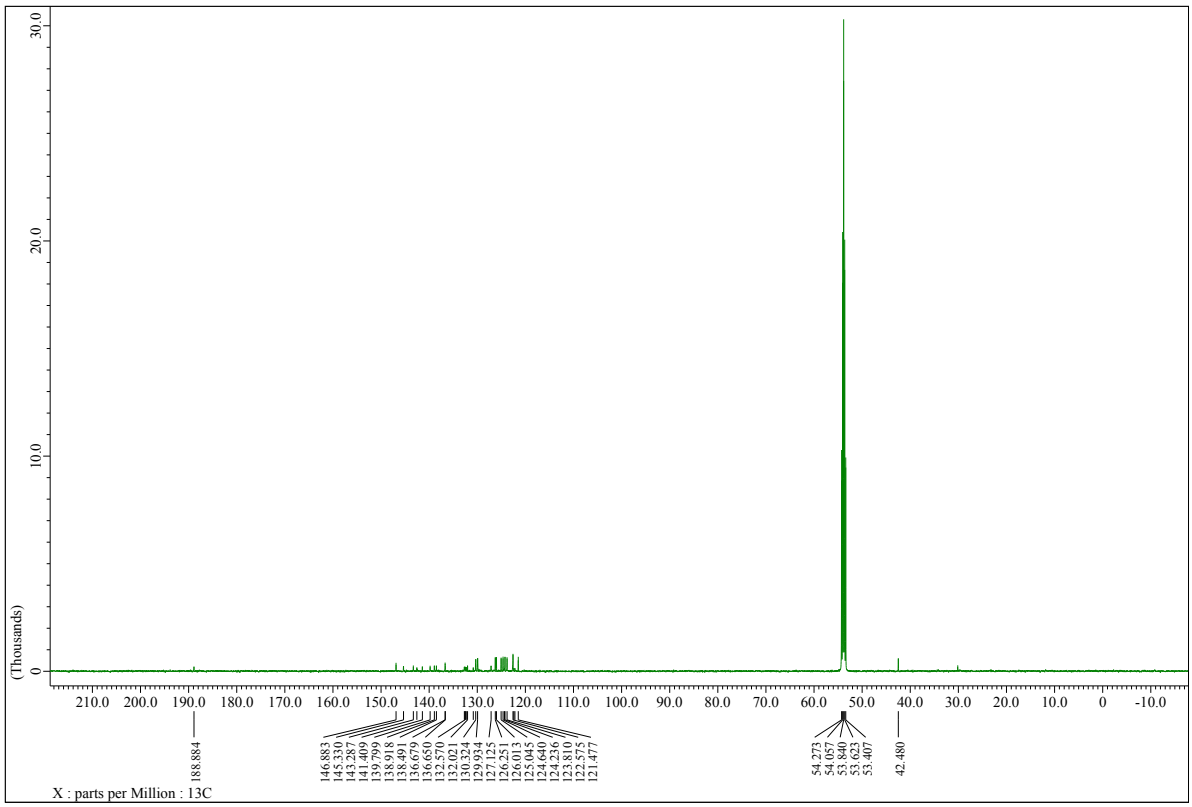

Fig. S17. ^{13}C{^{1}H} NMR spectrum of **13a** (126 MHz, CD_2Cl_2).

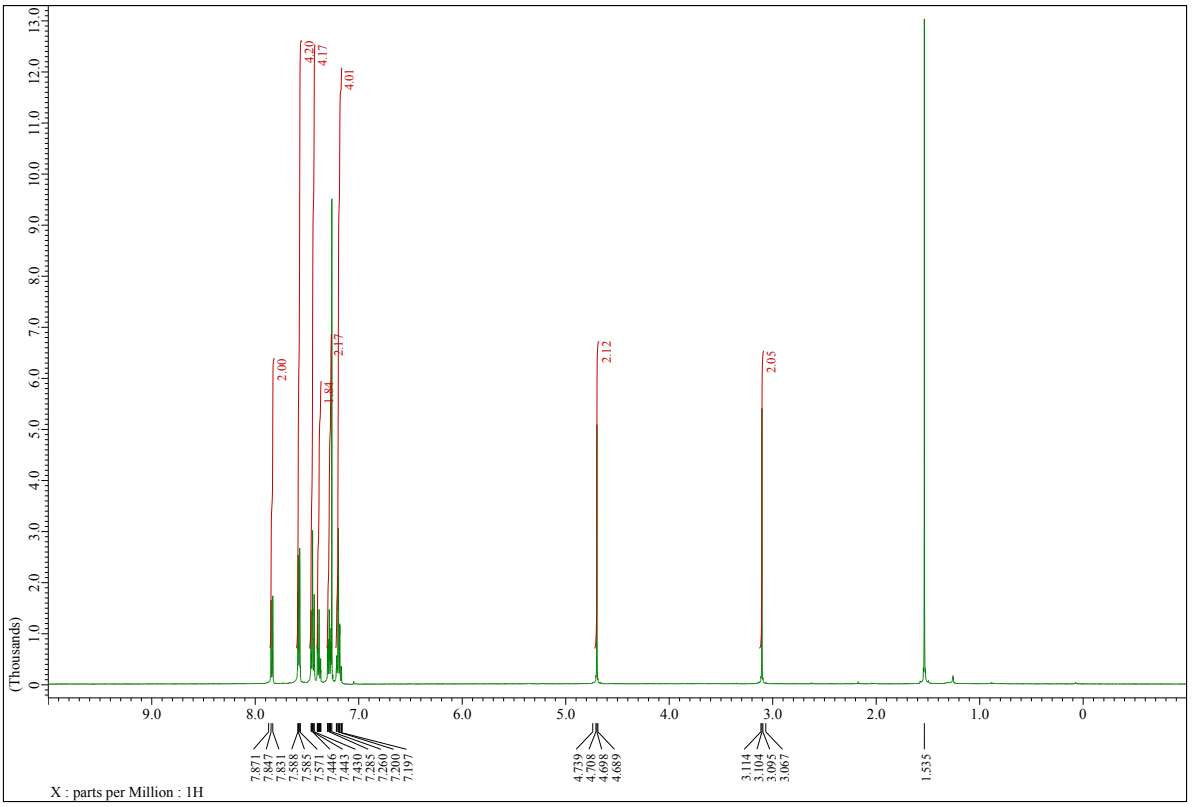

Fig. S18. ^{1}H NMR spectrum of **12b** (500 MHz, $CDCl_3$).

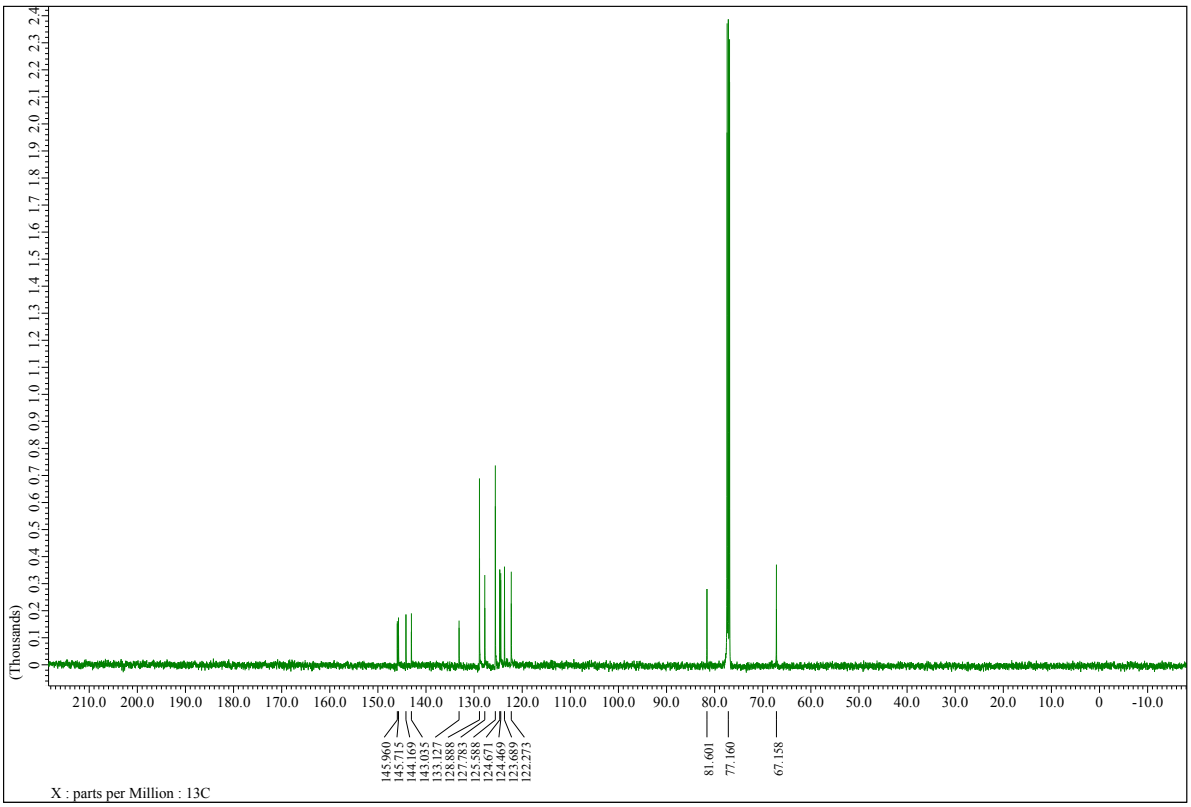

Fig. S19. ^{13}C{^{1}H} NMR spectrum of **12b** (126 MHz, $CDCl_3$).

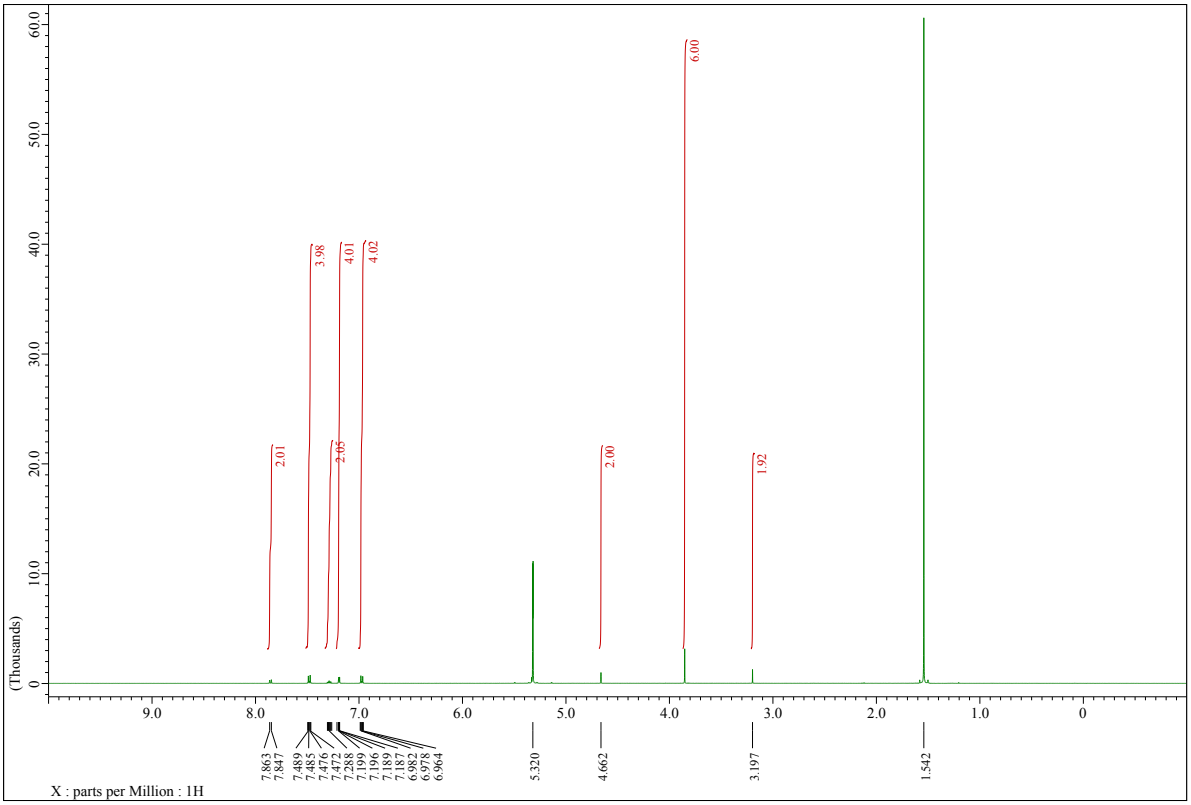

Fig. S20. ^{1}H NMR spectrum of **12c** (500 MHz, CD_2Cl_2).

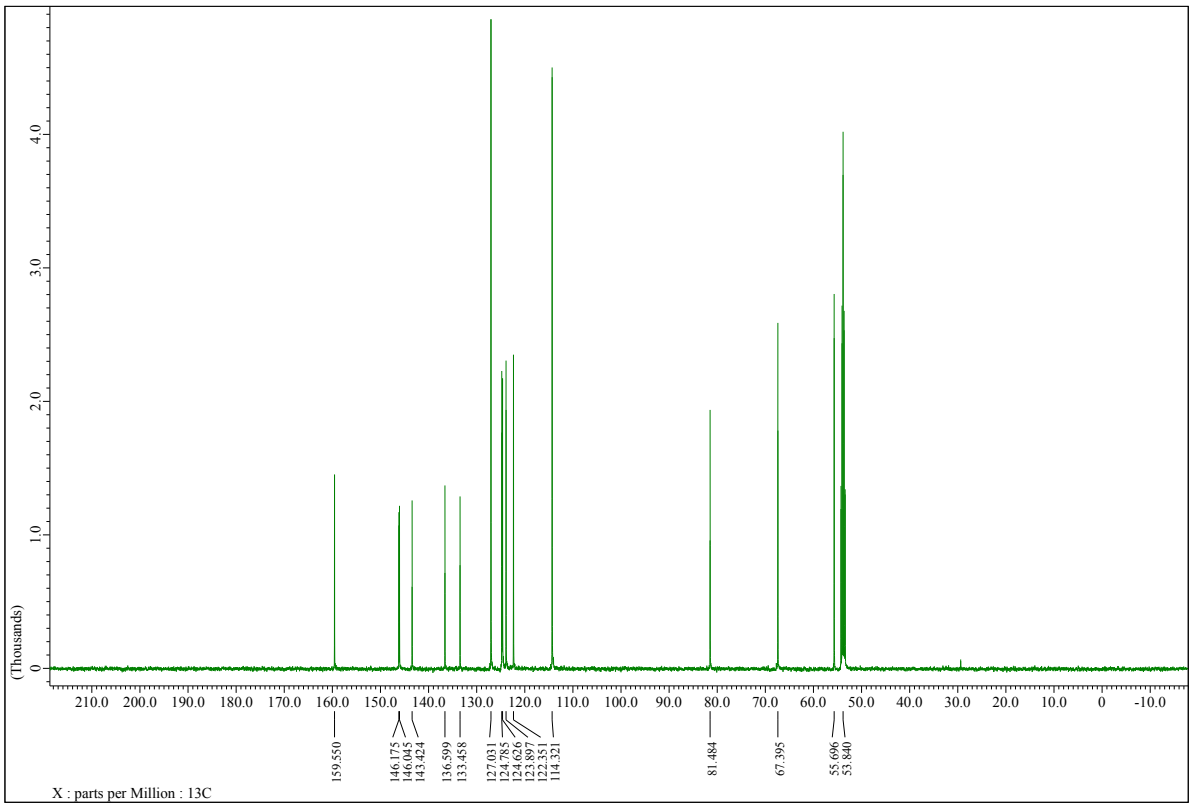

Fig. S21. ^{13}C{^{1}H} NMR spectrum of **12c** (126 MHz, CD_2Cl_2).

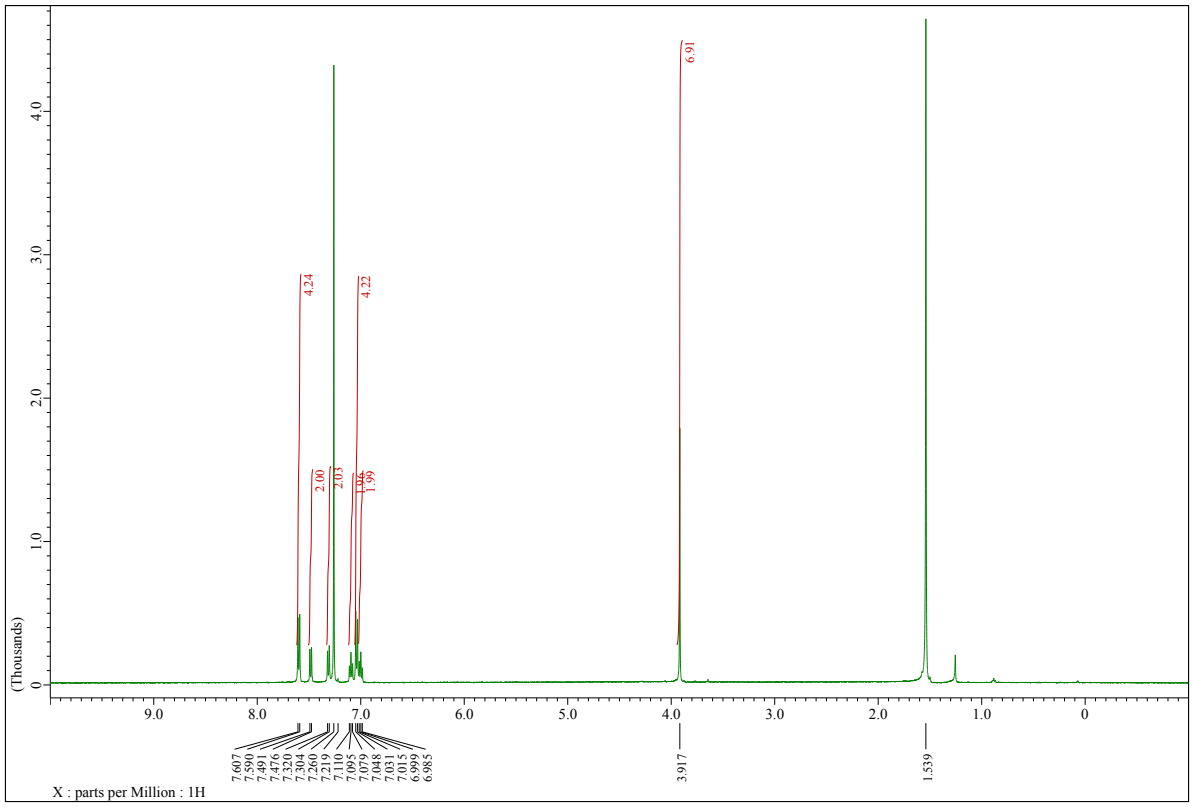

Fig. S22. ^{1}H NMR spectrum of **4c** (500 MHz, $CDCl_3$).

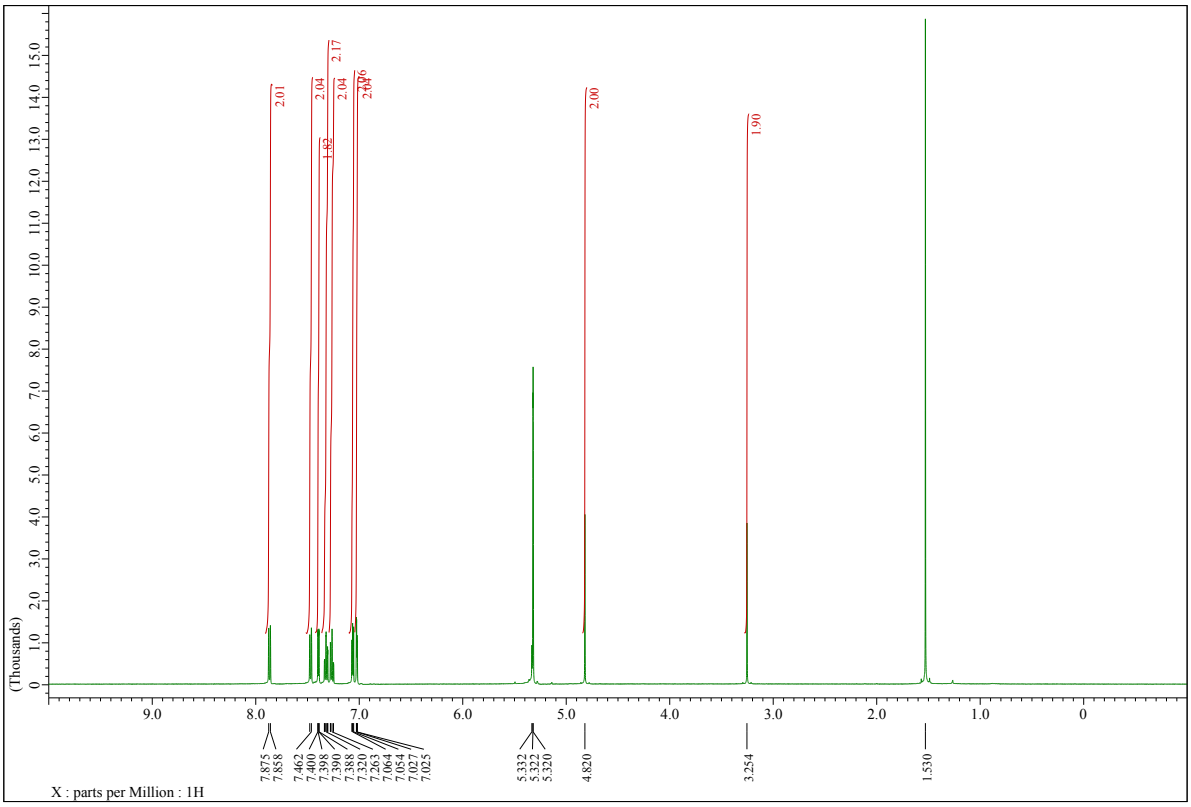

Fig. S23. ^{1}H NMR spectrum of **12d** (500 MHz, CD_2Cl_2).

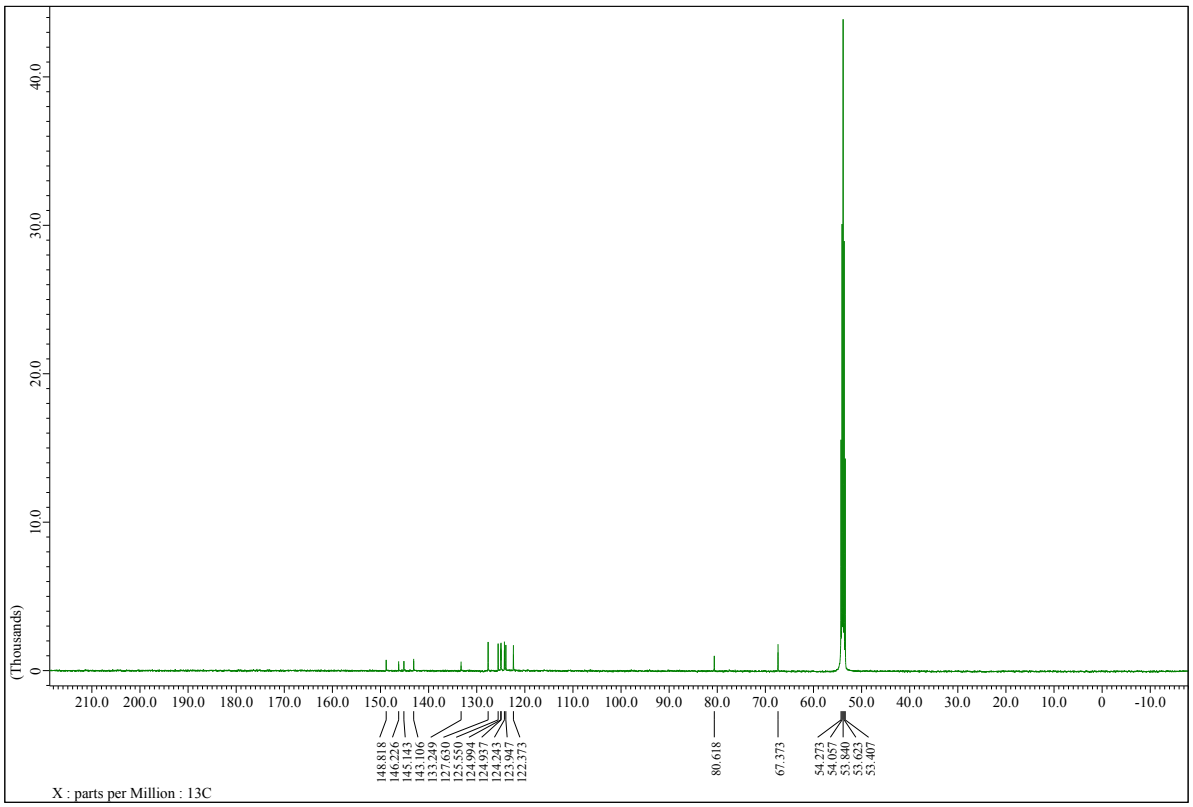

Fig. S24. $^{13}C\{^{1}H\}$ NMR spectrum of **12d** (126 MHz, CD_2Cl_2).

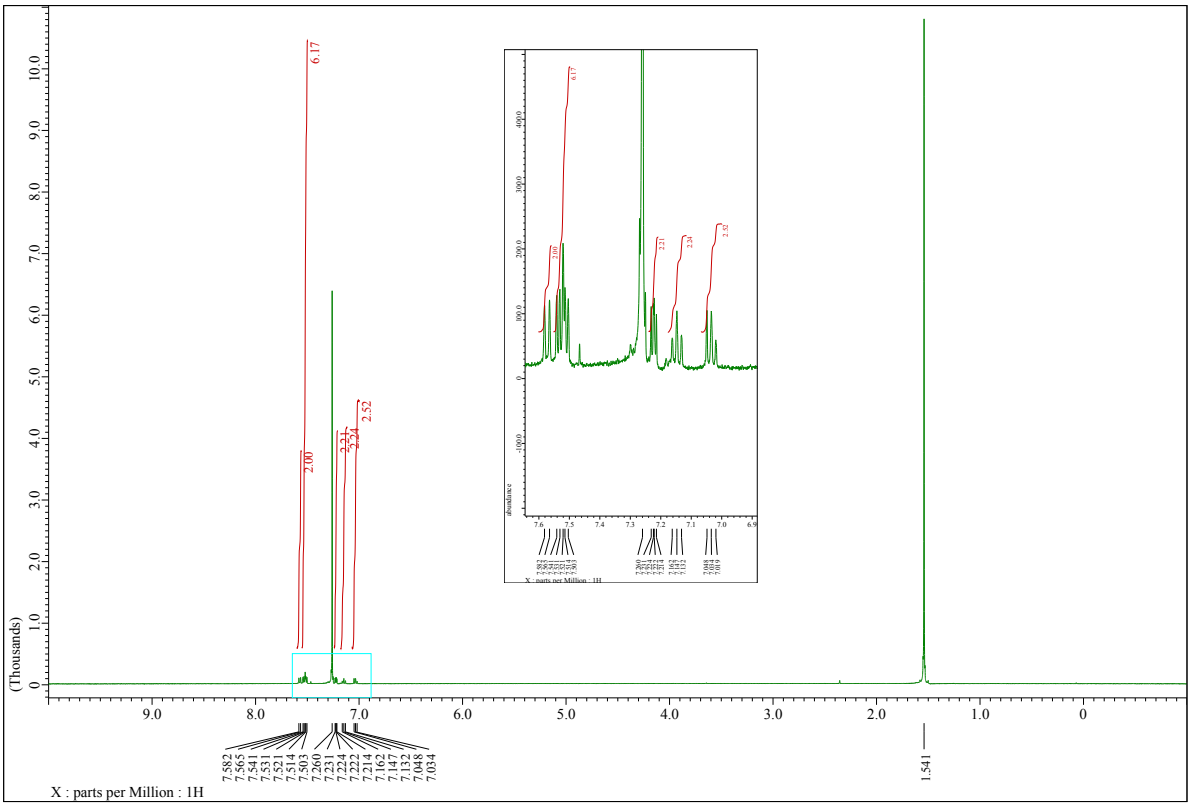

Fig. S25. ^{1}H NMR spectrum of **4d** (500 MHz, $CDCl_3$).

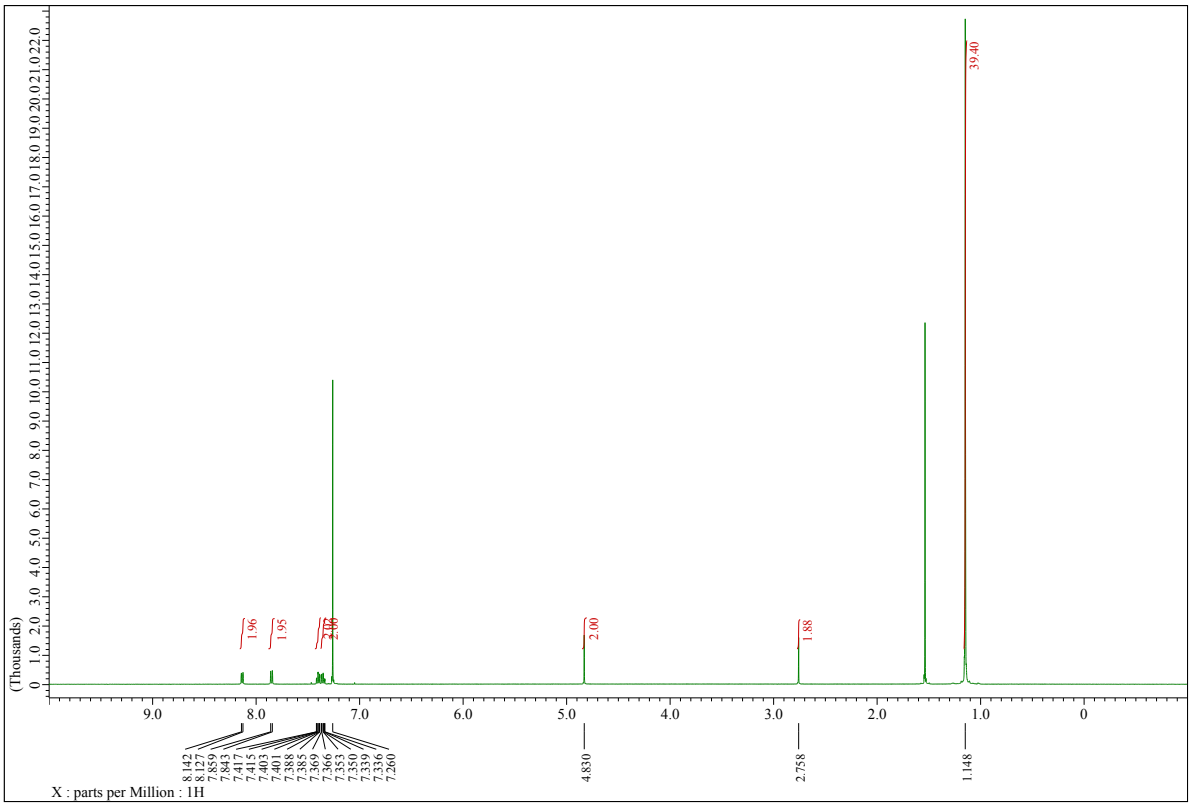

Fig. S26. ^{1}H NMR spectrum of **12e** (500 MHz, $CDCl_3$).

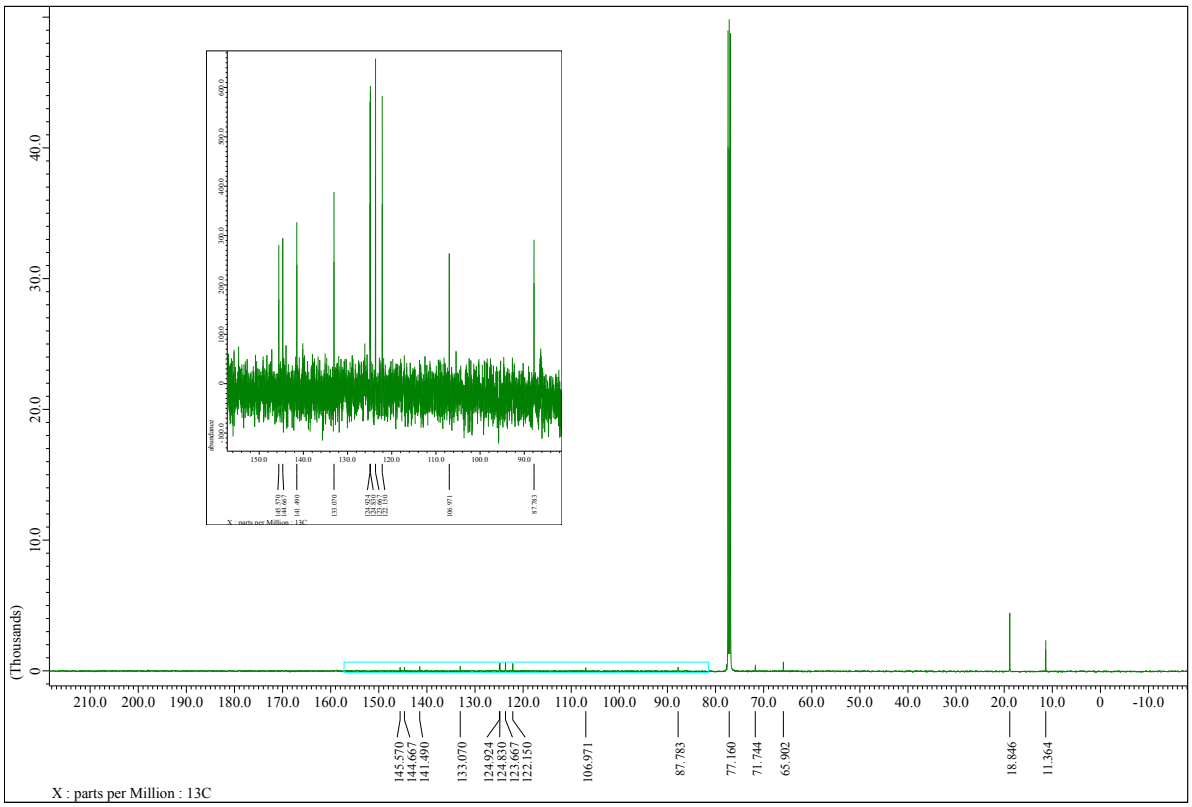

Fig. S27. $^{13}C\{^{1}H\}$ NMR spectrum of **12e** (126 MHz, $CDCl_3$).

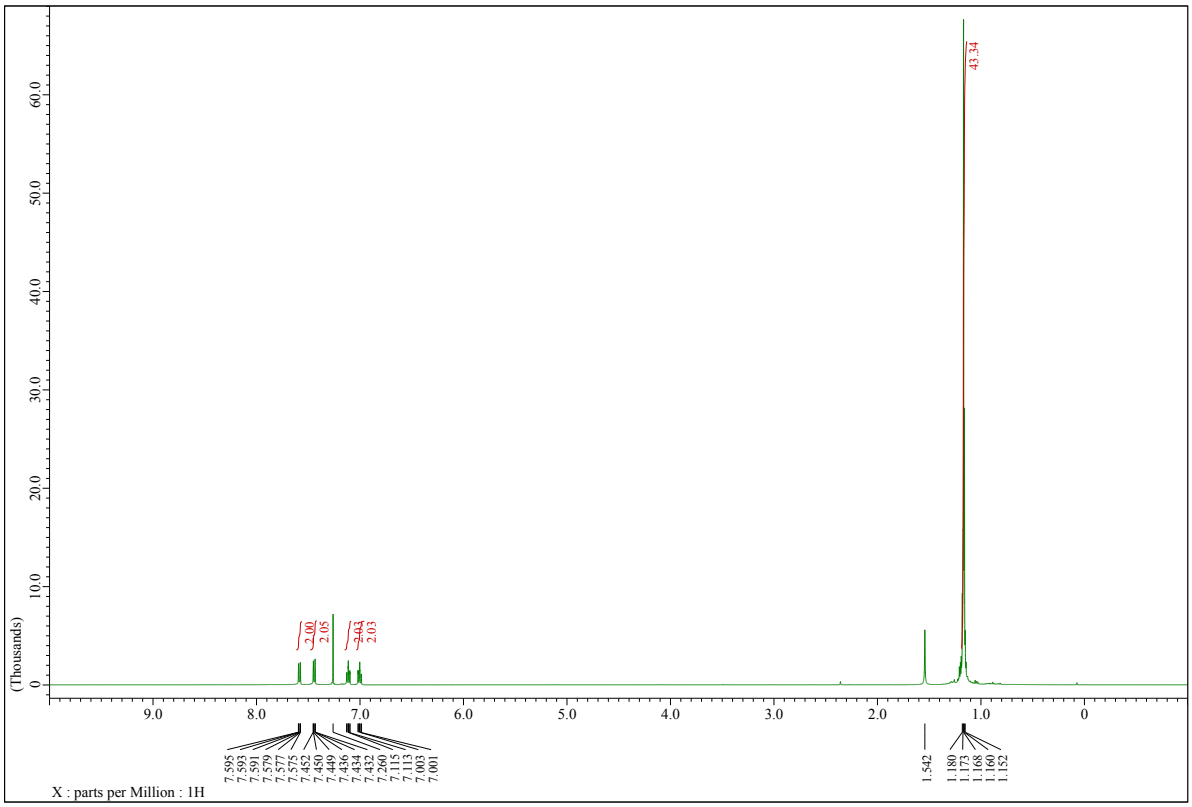

Fig. S28. ^{1}H NMR spectrum of **4e** (500 MHz, $CDCl_3$).

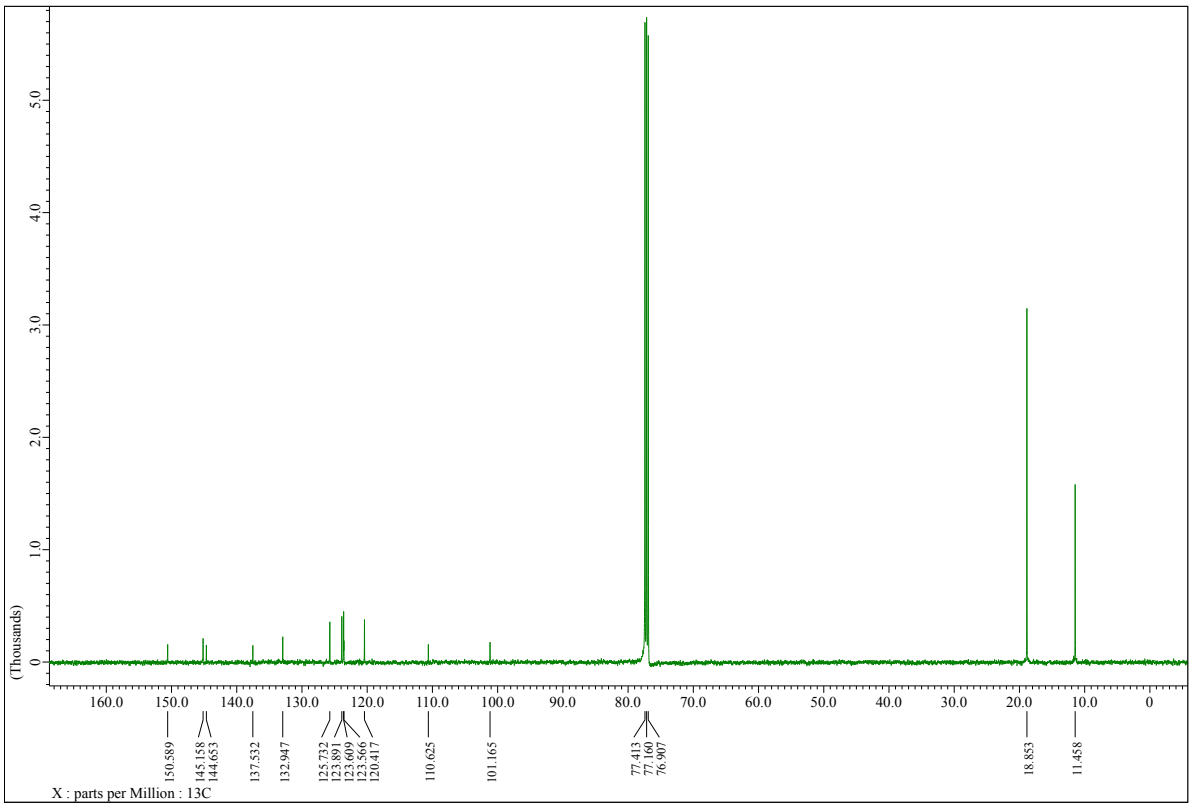

Fig. S29. ^{13}C{^{1}H} NMR spectrum of **4e** (126 MHz, $CDCl_3$).

7.2 High-Resolution Mass Spectra of New Compounds

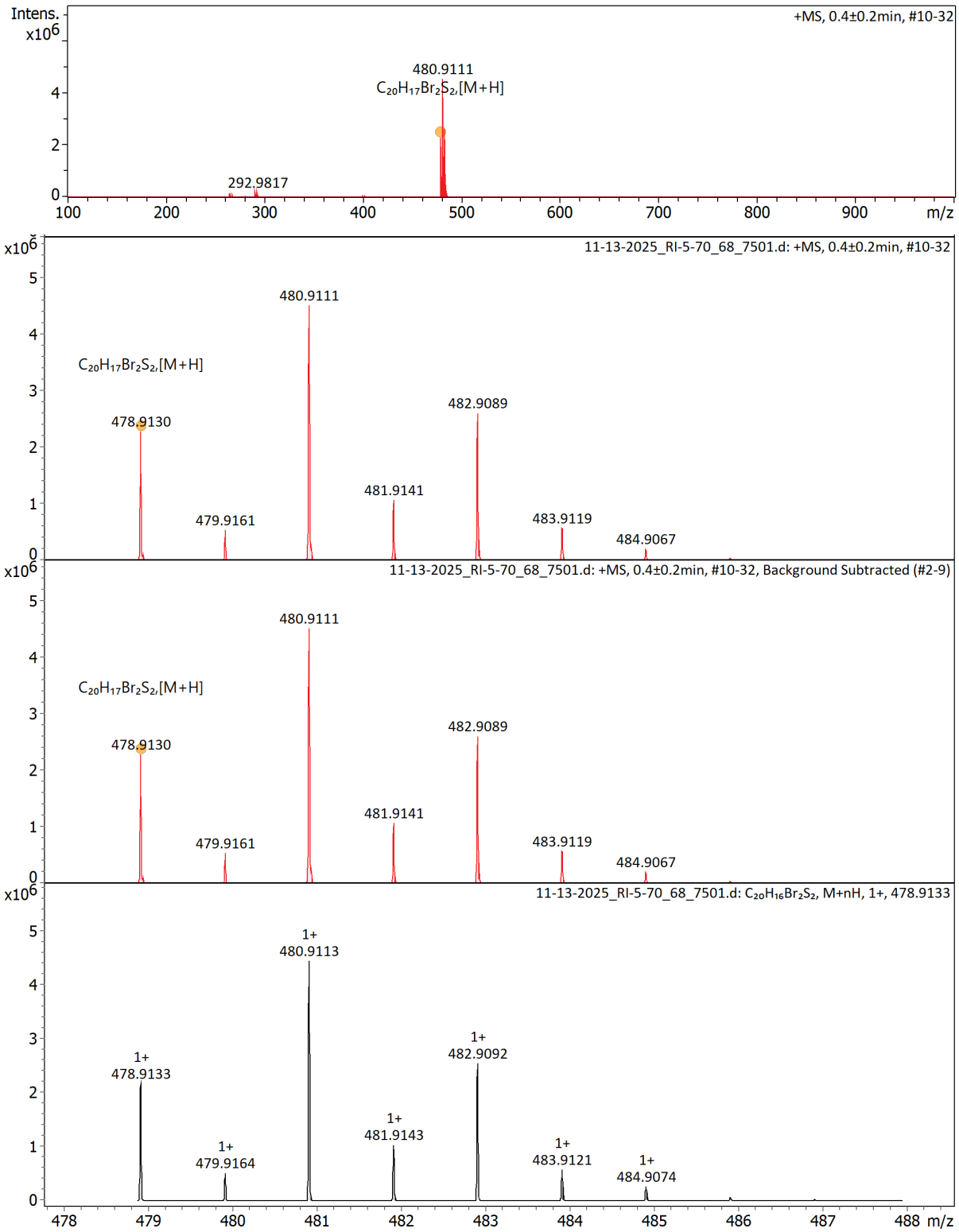

Fig S30. High-resolution mass spectrum of **9** (APCI). Top: full experimental spectrum; middle: enlarged view of the $[M+H]^+$ signals; bottom: simulated spectrum.

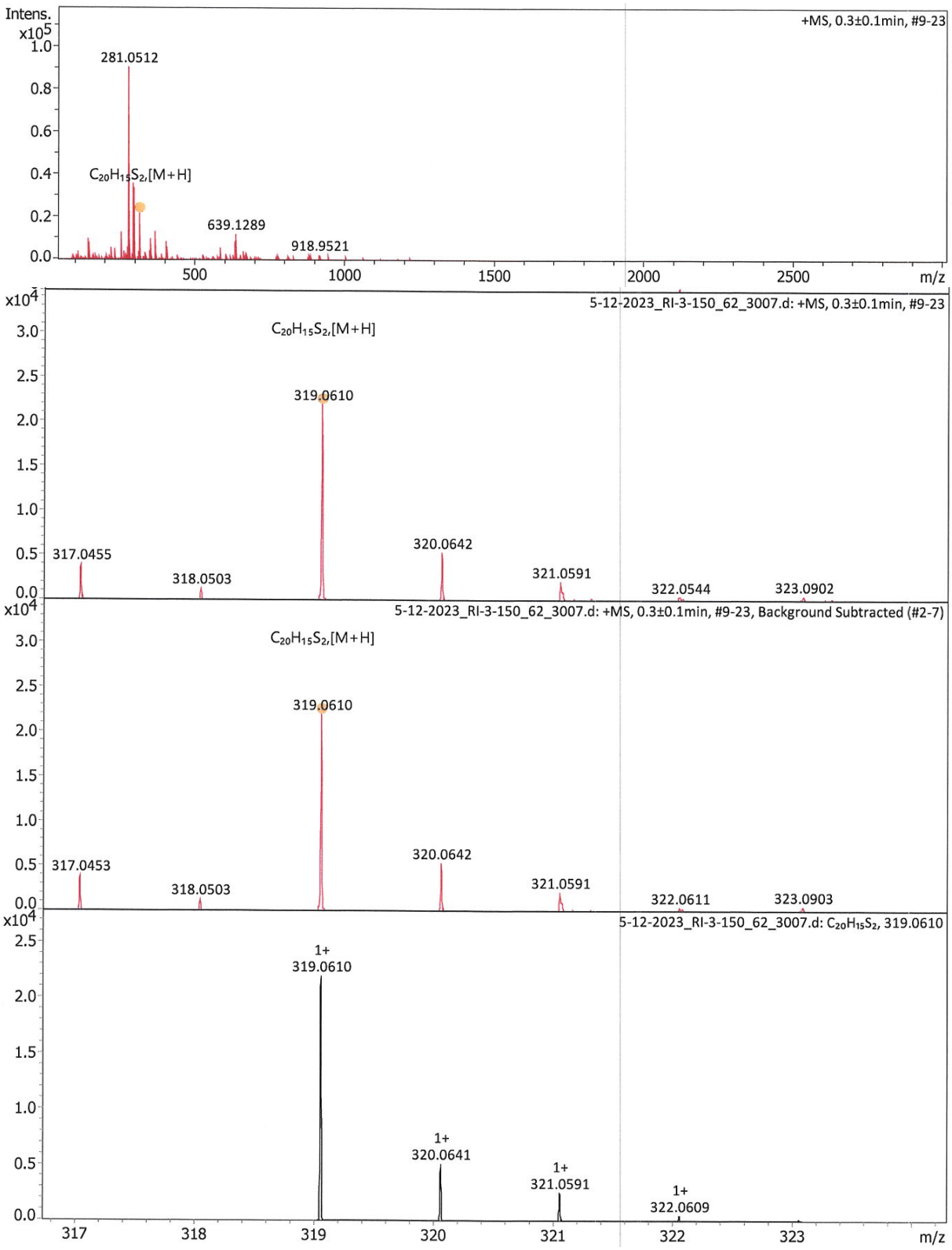

Fig S31. High-resolution mass spectrum of **8** (APCI). Top: full experimental spectrum; middle: enlarged view of the $[M+H]^+$ signals; bottom: simulated spectrum.

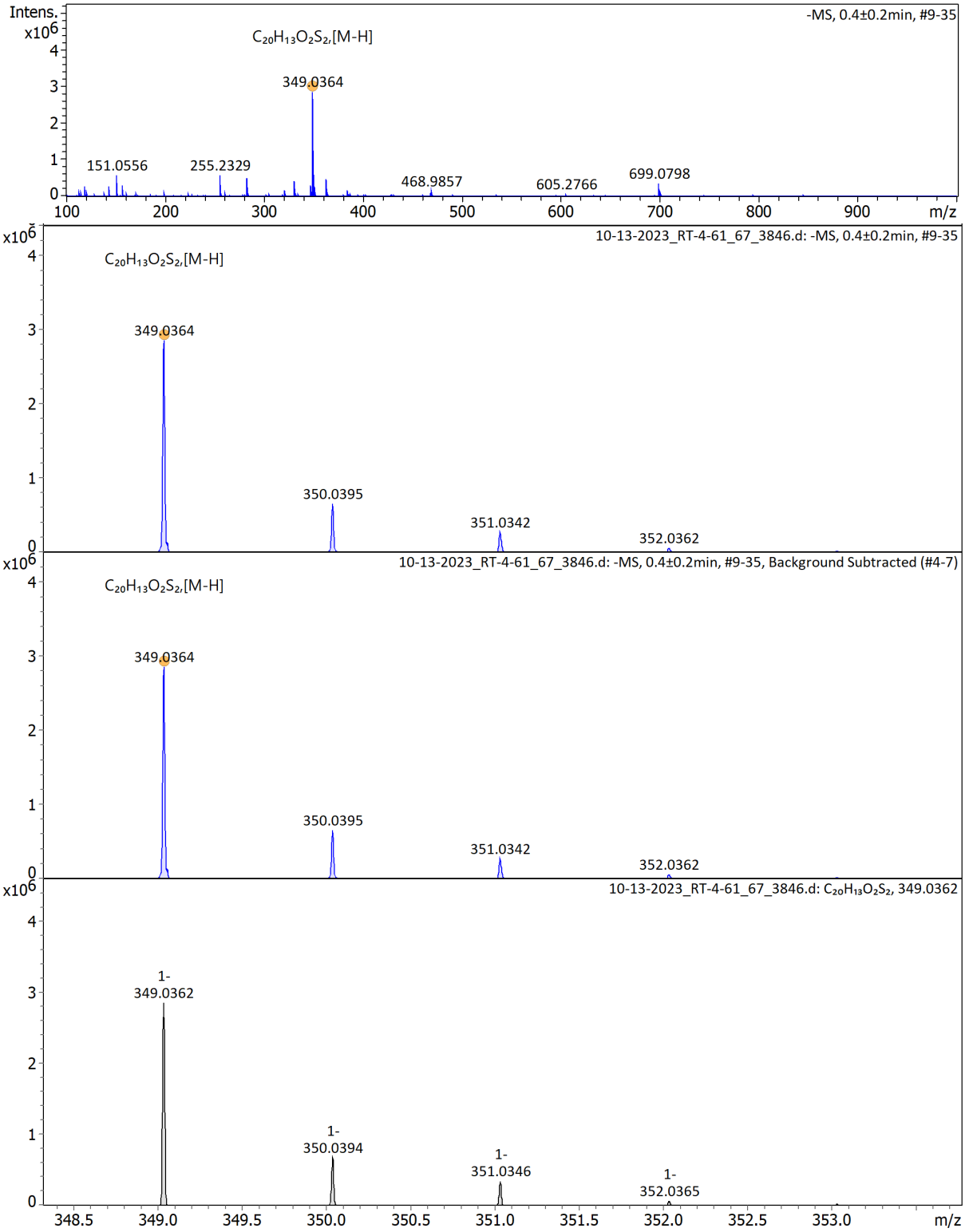

Fig S32. High-resolution mass spectrum of **11** (ESI). Top: full experimental spectrum; middle: enlarged view of the $[M–H]^-$ signals; bottom: simulated spectrum.

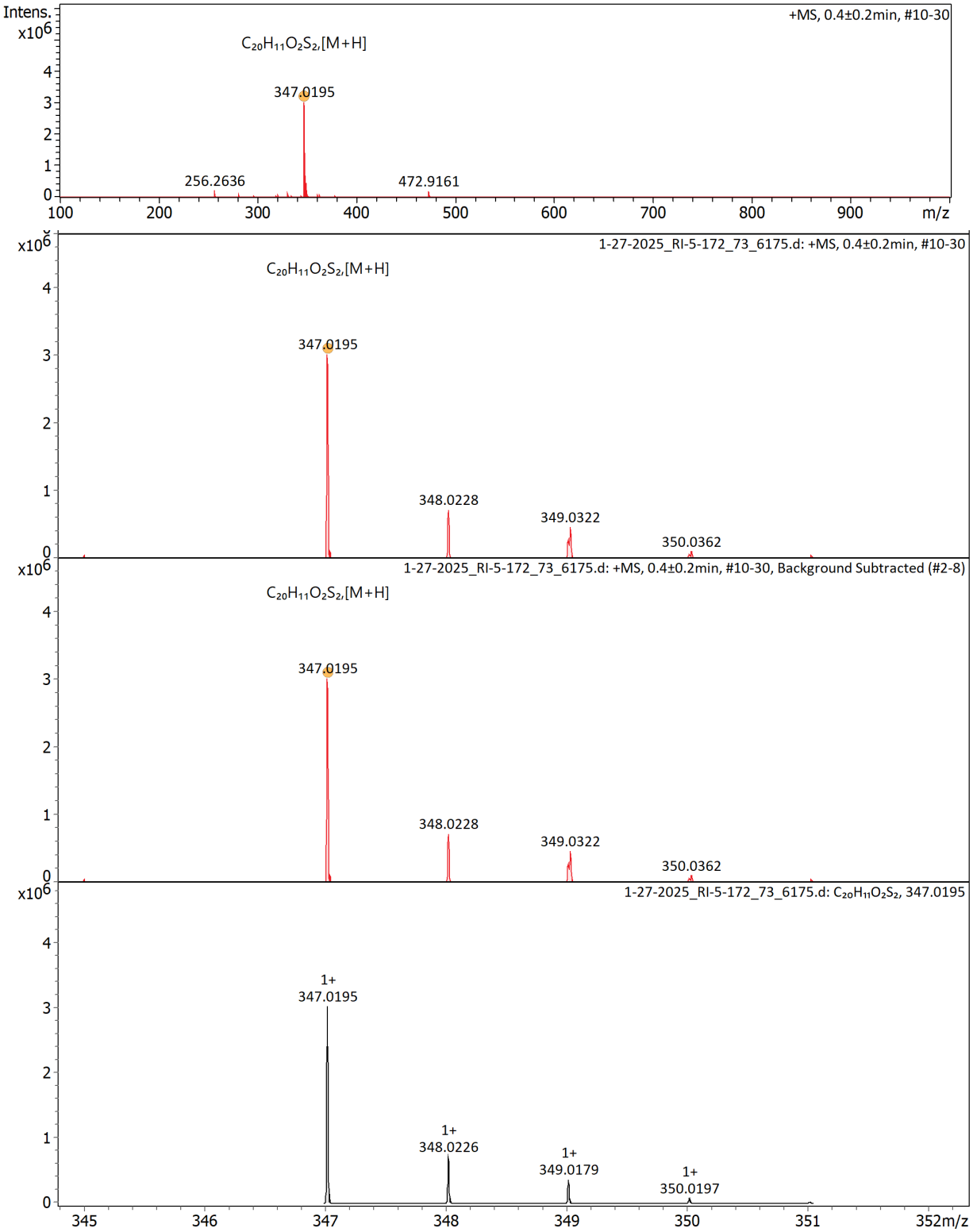

Fig S33. High-resolution mass spectrum of **6** (APCI). Top: full experimental spectrum; middle: enlarged view of the $[M+H]^+$ signals; bottom: simulated spectrum.

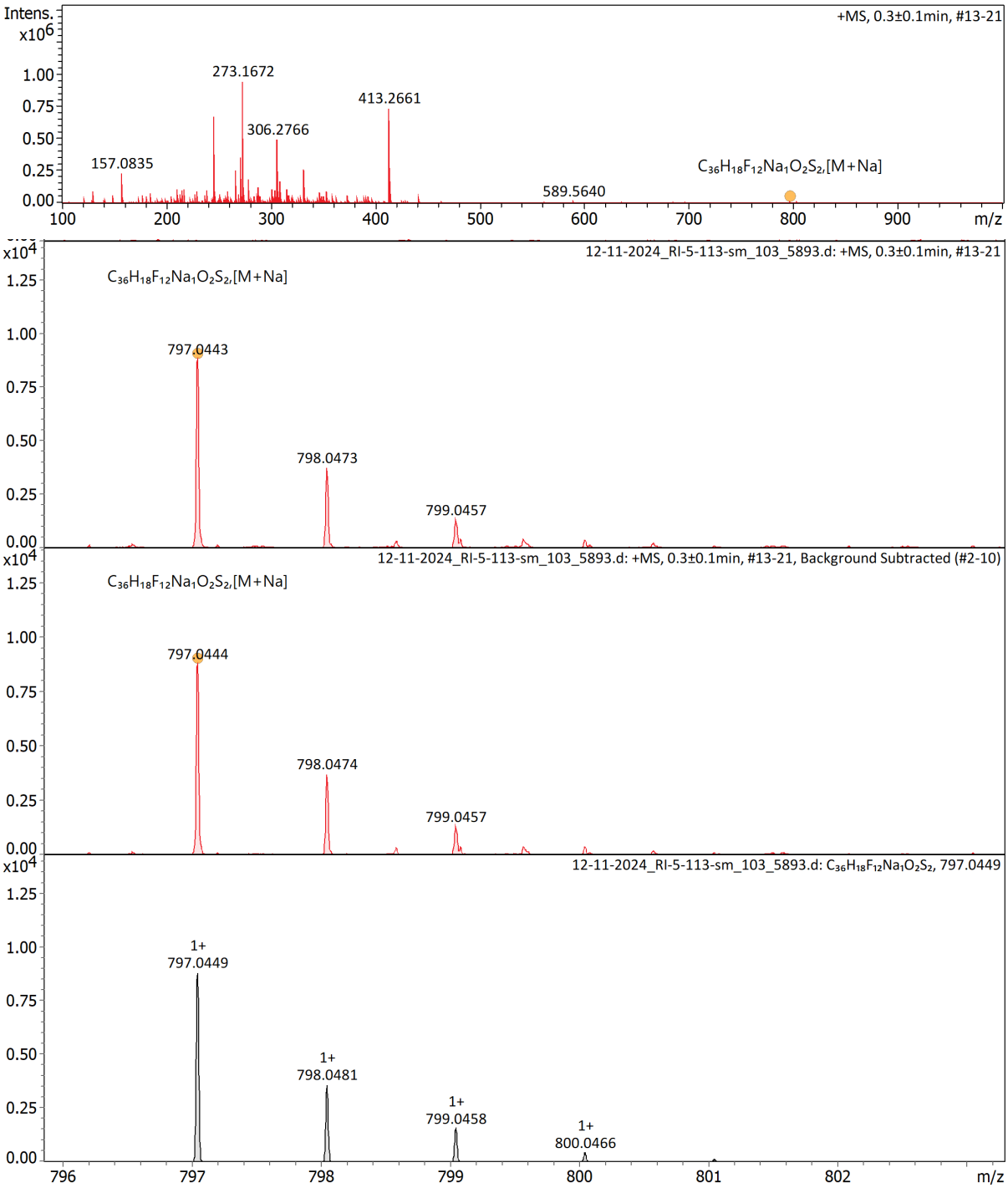

Fig S34. High-resolution mass spectrum of **12a** (ESI). Top: full experimental spectrum; middle: enlarged view of the $[M+Na]^+$ signals; bottom: simulated spectrum.

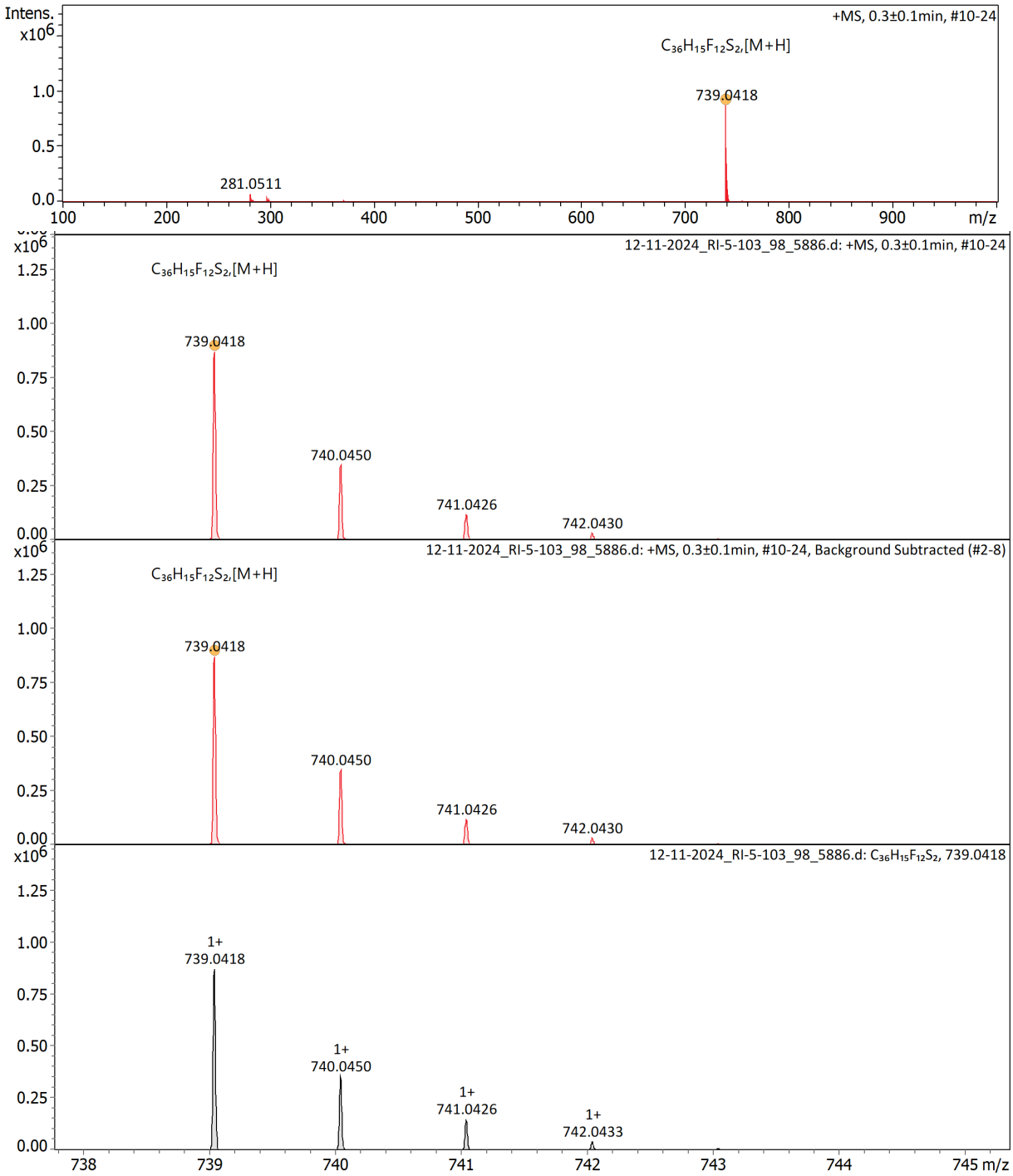

Fig S35. High-resolution mass spectrum of **4a** (APCI). Top: full experimental spectrum; middle: enlarged view of the $[M+H]^+$ signals; bottom: simulated spectrum.

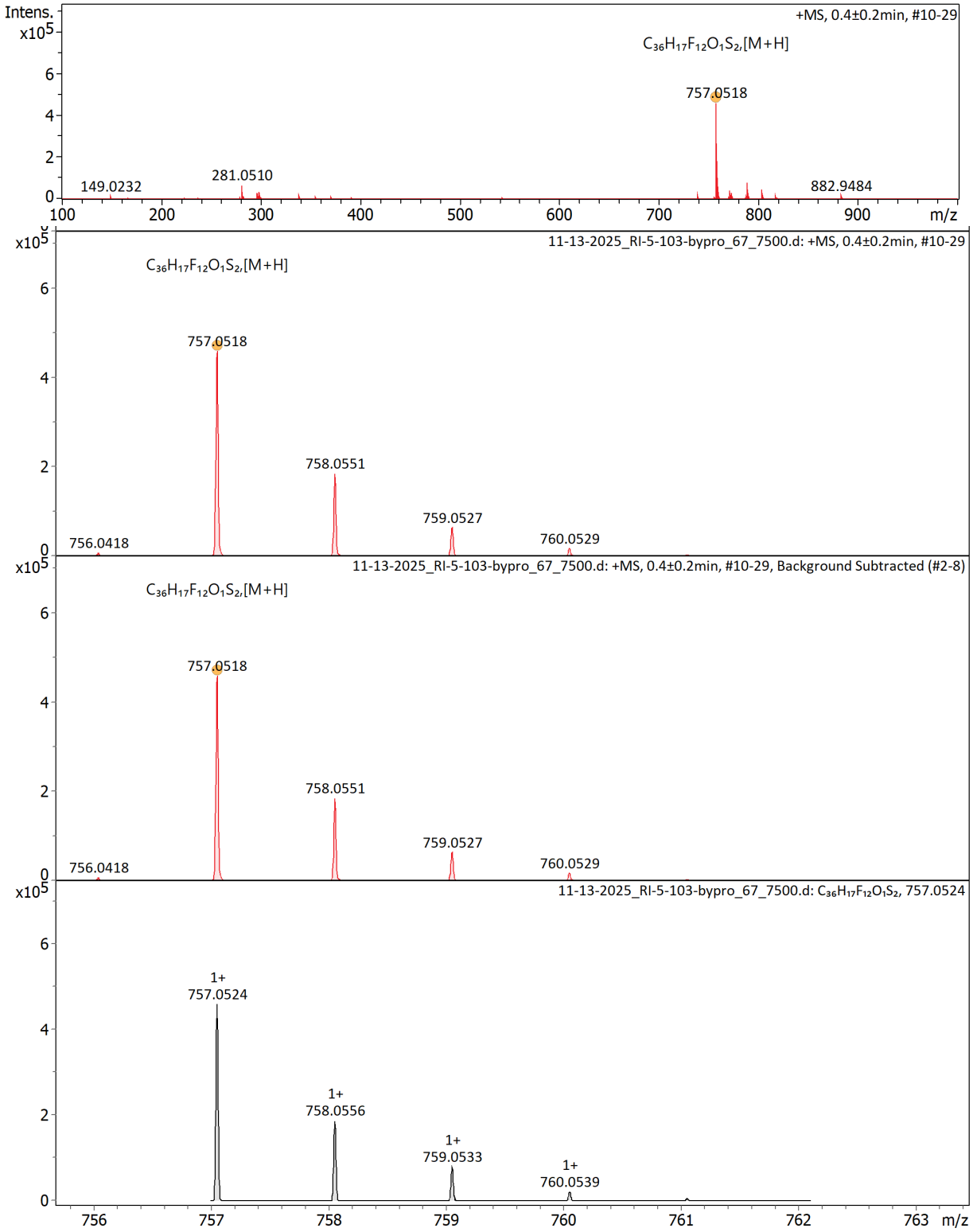

Fig S36. High-resolution mass spectrum of **13a** (APCI). Top: full experimental spectrum; middle: enlarged view of the $[M+H]^+$ signals; bottom: simulated spectrum.

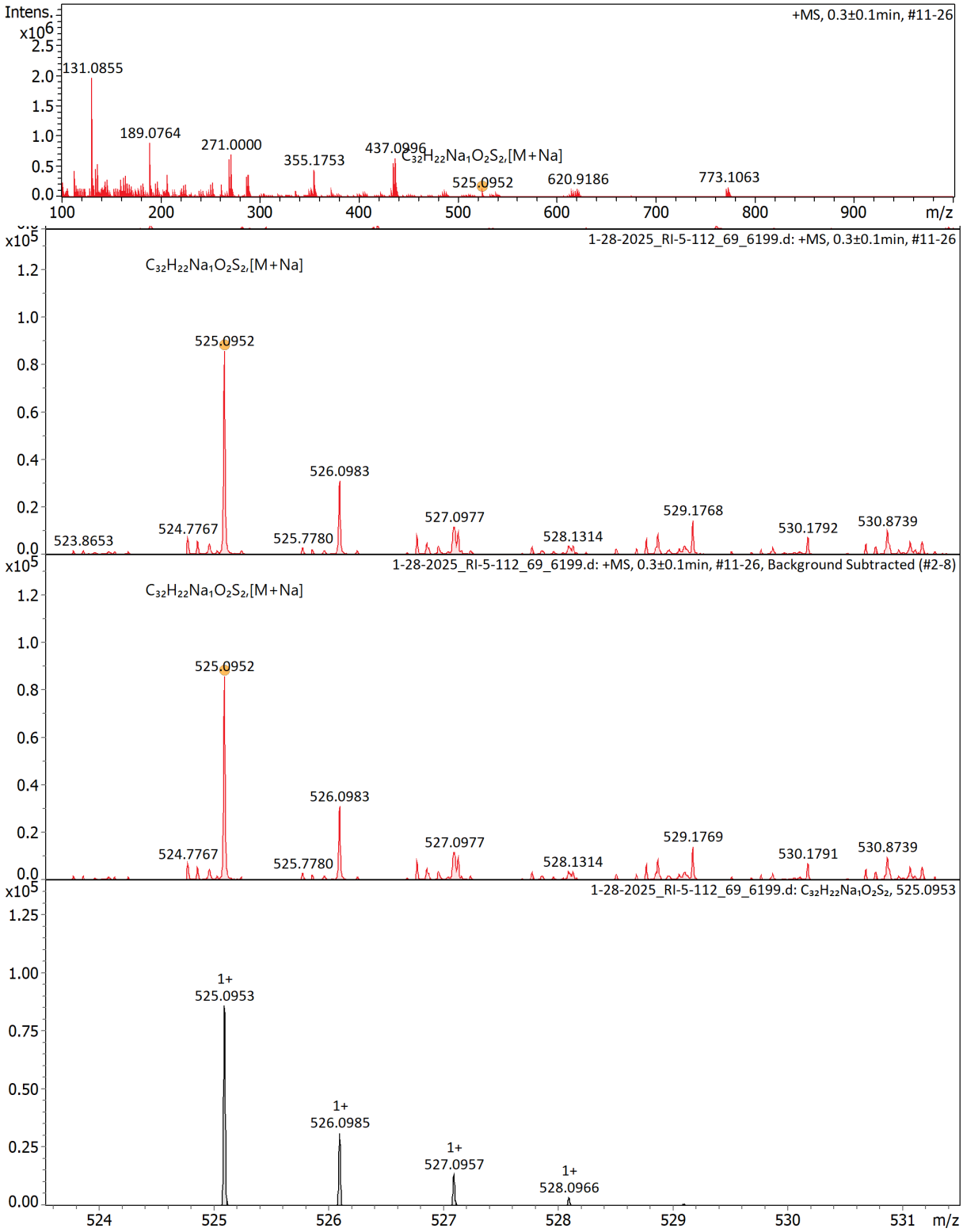

Fig S37. High-resolution mass spectrum of **12b** (ESI). Top: full experimental spectrum; middle: enlarged view of the $[M+Na]^+$ signals; bottom: simulated spectrum.

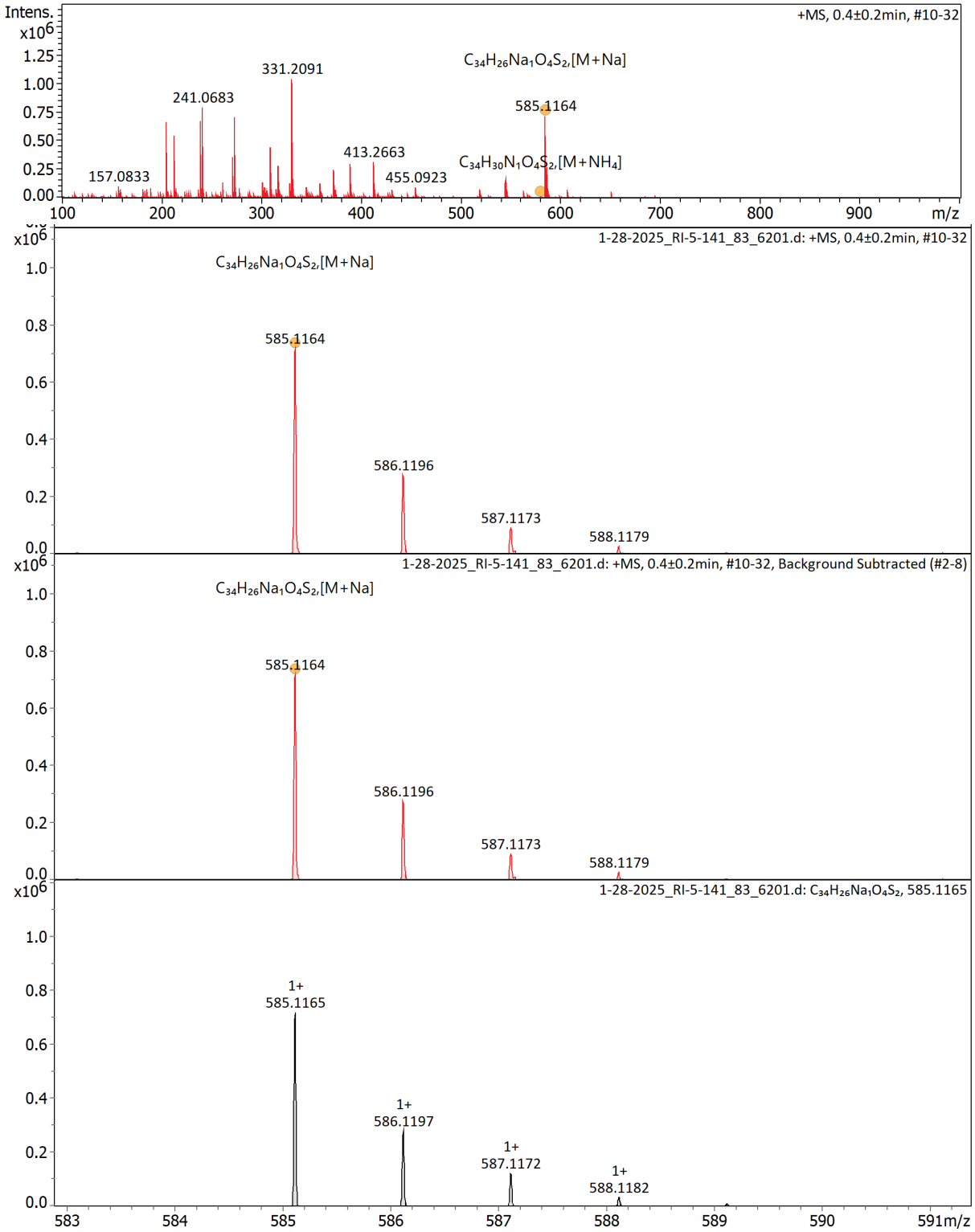

Fig S38. High-resolution mass spectrum of **12c** (ESI). Top: full experimental spectrum; middle: enlarged view of the $[M+Na]^+$ signals; bottom: simulated spectrum.

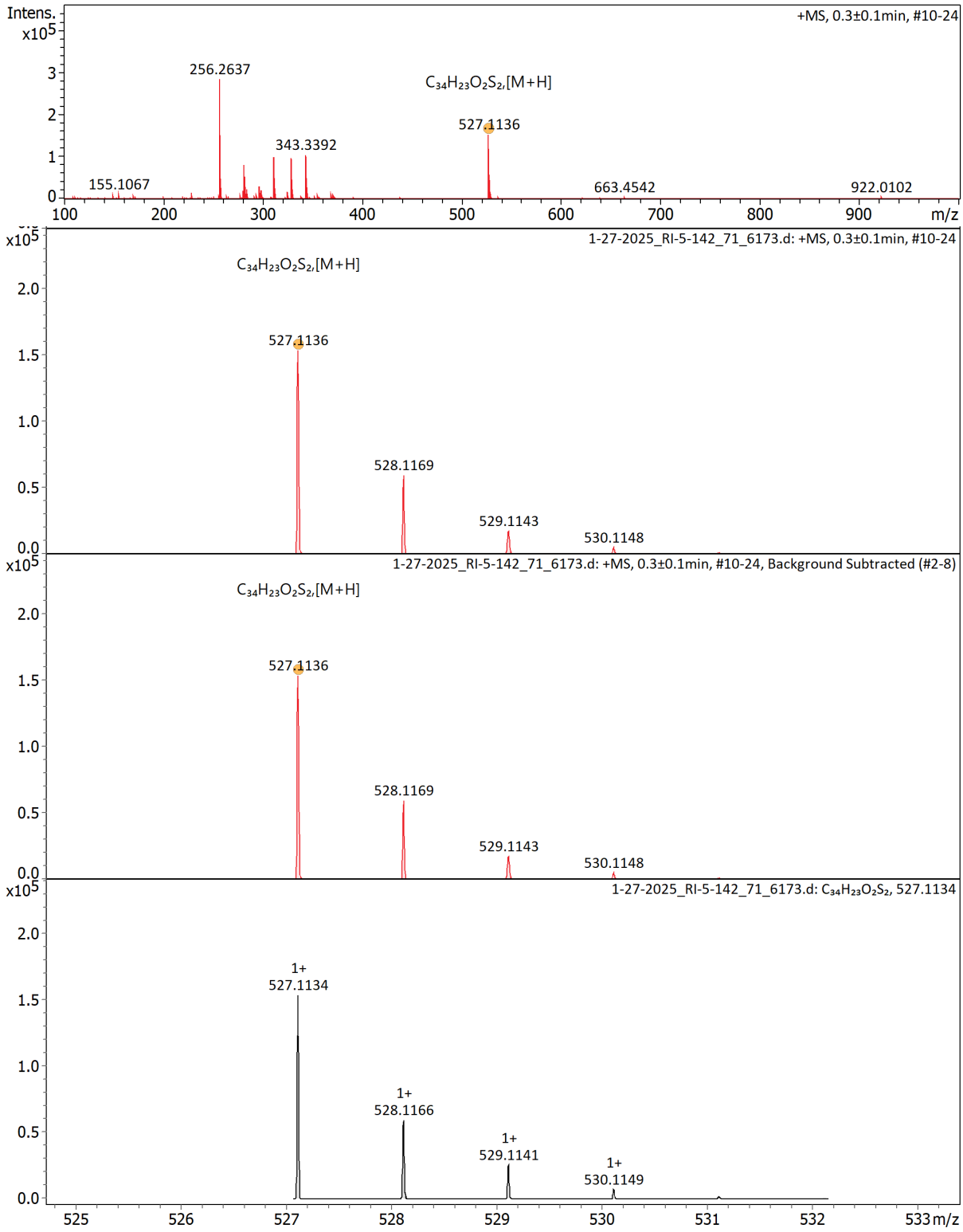

Fig S39. High-resolution mass spectrum of **4c** (APCI). Top: full experimental spectrum; middle: enlarged view of the $[M+H]^+$ signals; bottom: simulated spectrum.

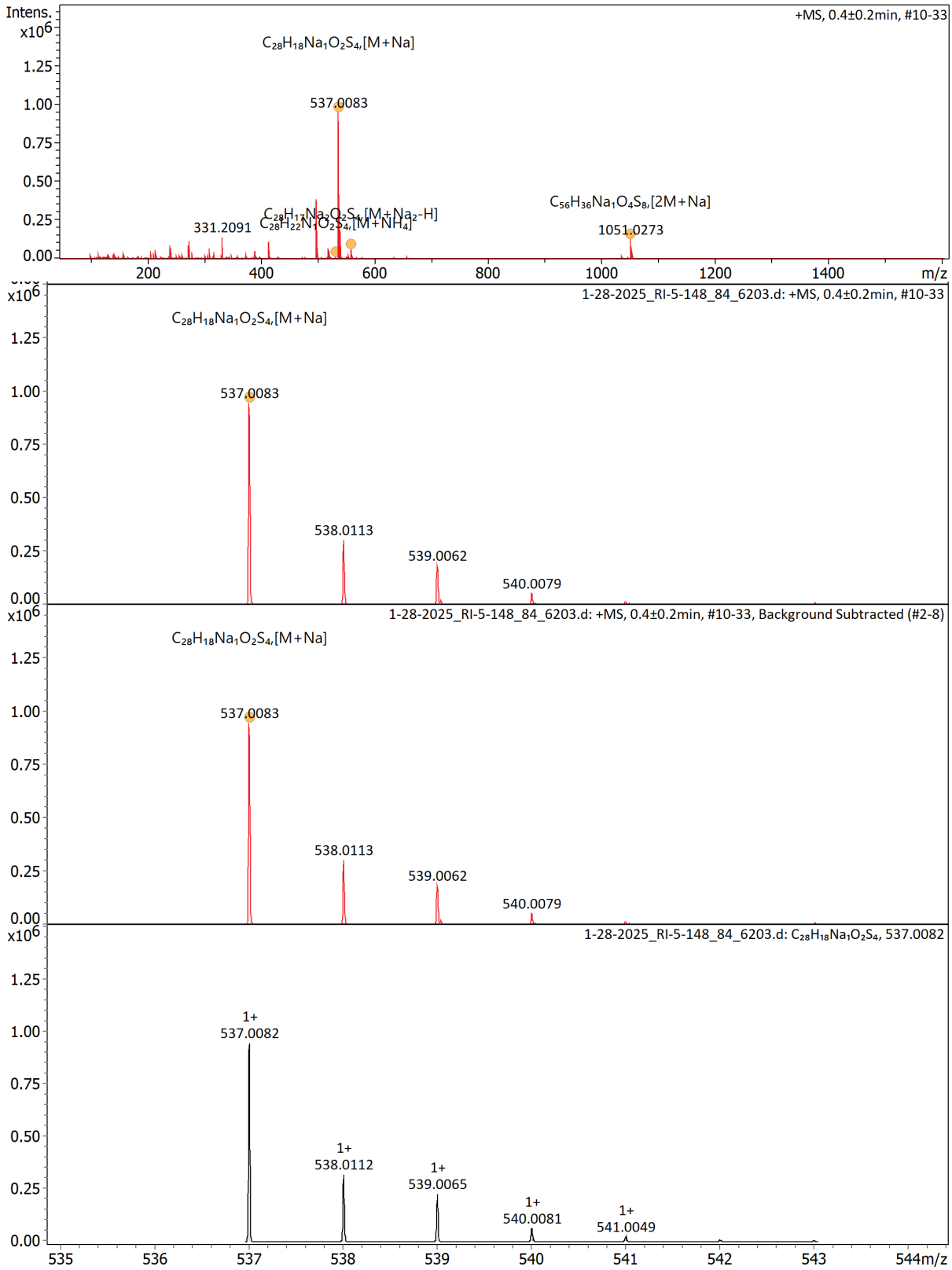

Fig S40. High-resolution mass spectrum of **12d** (ESI). Top: full experimental spectrum; middle: enlarged view of the $[M+Na]^+$ signals; bottom: simulated spectrum.

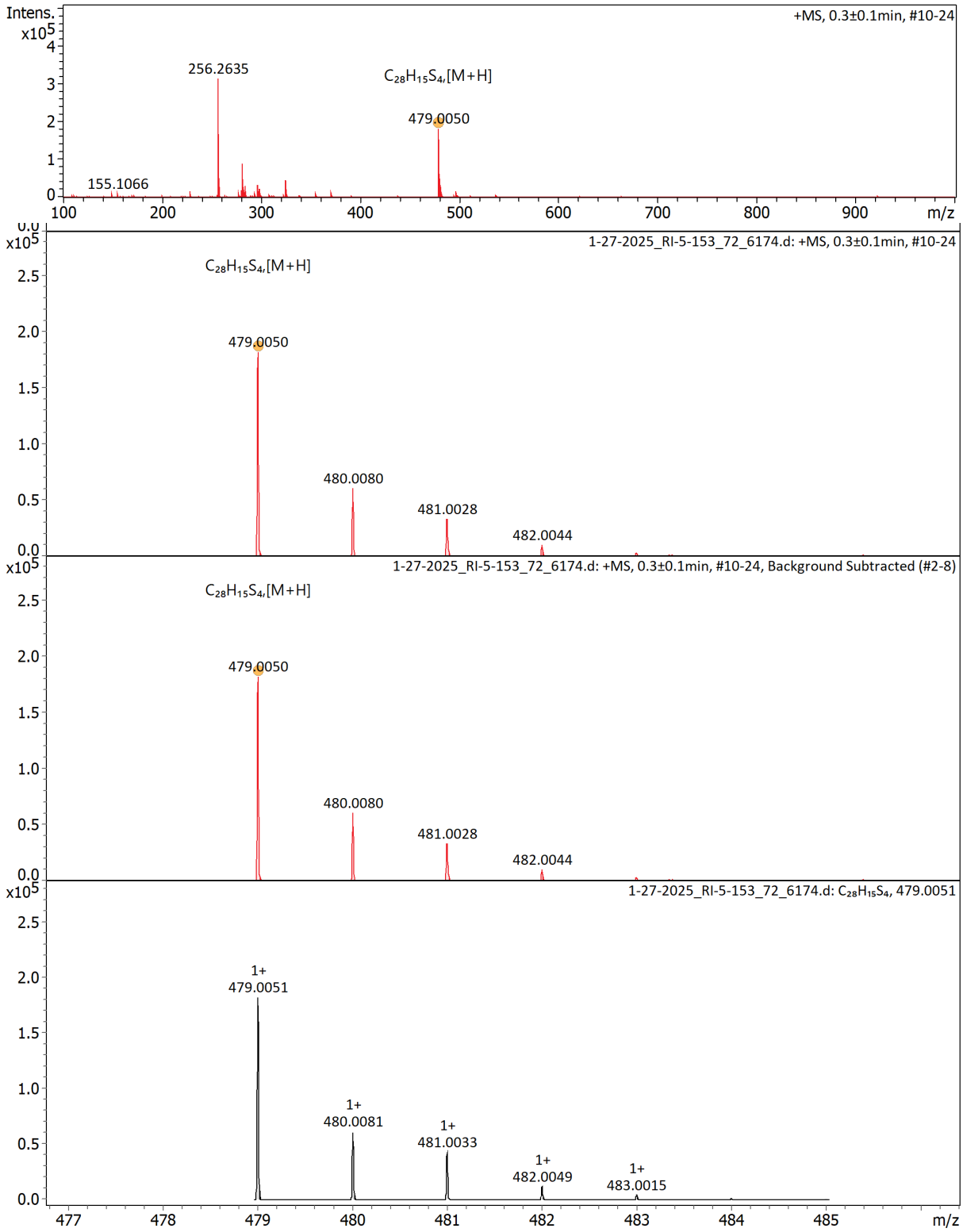

Fig S41. High-resolution mass spectrum of **4d** (APCI). Top: full experimental spectrum; middle: enlarged view of the $[M+H]^+$ signals; bottom: simulated spectrum.

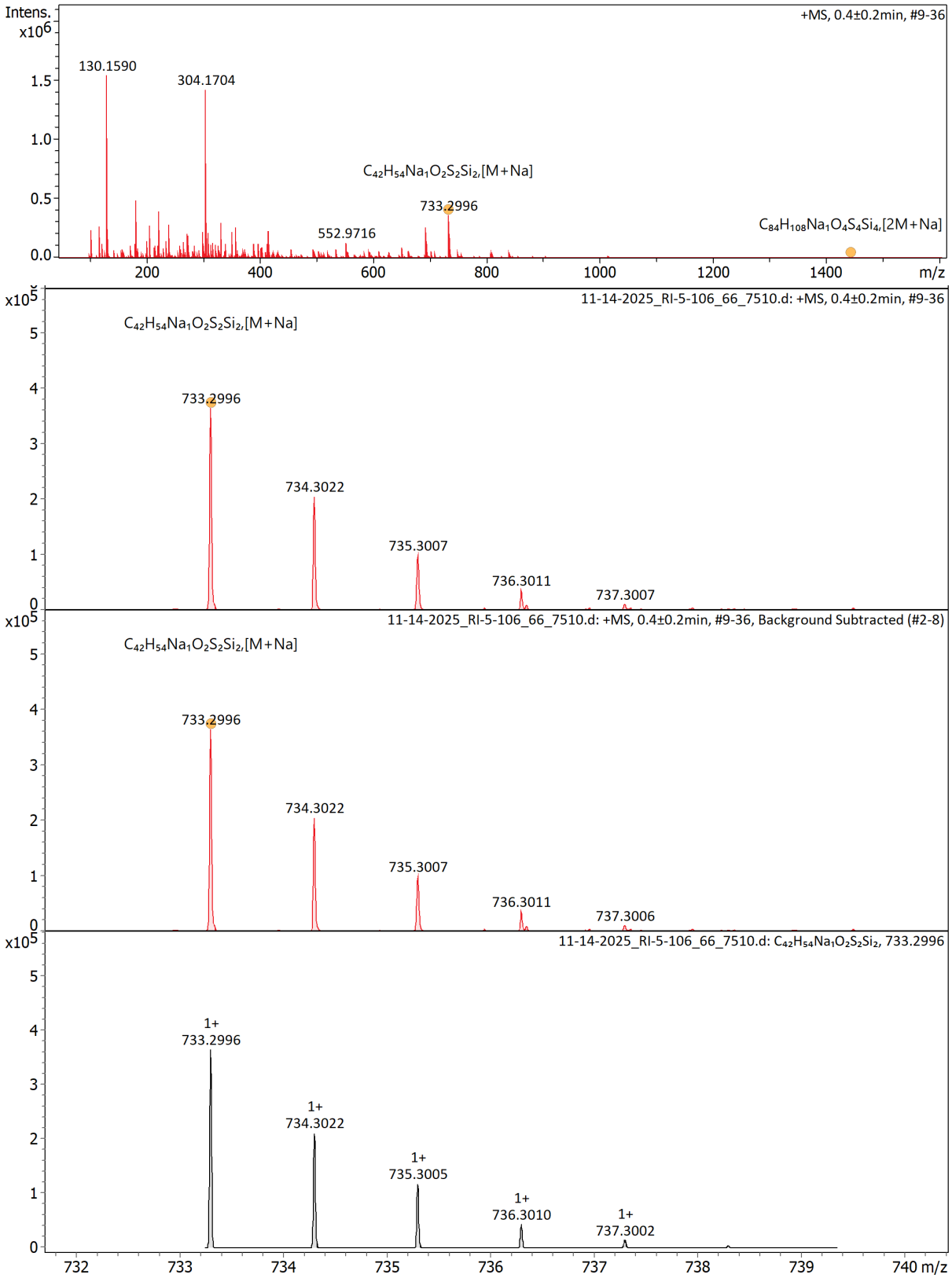

Fig S42. High-resolution mass spectrum of **12e** (ESI). Top: full experimental spectrum; middle: enlarged view of the $[M+Na]^+$ signals; bottom: simulated spectrum.

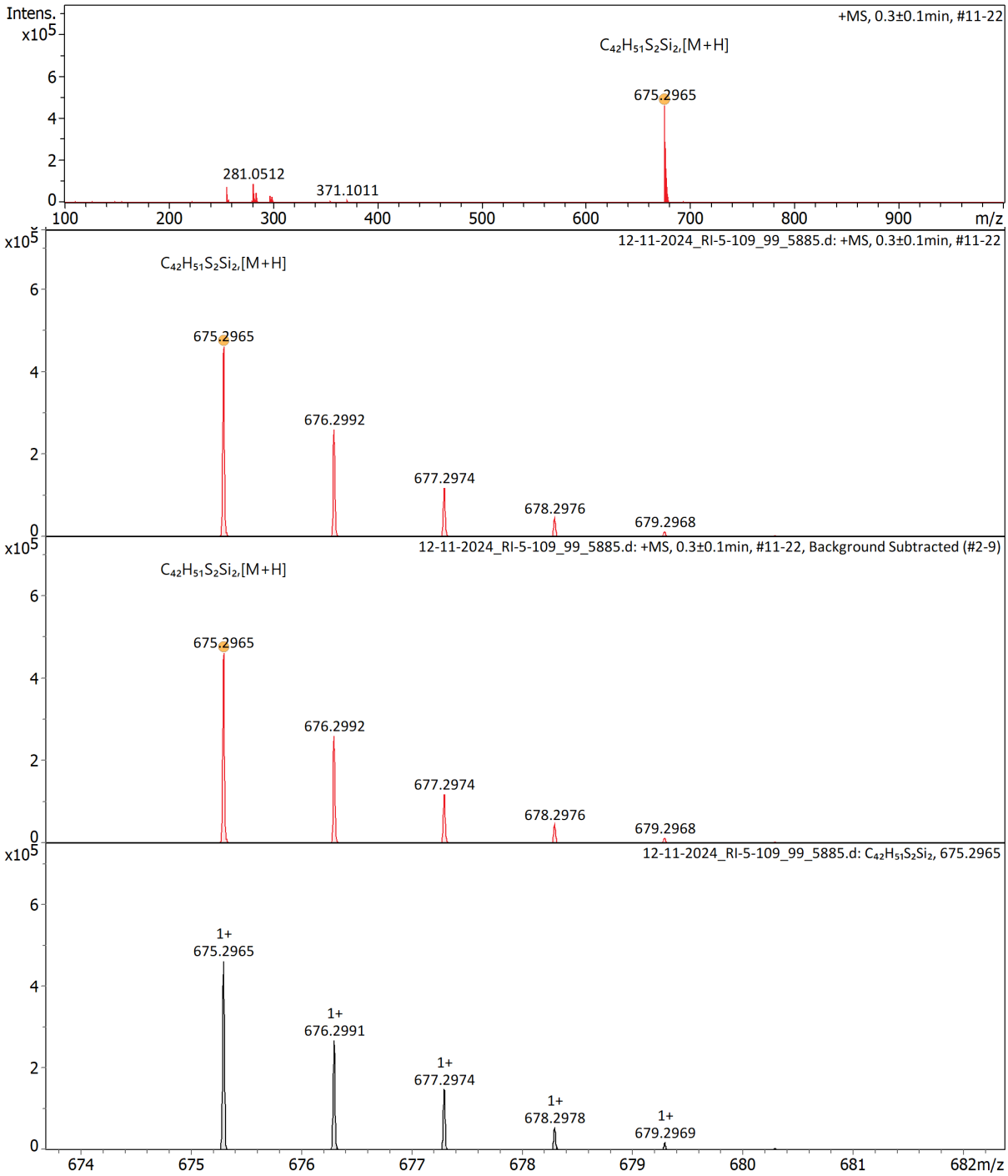

Fig S43. High-resolution mass spectrum of **4e** (APCI). Top: full experimental spectrum; middle: enlarged view of the $[M+H]^+$ signals; bottom: simulated spectrum.

7.3 Cartesian Coordinates of the Optimized Geometries

Table S5. Cartesian Coordinates (Å) of the Optimized Geometry for **4e′** Calculated at the B3LYP/6-31++G(d) Level of Theory

C	0.004358	-1.793041	0.000411
C	1.387871	-1.689323	0.000524
C	1.751715	-0.248372	0.000394
C	0.563358	0.461236	0.000341
C	-1.751645	0.248179	0.000425
C	-1.387793	1.689133	0.000499
C	-0.004281	1.792842	0.000357
C	-2.056518	2.956000	0.000857
C	-1.107676	4.021623	0.000870
S	0.562417	3.429585	0.000546
S	-0.562329	-3.429786	0.000580
C	2.056603	-2.956185	0.000854
C	-0.563290	-0.461435	0.000365
C	-3.428621	3.280321	0.001297
C	-3.819791	4.614276	0.001653
C	-2.867596	5.651477	0.001551
C	-1.504287	5.361132	0.001182
H	-4.169066	2.486134	0.001465
H	-4.878361	4.861388	0.002038
H	-3.195522	6.687399	0.001820
H	-0.767431	6.160110	0.001170
C	1.107769	-4.021815	0.000876
C	3.428709	-3.280493	0.001261
C	3.819891	-4.614444	0.001605
C	2.867704	-5.651653	0.001524
C	1.504392	-5.361321	0.001183
H	4.169146	-2.486298	0.001407
H	4.878463	-4.861548	0.001961
H	3.195638	-6.687572	0.001784
H	0.767543	-6.160305	0.001186
C	-3.058344	-0.276862	0.000189
C	-4.193420	-0.739252	-0.000155
C	3.058395	0.276713	0.000163
C	4.193421	0.739230	-0.000185
Si	5.895173	1.465128	-0.001330
Si	-5.895308	-1.464818	-0.001321
C	-7.145994	-0.049869	0.051199
C	-6.063995	-2.563279	1.526251
C	6.065067	2.560330	1.528449
C	6.095905	2.481523	-1.581016
C	7.146149	0.050284	0.047035
H	-5.920063	-1.988659	2.448990
H	7.062661	3.016931	1.569257
H	7.094006	2.936763	-1.624646
H	7.040412	-0.607294	-0.824255
C	-6.097724	-2.477708	-1.583057
H	-7.020289	0.561889	0.952679
H	-8.172309	-0.439558	0.052729
H	-7.041098	0.609401	-0.818915
H	-5.357851	-3.285162	-1.636473
H	-5.974328	-1.852941	-2.475685
H	-7.095971	-2.932624	-1.626732
H	-7.061586	-3.019891	1.566976
H	-5.324126	-3.372467	1.518717
H	5.921996	1.983739	2.450092
H	5.325132	3.369476	1.523284
H	5.355794	3.288918	-1.631951
H	5.971800	1.858704	-2.474907
H	7.021490	-0.563263	0.947446
H	8.172408	0.440121	0.048250

Table S6. Cartesian Coordinates (Å) of the Optimized Geometry for **4e'** Calculated at the M06/6-31++G(d) Level of Theory

C	-0.095105	1.785656	0.007938
C	-1.465127	1.605723	0.006357
C	-1.751223	0.158046	0.007753
C	-0.536808	-0.488356	0.009359
C	1.751214	-0.158026	0.007513
C	1.465115	-1.605702	0.006208
C	0.095094	-1.785636	0.008017
C	2.200397	-2.826586	0.001790
C	1.314513	-3.935654	0.001275
S	-0.380655	-3.443302	0.005551
S	0.380643	3.443321	0.005314
C	-2.200409	2.826606	0.001998
C	0.536799	0.488378	0.009262
C	3.583812	-3.070072	-0.002949
C	4.045600	-4.375427	-0.007317
C	3.154494	-5.459914	-0.007070
C	1.782768	-5.247451	-0.002897
H	4.279572	-2.230747	-0.003646
H	5.117977	-4.565095	-0.011146
H	3.540852	-6.477674	-0.010508
H	1.088385	-6.086771	-0.003117
C	-1.314526	3.935673	0.001281
C	-3.583825	3.070094	-0.002542
C	-4.045613	4.375450	-0.006906
C	-3.154506	5.459935	-0.006852
C	-1.782779	5.247471	-0.002883
H	-4.279586	2.230769	-0.003090
H	-5.117990	4.565116	-0.010585
H	-3.540862	6.477696	-0.010282
H	-1.088394	6.086789	-0.003260
C	3.034218	0.418482	0.006291
C	4.156667	0.904941	0.005158
C	-3.034223	-0.418469	0.006823
C	-4.156665	-0.904942	0.005773
Si	-5.878578	-1.575981	-0.003372
Si	5.878592	1.575956	-0.003074
C	7.043374	0.109333	-0.106986
C	6.066735	2.692961	-1.496648
C	6.145072	2.534295	1.585783
C	-7.043335	-0.109394	-0.108006
C	-6.145899	-2.534269	1.585366
C	-6.065869	-2.693068	-1.496992
H	7.082606	3.108869	-1.543085
H	-6.857570	0.478431	-1.016679
H	-7.165078	-2.942988	1.622682
H	-7.081634	-3.109178	-1.543857
H	6.916390	-0.557325	0.756337
H	8.091307	0.438367	-0.126212
H	6.858448	-0.478269	-1.015972
H	5.360167	3.531864	-1.456301
H	5.883356	2.145094	-2.429692
H	5.441995	3.373143	1.666648
H	7.164259	2.942937	1.623683
H	6.005416	1.893782	2.465900
H	-8.091231	-0.438479	-0.128309
H	-6.917204	0.557072	0.755590
H	-6.006801	-1.893733	2.465552
H	-5.442809	-3.373067	1.666652
H	-5.882182	-2.145194	-2.429970
H	-5.359158	-3.531836	-1.456311

Table S7. Cartesian Coordinates (Å) of the Optimized Geometry for **4e′** Calculated at the M06-2X/6-31++G(d) Level of Theory

C	-0.091420	1.797054	0.000497
C	-1.454366	1.615846	-0.000088
C	-1.747643	0.157201	0.000492
C	-0.543779	-0.489840	0.000551
C	1.747715	-0.157391	0.000534
C	1.454439	-1.616036	-0.000231
C	0.091494	-1.797245	0.000296
C	2.191485	-2.842976	-0.002339
C	1.302649	-3.948189	-0.002849
S	-0.384597	-3.452858	-0.001210
S	0.384673	3.452665	-0.000817
C	-2.191410	2.842787	-0.002069
C	0.543850	0.489647	0.000627
C	3.577287	-3.083394	-0.004512
C	4.039175	-4.388619	-0.006728
C	3.144539	-5.474077	-0.006751
C	1.773108	-5.263404	-0.004883
H	4.268109	-2.244972	-0.004787
H	5.108275	-4.579332	-0.008593
H	3.529834	-6.489085	-0.008439
H	1.081153	-6.100687	-0.005169
C	-1.302572	3.947999	-0.002425
C	-3.577213	3.083209	-0.004242
C	-4.039097	4.388436	-0.006322
C	-3.144458	5.473891	-0.006205
C	-1.773027	5.263215	-0.004325
H	-4.268037	2.244789	-0.004622
H	-5.108196	4.579151	-0.008177
H	-3.529751	6.488901	-0.007809
H	-1.081070	6.100497	-0.004492
C	3.044255	0.411785	0.001661
C	4.168816	0.884659	0.003152
C	-3.044189	-0.411962	0.001499
C	-4.168782	-0.884760	0.002886
Si	-5.889167	-1.571843	0.003483
Si	5.889029	1.572180	0.003972
C	7.075346	0.119709	-0.096128
C	6.068405	2.694352	-1.489652
C	6.131996	2.530311	1.599315
C	-7.075119	-0.119135	-0.097547
C	-6.132835	-2.529429	1.599039
C	-6.068312	-2.694481	-1.489831
H	7.076383	3.122803	-1.529871
H	-6.906408	0.463580	-1.009299
H	-7.143647	-2.950752	1.643663
H	-7.076264	-3.122984	-1.530135
H	6.949903	-0.549583	0.761643
H	8.114649	0.467275	-0.103756
H	6.907608	-0.462984	-1.008077
H	5.350287	3.519764	-1.448922
H	5.896335	2.143538	-2.419923
H	5.416455	3.355390	1.675510
H	7.142652	2.951988	1.644099
H	5.995093	1.883852	2.472115
H	-8.114479	-0.466520	-0.106214
H	-6.950400	0.550053	0.760407
H	-5.995954	-1.882800	2.471717
H	-5.417604	-3.354737	1.675642
H	-5.896106	-2.143930	-2.420240
H	-5.350133	-3.519819	-1.448728

Table S8. Cartesian Coordinates (Å) of the Optimized Geometry for **4e′** Calculated at the ωB97X-D/6-31++G(d) Level of Theory

C	-0.101296	1.794965	-0.011442
C	-1.461143	1.605939	-0.011408
C	-1.746511	0.146860	-0.011365
C	-0.540677	-0.491727	-0.011510
C	1.746632	-0.146983	-0.011393
C	1.461266	-1.606061	-0.011400
C	0.101420	-1.795089	-0.011431
C	2.206766	-2.827825	-0.011488
C	1.327335	-3.938695	-0.011543
S	-0.365090	-3.453422	-0.011548
S	0.365217	3.453296	-0.011542
C	-2.206640	2.827705	-0.011477
C	0.540794	0.491599	-0.011521
C	3.593105	-3.056432	-0.011560
C	4.066480	-4.357356	-0.011656
C	3.181478	-5.449031	-0.011670
C	1.808709	-5.249402	-0.011615
H	4.277621	-2.213261	-0.011566
H	5.137480	-4.538663	-0.021733
H	3.574895	-6.461223	-0.011744
H	1.125565	-6.093870	-0.011643
C	-1.327207	3.938572	-0.011538
C	-3.592979	3.056318	-0.011557
C	-4.066349	4.357244	-0.011661
C	-3.181344	5.448916	-0.011674
C	-1.808576	5.249281	-0.011620
H	-4.277498	2.213150	-0.011568
H	-5.137349	4.538553	-0.021737
H	-3.574756	6.461110	-0.021745
H	-1.125429	6.093748	-0.011662
C	3.037775	0.428688	-0.001174
C	4.159941	0.903894	-0.000916
C	-3.037673	-0.428769	-0.001131
C	-4.159868	-0.903908	-0.000870
Si	-5.878003	-1.585296	0.019609
Si	5.877993	1.585500	0.019609
C	7.063104	0.126741	-0.148459
C	6.050664	2.773857	-1.434067
C	6.134962	2.479984	1.662031
C	-7.062925	-0.126377	-0.148006
C	-6.135006	-2.480161	1.651776
C	-6.050913	-2.773233	-1.434318
H	7.062044	3.205954	-1.468732
H	-6.895284	0.417777	-1.086721
H	-7.146601	-2.901660	1.717420
H	-7.062351	-3.195189	-1.469079
H	6.948022	-0.584880	0.675386
H	8.104538	0.470683	-0.148482
H	6.895409	-0.417239	-1.087286
H	5.336792	3.604933	-1.358289
H	5.862162	2.260027	-2.391080
H	5.421206	3.310946	1.775687
H	7.146493	2.901620	1.717766
H	5.998882	1.798009	2.514075
H	-8.104405	-0.470181	-0.147967
H	-6.947632	0.575028	0.685962
H	-5.998809	-1.798483	2.503997
H	-5.421373	-3.311235	1.775129
H	-5.872328	-2.259186	-2.391172
H	-5.337148	-3.604403	-1.358787

Table S9. Cartesian Coordinates (Å) of the Optimized Geometry for **4e′** Calculated at the M11/6-31++G(d) Level of Theory

C	-0.122400	1.800852	0.000162
C	-1.477592	1.593488	0.000066
C	-1.746981	0.125618	-0.000108
C	-0.538272	-0.499648	-0.000023
C	1.746982	-0.125623	0.000085
C	1.477594	-1.593492	0.000058
C	0.122402	-1.800857	-0.000030
C	2.239592	-2.809412	0.000145
C	1.373498	-3.928531	0.000093
S	-0.324953	-3.465687	-0.000098
S	0.324956	3.465681	0.000332
C	-2.239589	2.809408	0.000195
C	0.538273	0.499643	0.000098
C	3.629765	-3.021046	0.000299
C	4.117455	-4.315924	0.000385
C	3.243759	-5.419052	0.000317
C	1.869992	-5.235703	0.000175
H	4.306760	-2.164914	0.000367
H	5.195278	-4.486060	0.000504
H	3.651075	-6.431112	0.000381
H	1.191295	-6.090117	0.000120
C	-1.373495	3.928526	0.000370
C	-3.629763	3.021043	0.000206
C	-4.117451	4.315922	0.000373
C	-3.243755	5.419048	0.000530
C	-1.869988	5.235699	0.000535
H	-4.306758	2.164911	0.000099
H	-5.195274	4.486058	0.000384
H	-3.651070	6.431109	0.000648
H	-1.191290	6.090112	0.000654
C	3.040826	0.461510	0.000144
C	4.160421	0.941887	0.000213
C	-3.040826	-0.461511	-0.000289
C	-4.160423	-0.941885	-0.000398
Si	-5.892265	-1.610014	-0.000611
Si	5.892265	1.610019	0.000044
C	7.051004	0.131742	0.001396
C	6.117993	2.645308	-1.548643
C	6.117351	2.647860	1.547102
C	-7.051004	-0.131738	0.000581
C	-6.117420	-2.647706	1.546548
C	-6.117946	-2.645438	-1.549209
H	7.136995	3.058099	-1.596827
H	-6.891303	0.497229	-0.887486
H	-7.136673	-3.059853	1.594895
H	-7.136933	-3.058260	-1.597381
H	6.892506	-0.494876	0.891330
H	8.103215	0.453674	0.000257
H	6.891337	-0.497274	-0.886640
H	5.411512	3.487320	-1.570271
H	5.953215	2.046253	-2.455555
H	5.411380	3.490353	1.566654
H	7.136568	3.060100	1.595433
H	5.951436	2.050512	2.454932
H	-8.103221	-0.453649	-0.000581
H	-6.892536	0.494941	0.890481
H	-5.951453	-2.050268	2.454304
H	-5.411514	-3.490250	1.566155
H	-5.953161	-2.046468	-2.456176
H	-5.411443	-3.487436	-1.570750

Table S10. Cartesian Coordinates (Å) of the Optimized Geometry for **2** Calculated at the M06-2X/6-31++G(d) Level of Theory

C	0.251697	-1.804903	-0.073680
C	-1.169320	-1.839913	-0.066574
C	-1.693914	-0.446353	-0.013211
C	-0.621188	0.387327	0.008716
C	1.694317	0.446946	0.013584
C	1.169586	1.840539	0.066815
C	-0.251393	1.805497	0.074036
C	0.621500	-0.386712	-0.007845
C	0.981899	-2.978514	-0.178028
C	0.292361	-4.196876	-0.267874
C	-1.098995	-4.230824	-0.262959
C	-1.844450	-3.046318	-0.170329
C	-0.981758	2.979066	0.177790
C	-0.292369	4.197549	0.266845
C	1.098999	4.231587	0.261893
C	1.844524	3.047077	0.170051
H	2.067550	-2.959984	-0.205599
H	0.853297	-5.123134	-0.350817
H	-1.614982	-5.183169	-0.342063
H	-2.930305	-3.078190	-0.198127
H	-2.067407	2.960327	0.205315
H	-0.853370	5.123817	0.349229
H	1.614927	5.184004	0.340481
H	2.930341	3.079076	0.198005
C	3.120609	0.091141	0.018476
C	-3.120751	-0.090867	-0.018553
C	3.595345	-0.909681	0.876982
C	4.942113	-1.261744	0.877474
C	5.834031	-0.618604	0.019276
C	5.372087	0.381107	-0.836211
C	4.026271	0.738453	-0.833532
C	-3.596265	0.909018	-0.877620
C	-4.943397	1.259868	-0.878030
C	-5.834431	0.616539	-0.019046
C	-5.371476	-0.381914	0.837369
C	-4.025547	-0.738183	0.834435
H	-2.900859	1.394801	-1.557837
H	-5.299547	2.032002	-1.553979
H	-6.885350	0.890341	-0.018971
H	-6.059947	-0.882531	1.512024
H	-3.662561	-1.503762	1.515354
H	2.899424	-1.395251	1.556822
H	5.297298	-2.034633	1.553073
H	6.884717	-0.893294	0.019218
H	6.061150	0.882001	-1.510048
H	3.665110	1.505734	-1.513578

Table S11. Cartesian Cartesian Coordinates (Å) of the Optimized Geometry for **4a** Calculated at the M06-2X/6-31++G(d) Level of Theory

C	0.217273	1.768815	0.247841
C	-1.156138	1.817923	0.350504
C	-1.694298	0.441447	0.162022
C	-0.625838	-0.384238	-0.018308
C	1.684679	-0.437875	-0.172782
C	1.146040	-1.814370	-0.361507
C	-0.227389	-1.764570	-0.260464
C	1.633284	-3.125207	-0.702205
C	0.552448	-4.040939	-0.793032
S	-1.004298	-3.279249	-0.510467
S	0.992785	3.284408	0.497721
C	-1.644103	3.128116	0.692193
C	0.616156	0.388780	0.004426
C	2.930022	-3.602957	-0.975497
C	3.119765	-4.939228	-1.285598
C	2.037304	-5.833383	-1.339511
C	0.745723	-5.389130	-1.100366
C	3.096943	-0.044738	-0.130454
H	3.779336	-2.927631	-0.964099
H	4.122253	-5.299526	-1.495118
H	2.210341	-6.877293	-1.581226
H	-0.098523	-6.069985	-1.157563
C	-0.564074	4.044737	0.782783
C	-2.941160	3.604467	0.966308
C	-3.131970	4.940363	1.277310
C	-2.050264	5.835459	1.331198
C	-0.758409	5.392583	1.090974
C	-3.106505	0.046890	0.125307
H	-3.789862	2.928335	0.954800
H	-4.134677	5.299659	1.487497
H	-2.224123	6.879062	1.573637
H	0.085163	6.074287	1.147972
C	-3.523147	-1.145397	0.730613
C	-4.852154	-1.543765	0.647215
C	-5.792554	-0.770789	-0.030383
C	-5.373816	0.412230	-0.630129
C	-4.045861	0.823066	-0.560360
C	3.513922	1.154322	-0.727953
C	4.839569	1.552496	-0.635633
C	5.779323	0.774320	0.042135
C	5.361754	-0.410941	0.632325
C	4.032605	-0.823336	0.553540
H	-2.809061	-1.744900	1.289911
C	-5.262198	-2.855135	1.263915
H	-6.830145	-1.081993	-0.084553
C	-6.352764	1.298845	-1.352763
H	-3.733073	1.738439	-1.057538
H	2.800686	1.756766	-1.283431
C	5.296575	2.849286	-1.249494
H	6.816175	1.089605	0.104415
C	6.337140	-1.298742	1.358113
H	3.718864	-1.741353	1.045165
F	-7.568660	0.744147	-1.447698
F	-5.936500	1.580404	-2.598328
F	-6.497834	2.478009	-0.718668
F	-6.573985	-2.890515	1.542385
F	-5.006493	-3.885176	0.436525
F	-4.597575	-3.097345	2.404352
F	4.349005	3.412700	-2.010888
F	5.634667	3.743375	-0.302868
F	6.384089	2.672493	-2.019222
F	5.923721	-1.566820	2.607644
F	6.470469	-2.483918	0.733079
F	7.557271	-0.752068	1.443727

Table S12. Cartesian Coordinates (Å) of the Optimized Geometry for **4b** Calculated at the M06-2X/6-31++G(d) Level of Theory

C	1.183287	-1.347460	-0.069264
C	2.146943	-0.361403	-0.030908
C	1.470486	0.964369	0.019086
C	0.128311	0.717939	0.036745
C	-1.470495	-0.964373	-0.019259
C	-2.146950	0.361400	0.030832
C	-1.183292	1.347456	0.069132
C	-3.482192	0.891472	-0.055274
C	-3.452902	2.310223	-0.024034
S	-1.818310	2.948258	0.064064
S	1.818315	-2.948258	-0.064192
C	3.482182	-0.891469	0.055269
C	-0.128318	-0.717941	-0.037018
C	-4.732080	0.258116	-0.196770
C	-5.886567	1.020910	-0.265831
C	-5.836013	2.423340	-0.200795
C	-4.617736	3.077072	-0.085767
C	-2.116122	-2.281211	-0.009360
H	-4.788720	-0.822867	-0.271270
H	-6.846487	0.525718	-0.378514
H	-6.753501	3.001192	-0.254007
H	-4.567876	4.161781	-0.054533
C	3.452901	-2.310219	0.024020
C	4.732057	-0.258105	0.196841
C	5.886544	-1.020893	0.265975
C	5.836001	-2.423324	0.200938
C	4.617735	-3.077062	0.085831
C	2.116122	2.281206	0.009317
H	4.788685	0.822879	0.271337
H	6.846454	-0.525696	0.378716
H	6.753489	-3.001171	0.254204
H	4.567882	-4.161772	0.054588
C	1.631356	3.311491	0.826580
C	2.207433	4.577699	0.780342
C	3.269470	4.831670	-0.087127
C	3.753905	3.813448	-0.909054
C	3.184391	2.544740	-0.859541
C	-1.631488	-3.311507	-0.826691
C	-2.207552	-4.577715	-0.780342
C	-3.269442	-4.831680	0.087311
C	-3.753744	-3.813450	0.909305
C	-3.184247	-2.544740	0.859677
H	0.815859	3.104708	1.515583
H	1.829226	5.365718	1.424877
H	3.718051	5.819995	-0.123684
H	4.573901	4.009895	-1.593651
H	3.546415	1.755501	-1.513932
H	-0.816121	-3.104725	-1.515847
H	-1.829454	-5.365740	-1.424934
H	-3.718012	-5.820007	0.123955
H	-4.573622	-4.009894	1.594044
H	-3.546159	-1.755497	1.514125

Table S13. Cartesian Coordinates (Å) of the Optimized Geometry for **4c** Calculated at the M06-2X/6-31++G(d) Level of Theory

C	0.058020	-1.740121	0.021193
C	-1.319613	-1.667710	-0.027513
C	-1.718543	-0.235079	-0.083329
C	-0.559871	0.490859	-0.094280
C	1.756748	0.334416	-0.020464
C	1.358630	1.766797	-0.077259
C	-0.019048	1.840226	-0.125381
C	1.981290	3.061289	0.019235
C	0.999659	4.085962	-0.018819
S	-0.634613	3.449047	-0.121313
S	0.675035	-3.348676	0.018809
C	-1.940950	-2.962850	-0.124882
C	0.597763	-0.391014	-0.010136
C	3.327894	3.442790	0.176059
C	3.660105	4.786051	0.250256
C	2.674214	5.783743	0.175928
C	1.336406	5.438845	0.047369
C	3.120109	-0.196481	-0.009985
H	4.101716	2.686747	0.259083
H	4.700625	5.071309	0.374297
H	2.957087	6.830327	0.232565
H	0.564889	6.202676	0.009243
C	-0.958679	-3.987029	-0.085538
C	-3.286789	-3.345866	-0.285184
C	-3.617748	-4.689428	-0.360915
C	-2.631425	-5.686414	-0.284385
C	-1.294212	-5.340058	-0.152882
C	-3.082502	0.294342	-0.089792
H	-4.060450	-2.590089	-0.371692
H	-4.657561	-4.975582	-0.489040
H	-2.913141	-6.733218	-0.342667
H	-0.522049	-6.103241	-0.114236
C	-3.416641	1.403244	-0.887228
C	-4.688756	1.946158	-0.854550
C	-5.664144	1.398262	-0.010208
C	-5.349620	0.300469	0.796243
C	-4.066537	-0.241780	0.745396
C	3.451401	-1.292522	0.791219
C	4.730290	-1.846672	0.772513
C	5.700975	-1.302952	-0.072882
C	5.382043	-0.208472	-0.889435
C	4.111298	0.337321	-0.852803
H	-2.669777	1.820695	-1.558256
H	-4.958634	2.794050	-1.475998
O	-6.879978	1.998437	-0.045287
H	-6.083043	-0.132669	1.466587
H	-3.818358	-1.080109	1.391709
H	2.703249	-1.705154	1.463936
H	4.953600	-2.688509	1.417621
O	6.973198	-1.762319	-0.173210
H	6.149711	0.187000	-1.547005
H	3.863972	1.170678	-1.505711
C	7.339855	-2.872074	0.621195
C	-7.896628	1.483260	0.789940
H	8.383260	-3.078156	0.384606
H	6.728614	-3.749519	0.378954
H	7.245044	-2.641423	1.688963
H	-8.776109	2.099717	0.606514
H	-7.613130	1.554794	1.846744
H	-8.121993	0.439703	0.539648

Table S14. Cartesian Coordinates (Å) of the Optimized Geometry for **4d** Calculated at the M06-2X/6-31++G(d) Level of Theory

C	1.289591	1.248462	0.060880
C	2.171303	0.186636	0.056951
C	1.389752	-1.078155	0.034267
C	0.067683	-0.726122	-0.017362
C	-1.389755	1.078159	-0.034335
C	-2.171306	-0.186632	-0.056994
C	-1.289593	-1.248458	-0.060985
C	-3.546888	-0.601005	0.029792
C	-3.632997	-2.017439	0.024005
S	-2.058368	-2.790391	-0.039159
S	2.058369	2.790394	0.038975
C	3.546888	0.601002	-0.029828
C	-0.067682	0.726126	0.017172
C	-4.742652	0.132019	0.159124
C	-5.955140	-0.534148	0.234192
C	-6.018510	-1.936724	0.188047
C	-4.856187	-2.687199	0.089924
C	-1.951219	2.413852	-0.103895
H	-4.712918	1.213944	0.225852
H	-6.871801	0.038810	0.338490
H	-6.979834	-2.437823	0.244999
H	-4.892567	-3.772816	0.076477
C	3.632998	2.017437	-0.024109
C	4.742654	-0.132030	-0.159093
C	5.955145	0.534131	-0.234163
C	6.018516	1.936710	-0.188082
C	4.856191	2.687191	-0.090023
C	1.951212	-2.413840	0.103945
H	4.712921	-1.213959	-0.225765
H	6.871807	-0.038833	-0.338411
H	6.979841	2.437805	-0.245034
H	4.892573	3.772809	-0.076625
S	1.227637	-3.742972	-0.744385
C	2.348724	-4.856775	-0.068393
C	3.237096	-4.242519	0.771456
C	3.012153	-2.841534	0.868742
S	-1.227613	3.742919	0.744511
C	-2.348731	4.856774	0.068653
C	-3.237123	4.242584	-0.771222
C	-3.012179	2.841608	-0.868630
H	-3.577457	2.172706	-1.508550
H	4.020530	-4.770582	1.302292
H	2.301716	-5.903188	-0.338735
H	-2.301718	5.903164	0.339080
H	-4.020575	4.770687	-1.301993
H	3.577413	-2.172581	1.508624

Table S15. Cartesian Coordinates (Å) of the Optimized Geometry for **4f** Calculated at the M06-2X/6-31++G(d) Level of Theory

C	1.53706	-0.94328	-0.00022
C	0.71781	-2.04823	-0.00026
C	-0.69588	-1.60462	-0.00049
C	-0.69588	-0.25133	-0.00034
C	0.69588	1.60462	-0.00049
C	-0.71781	2.04823	-0.00026
C	-1.53706	0.94328	-0.00022
C	-1.44203	3.28492	-0.00003
C	-2.83906	3.04162	0.00014
S	-3.21664	1.32553	-0.00017
S	3.21664	-1.32553	-0.00017
C	1.44203	-3.28492	-0.00003
C	0.69588	0.25133	-0.00034
C	-0.98779	4.61540	0.00009
C	-1.90670	5.65130	0.00038
C	-3.28859	5.39099	0.00055
C	-3.76451	4.08744	0.00043
H	1.55455	2.26680	-0.00051
H	0.07873	4.82303	-0.00002
H	-1.55717	6.67935	0.00047
H	-3.99219	6.21771	0.00076
H	-4.83154	3.88457	0.00052
C	2.83906	-3.04162	0.00014
C	0.98779	-4.61540	0.00009
C	1.90670	-5.65130	0.00038
C	3.28859	-5.39099	0.00055
C	3.76451	-4.08744	0.00043
H	-1.55455	-2.26680	-0.00051
H	-0.07873	-4.82303	-0.00002
H	1.55717	-6.67935	0.00047
H	3.99219	-6.21771	0.00076
H	4.83154	-3.88457	0.00052

8. References

S1 N. Cramer, M. Buchweitz, S. Laschat, W. Frey, A. Baro, D. Mathieu, C. Richter and H. Schwalbe, *Chem. Eur. J.*, 2006, **12**, 2488–2503.

S2 R. Kuwata, T. Imanishi, S. Hasegawa, Z. Wang, J. Usuba, K. Yasui, M. U. G. Khan, J. I. Wu, Y. Uetake and A. Fukazawa, *ChemRxiv*, 2025, DOI: 10.2634/chemrxiv-2025-l8c87-v2.

S3 G. M. Sheldrick, *Acta Cryst.*, 2015, **71**, 3–8.

S4 a) G. M. Sheldrick, *SHELX-2018, Program for the Refinement of Crystal Structures*, University of Göttingen, Göttingen, Germany, 2018. b) G. M. Sheldrick, *Acta Crystallogr., Sect. C*, 2015, **71**, 3–8.

S5 C. M. Cardona, W. Li, A. E. Kaifer, D. Stockdale and G. C. Bazan, *Adv. Mater.*, 2011, **23**, 2367–2371.

S6 Gaussian 16, Revision B.01, M. J. Frisch, G. W. Trucks, H. B. Schlegel, G. E. Scuseria, M. A. Robb, J. R. Cheeseman, G. Scalmani, V. Barone, G. A. Petersson, H. Nakatsuji, X. Li, M. Caricato, A. V. Marenich, J. Bloino, B. G. Janesko, R. Gomperts, B. Mennucci, H. P. Hratchian, J. V. Ortiz, A. F. Izmaylov, J. L. Sonnenberg, D. Williams-Young, F. Ding, F. Lipparini, F. Egidi, J. Goings, B. Peng, A. Petrone, T. Henderson, D. Ranasinghe, V. G. Zakrzewski, J. Gao, N. Rega, G. Zheng, W. Liang, M. Hada, M. Ehara, K. Toyota, R. Fukuda, J. Hasegawa, M. Ishida, T. Nakajima, Y. Honda, O. Kitao, H. Nakai, T. Vreven, K. Throssell, J. A. Montgomery, Jr., J. E. Peralta, F. Ogliaro, M. J. Bearpark, J. J. Heyd, E. N. Brothers, K. N. Kudin, V. N. Staroverov, T. A. Keith, R. Kobayashi, J. Normand, K. Raghavachari, A. P. Rendell, J. C. Burant, S. S. Iyengar, J. Tomasi, M. Cossi, J. M. Millam, M. Klene, C. Adamo, R. Cammi, J. W. Ochterski, R. L. Martin, K. Morokuma, O. Farkas, J. B. Foresman and D. J. Fox, Gaussian, Inc., Wallingford CT, 2016.

S7 a) P. v. R. Schleyer, C. Maerker, A. Dransfeld, H. Jiao and N. J. R. van Eikema Hommes, *J. Am. Chem. Soc.*, 1996, **118**, 6317–6318. b) Z. Chen, C. S. Wannere, C. Corminboeuf, R. Puchta and P. v. R. Schleyer, *Chem. Rev.*, 2005, **105**, 3842–3888. c) H. Fallah-Bagher-Shaidaei, C. S. Wannere, C. Corminboeuf, R. Puchta and P. v. R. Schleyer, *Org. Lett.*, 2006, **8**, 863–866.

S8 R. Gershoni-Poranne and A. Stanger, *Chem. Eur. J.*, 2014, **20**, 5673–5688.

S9 Z. Wang. *Chemistry*, 2024, **6**, 1692–1703.

S10 D. Geuenich, K. Hess, F. Köhler and R. Herges, *Chem. Rev.*, 2005, **105**, 3758–3772.

S11 E. D. Glendening, J. K. Badenhoop, A. E. Reed, J. E. Carpenter, J. A. Bohmann, C. M Morales, P. Karafiloglou, C. R. Landis, F. Weinhold, NBO 7.0, Theoretical Chemistry Institute, University of Wisconsin, Madison, 2018.